Minimization of Crosstalk in Multi-Actuator Hydraulic Systems

A Thesis
SUBMITTED TO THE FACULTY OF THE
UNIVERSITY OF MINNESOTA
BY

Kshitij Suresh Sonkar

IN PARTIAL FULFILLMENT OF THE REQUIREMENTS
FOR THE DEGREE OF
MASTER OF SCIENCE

James D. Van de Ven, PhD

February 2022

Acknowledgements

I would like to thank my advisor Dr. James Van de Ven, for his boundless patience, unfaltering support and the opportunity to take on this journey. I would like to thank my lab mates from the Mechanical Energy and Power Systems Laboratory – Jeremy Simmons, Grey Boyce-Erickson, Nate Fulbright, Jenny Swanson, Chris Heen, Jonatan Pozo-Palacios, Caroline Dai and Steven Thomalla for their help and support during my time at the University of Minnesota. I would like to thank Paul Carrol, Scott Johnson and Steve Lemmer from MTS Systems for their mentorship and advice as I figure out how to be an engineer. I would like to thank Dr. Frank Kelso, Dr. Tom Chase, Dr. Tim Kowalewski and Dr. Sungyon Lee for some of the most incredible lectures I have ever attended. I would also like to thank the committee members Dr. Kim Stelson and Dr. Ryan Caverly.

Dedication

To my family and the coffeeshops in the city of Minneapolis.

Abstract

The field of material testing is dominated by servo-hydraulic control systems owing to their large power to weight ratio compared to servo-electric control systems. Hydraulic systems are capable of producing large forces and torques with a fast response time, making them ideal to conduct fatigue, failure, and wear type tests. Material testing requires high positional and force control accuracy, which is achieved in hydraulics with fast responding servo-hydraulic valves. In this thesis, the impact on the accuracy in positional control of hydraulic test systems is explored, specifically in the case of multiple actuators simultaneously being powered by a singular pressurized flow source. The reduction in performance and position control accuracy of a loadframe due to the dynamics introduced in the system by another loadframe connected to the same hydraulic circuit is called crosstalk.

A system model is developed of a hydraulic testing laboratory as a tool to model pressure and flow dynamics in the hydraulic circuit and position dynamics of the actuators. The aim of this model is to measure impact on the position control accuracy of loadframes during simultaneous operation. The model consists of sub-system models of the components of a hydraulic testing laboratory - the loadframes, hydraulic pipeline and a hydraulic power unit. These sub-system models are developed and experimentally validated.

The system model is then used to evaluate crosstalk in a baseline test case. Three methods of crosstalk reduction, namely close coupled accumulation, RC Filtering, and 2nd Order RC Filters are analyzed and modelled and shown to be effective tools for the mitigation of crosstalk. The components involved in each method are sized to reduce the pressure fluctuations and improve the position control accuracy of the loadframes to an acceptable value in the baseline test case. The effectiveness of these methods is then evaluated by measuring the reduction of pressure fluctuations and improvement in position control accuracy showing that RC filters are the most effective tools for crosstalk mitigation tools. A cost comparison is conducted on the methods to corelate the expense with their effectiveness, concluding that 2nd order RC filters are the most cost-effective method for crosstalk reduction within the scope of this study.

Table of Contents

Acknowledgements i
Dedication ii
Abstract iii
Table of Contents iv
List of Tables vi
List of Figures vii
Chapter 1 Introduction 1
1.1 Background and Literature Review 3
1.1.1 Reduction of crosstalk 4
1.1.2 Modelling hydraulic systems 6
1.1.2.1 Pump Modelling 7
1.1.2.2 Actuator modelling 9
1.1.2.3 Pipeline Modelling 10
1.1.2.4 Modelling using Simscape 11
1.2 Thesis Overview 12
Chapter 2 Modelling of a Multiactuator Hydraulic System 13
2.1 Introduction 13
2.2 System Level Model 16
2.2.1 System Description 16
2.2.2 Component Models 20
2.2.2.1 Pump model – PID controlled Flow Source 20
2.2.2.1.1 Tuning of simplified pump model 22
2.2.2.1.2 Pump model validation 24
2.2.2.2 Segmented Pipeline Model 26
2.2.2.3 Accumulator Model 29
2.2.2.4 Loadframe Model 31
2.2.2.4.1 Servovalve Model 32
2.2.2.4.2 Actuator Model 35
2.2.2.4.3 Loadframe Controller Tuning 37

2.2.2.4.4 Loadframe Model Tuning 39
2.2.2.5 System model 40
2.2.2.6 Baseline System Parameters 42
2.2.2.7 Model Solver Configuration 43
2.3 Results 44
2.3.1 System Model – Baseline test case 44
2.4 Discussion 51
2.4.1 Baseline System Model Test Setup 51
2.5 Inferences and Conclusion 52
Chapter 3 Measurement and Reduction of Hydraulic Crosstalk in a Multiactuator System 55
3.1 Introduction 55
3.2 Modelling and Evaluation of Reduction Techniques for Crosstalk 57
3.2.1 Closed Coupled Accumulation 57
3.2.2 RC Filter 61
3.2.3 Second Order RC Filter 64
3.2.4 Cost Comparison of Crosstalk Reduction 66
3.3 Results 67
3.3.1 Case1 – Close Coupled Accumulation 67
3.3.2 Case 2 – RC Filter 75
3.3.3 Case 3 – 2nd Order RC Filter 80
3.4 Discussion 86
3.4.1 Pressure ripple due to sinusoidal displacement at Loadframe 2 87
3.4.2 Pressure variation in system due to step displacement at LF1 88
3.4.3 Error in displacement control of LF2 88
3.4.4 Cost evaluation in crosstalk reduction techniques 89
3.5 Conclusion 91
Chapter 4 Conclusion 93
4.1 Thesis Review 93
4.2 Recommendations for Future Work 95
Bibliography 97
Appendix A: Simscape Models 101
Appendix B: Convergence study of model 103

List of Tables

Table 2.1 Parameters of Hydraulic Lab Setup 19
Table 2.2 PID Controller gains for Pump Model.....26
Table 2.3 Tuning of Loadframe Model Parameters.....38
Table 2.4 PID Controller gains for Loadframe Model 39
Table 3.1 Comparison of Accumulation Volume on Crosstalk Reduction.....75
Table 3.2 Comparison of crosstalk reduction.....90
Table 3.3 Comparison of Resistance and Capacitance of system 91

List of Figures

Figure 1.1 An animated representation of a typical Materials Testing Lab 2
Figure 1.2 Loadframes 3
Figure 2.1 Loadframe for material testing [25] 13
Figure 2.2 MTS Bionix Knee wear simulation system[28] 14
Figure 2.3 Typical Material Testing Lab [2] 15
Figure 2.4 MTS Lab setup 17
Figure 2.5 Hydraulic Power Unit 17
Figure 2.6 Schematic of Hydraulic Lab Setup 18
Figure 2.7 Pump Model (PID Controlled flow source) 21
Figure 2.8 Lab setup for Pump Model validation 22
Figure 2.9 Pressure dynamics at pump outlet for 40% valve opening 25
Figure 2.10 Pressure dynamics at pump outlet for 90% valve opening 25
Figure 2.11 Segmented Pipeline Schematic Diagram 26
Figure 2.13 Commercial Bladder Style Accumulators [37] 29
Figure 2.14 Bladder Style Accumulator [38] 30
Figure 2.15 Schematic representation of the volumes in the accumulator 31
Figure 2.16 Schematic representation of a Servovalve [1] 32
Figure 2.17 Flow from servovalve to actuator [43] 34
Figure 2.18 Servovalve flow paths 34
Figure 2.19 Actuator Model 35
Figure 2.20 Tuning Loadframe Model 37
Figure 2.21 Position tracking of actuator (Model vs Experimental) 40
Figure 2.22 Schematic diagram of model for baseline test setup 41
Figure 2.23 Position tracking of Loadframe 1 45
Figure 2.24 Pressure study at Loadframe 1 and HPU 46
Figure 2.25 Pressure study at Loadframe 2 and HPU 47
Figure 2.26 Flow rate at Loadframe 1 and HPU 48
Figure 2.27 Flow rate at Loadframe 2 and HPU 49
Figure 2.28 Position tracking of loadframe 2 50

Figure 2.29 Error in position tracking for Loadframe 2 51
Figure 3.1 Line Accumulation 58
Figure 3.2 Close Coupled Accumulation.....58
Figure 3.3 Close Coupled Accumulation.....59
Figure 3.4 RC Filter 61
Figure 3.5 Hydraulic RC Filter 62
Figure 3.6 Second order RC Filter 64
Figure 3.7 Hydraulic 2nd order RC Filter.....65
Figure 3.8 Position tracking of Loadframe 1 68
Figure 3.9 Pressure study at Loadframe 1 and HPU.....70
Figure 3.10 Pressure study at Loadframe 2 and HPU.....71
Figure 3.11 Flow rate at Loadframe 1 and HPU.....72
Figure 3.12 Flow rate at Loadframe 2 and HPU.....73
Figure 3.13 Error in position tracking for Loadframe 2 74
Figure 3.14 Position tracking of Loadframe 1.....76
Figure 3.15 Pressure study at Loadframe 1 and HPU.....77
Figure 3.16 Pressure study at Loadframe 2 and HPU.....77
Figure 3.17 Flow rate at Loadframe 1 and HPU.....78
Figure 3.18 Flow rate at Loadframe 2 and HPU.....79
Figure 3.19 Error in position tracking for Loadframe 2 79
Figure 3.20 Position tracking of Loadframe 1.....81
Figure 3.21 Pressure study at Loadframe 1 and HPU.....82
Figure 3.22 Pressure study at Loadframe 2 and HPU.....83
Figure 3.23 Flow rate at Loadframe 1 and HPU.....84
Figure 3.24 Flow rate at Loadframe 2 and HPU.....85
Figure 3.25 Error in position tracking for Loadframe 2 86

Figure A. 1 Simscape Fluids Model for validation of Pump Model.....101
Figure A. 2 Simscape System Model for Evaluation of Crosstalk.....103

Figure B. 1 : Comparison of Loadframe 1 position with Relative tolerance 104
Figure B. 2 Comparison of flow rate of Loadframe 2 with Relative tolerance 105
Figure B. 3 Comparison of flow rate of Loadframe 2 with Relative tolerance 106

Figure B. 4 Comparison of Pressure at Loadframe 2 with Relative tolerance.....107
Figure B. 5 Comparison of Pressure at Loadframe 1 with Relative tolerance.....108
Figure B. 6 Comparison of error in position control of Loadframe 2 with Relative tolerance 109

Nomenclature

C_d	Coefficient of Flow
f_c	Friction factor
A	Area
c	Speed of sound
C	Capacitance
f	Frequency
i	Current
k	Specific heat ratio
L	Length
m	Mass
P	Pressure
R	Resistance
t	Time
V	Volume
D	Diameter
Q	Flow rate
Re	Reynolds Number
v	Voltage
x	Displacement
β	Bulk Modulus
λ	Characteristic length
ρ	Density

Chapter 1
Introduction

The field of material testing is dominated by servo-hydraulic control systems owing to their large power to weight ratio compared to servo-electric control systems [1]. Hydraulic systems are capable of producing large forces and torques with a fast response time, making them ideal to conduct fatigue, failure, and wear type tests. Material testing requires high positional and force control accuracy, which is achieved in hydraulics with fast responding servo-hydraulic valves. In this thesis, the impact on the accuracy in positional control of hydraulic test systems is explored, specifically in the case of multiple actuators simultaneously being powered by a singular pressurized flow source.

A hydraulic testing facility (Figure 1.1) typically consists of multiple test stations or loadframes that are powered by a singular pump and connected using flexible hoses and rigid pipelines. A loadframe is a hydraulic testing station comprising a hydraulic actuator mounted on a rigid frame, controlled by a servovalve (Figure 1.2) and capable of characterizing a wide range of materials, such as elastomers, alloys, composites such as carbon fiber, ceramics, and even medical device components. Specimens are mounted in the test space using grips and collets for the desired analysis of material properties. The reduction in performance and position control accuracy of a loadframe due to the dynamics introduced in the system by another loadframe connected to the same hydraulic circuit is called crosstalk.

Research in the field of servohydraulic control is typically focused on the improvement of the performance of components in a hydraulic circuit – pumps, valves, accumulator, actuators etc. There is a lack of research that study the system as whole and focus on the interactions between these components. This thesis focuses on exploring this space and

taking an initial step towards studying pressure dynamics and position control performance at a system level.

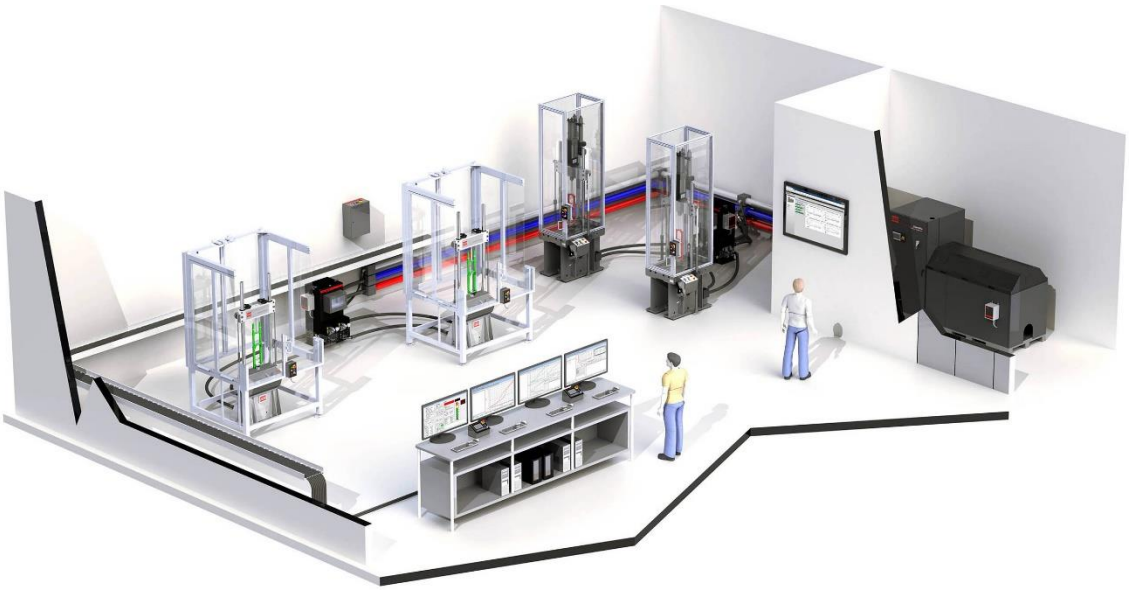

Figure 1.1 An animated representation of a typical Materials Testing Lab comprising of four loadframes (with enclosures around the test space), a pump, connecting pipelines and a controller station[2].

In this thesis, a system model is developed of a hydraulic testing laboratory as a tool to model pressure and flow dynamics in the hydraulic circuit and position dynamics of the actuators. The aim of this model is to measure impact on the position control accuracy of loadframes during simultaneous operation. The model consists of sub-system models of the components of a hydraulic testing laboratory - the loadframes, hydraulic pipeline and a hydraulic power unit. These sub-system models are developed and experimentally validated. The system model is then used to measure the crosstalk in system and evaluate the effectiveness of measures of reducing crosstalk that are implemented in the circuit.

Figure 1.2 Loadframes: These are two varieties of loadframes. The loadframe on the left is a 370.10 model with a frame and actuator rated for 100kN with a servovalve which has flow rating of 15gpm at 1000psi. The loadframe on the right is a 370.02 model, which has a frame and actuator rates for 25kN of force and a servovalve which has a flow rating of 5gpm at 1000psi. [3]

1.1 Background and Literature Review

This section provides a background on the research previously conducted on the topic of hydraulic noise and development of methods to attenuate it. Research on this topic primarily consists of 'localized' studies focusing on noise attenuation near one component in a hydraulic system, for example the reduction of pressure ripple generated by the pump at the pump outlet. Additionally, modelling methodologies for the components of a hydraulic testing system are discussed.

1.1.1 Reduction of crosstalk

A considerable amount of research has been conducted in the field of hydraulic noise attenuation. Pan and Johnston (2016) develop a hybrid method of active and passive hydraulic noise cancellation with a focus on the reduction of audible noise generated by the system, specifically at the pump outlet [4]. In this study, the primary disturbance generator in the system is the pump ripple produced by a gear pump metering flow through a loading valve. A passive flexible hose is used as added compliance to the system, to attenuate the high frequency pulsations. A variable piezoelectric valve is added to the system as a secondary flow path. The area of the piezoelectric valve is actively controlled to reduce harmonic pulsation in the system. The secondary flow path resulted in an attenuation of noise by 61.3dB at 200Hz and 52.5dB at 1000Hz showing that this device was more effective at lower frequencies.

In 2021, Pan and Yuan improved on this approach with the use of a piezo- actuator installed in the system [5]. The volume of the actuator is dynamically changed to vary the added compliance to the system with a feedforward controller that measures the pressure fluctuations in the system. The sizing of the flexible hose is optimized to maximize attenuation of noise in the higher frequencies. The effectiveness of the noise-reduction in these studies is measured as reduction in audible noise in the proximity to the pump and the reduction in pressure pulsation amplitudes at the pump outlet. The installation of the piezo- actuator resulted in an attenuation of noise by 11dB at 160Hz and 3dB at 640Hz showing that this device was more effective at lower frequencies. In this thesis, focus is placed on the reduction of pressure pulsations at the pump generated as a result of variation in flow demanded by a loadframe as well as the pressure ripple generated at the loadframes due to the position switching of the directional control servovalves. The accuracy in position control of hydraulic actuators is used as metric of evaluation of improvement methods implemented in the system

Haas and Lukachev explore the attenuation of pressure pulsations in short transmission lines generated by a switching valve using an RC filter [7]. This study is focused on the

pressure pulsations generated in the short transmission lines between a switching valve and the actuator controller by it. An RC Filter, consisting of a throttle as a resistance and an accumulator as added capacitance is used to reduce the pressure fluctuations in the transmission line to an acceptable value. The settling ties are seen to reduce by 75% and the amplitude of pressure ripple is reduced by 20% for the case studied. This thesis expands on this application, using the RC filter as an attenuation technique for the pressure ripple induced in long rigid pipelines by servovalves on material testing loadframes as well as the pressure fluctuations at the pump outlet of a pressure compensated variable displacement pump.

Yokota and Somada developed an active accumulator with the objective of reduction of high frequency pressure fluctuations produced by axial-piston pumps [7]. The active accumulator design consists of a piston controlled by piezoelectric sensor and a pressure transducer, and an accumulator installed at the pump outlet. The piston position determines the added capacitance volume to the system, dampening the pressure pulsations originating at the pump, similar to the piezo actuator developed by Pan and Yuan [6]. This method is shown to be effective in the frequency range of 500Hz – 1KHz.

Waitschat and Thielecke develop and evaluate a novel fluid-borne noise silencer for transmission lines in aviation systems called a ‘Disc Silencer’ [8] . The ‘Disc Silencer’ consists of an additional chamber shaped like a disc and of a height equivalent to the diameter of the transmission lines installed at the pump outlet for added compliance. The installation of this device was shown to considerably reduce the pressure fluctuations in the transmission lines with a reduction in noise by 10-11dB.

Earnhart and Cunafare have designed a ‘Compact Helmholtz Resonator’ for the reduction of pressure fluctuations in hydraulic lines [10]. The device consists of an additional chamber (resonator) installed on the hydraulic pipeline, with a compliant lining on the inside to dampen the pressure oscillations in the system. This device was shown to reduce the pressure oscillations by 5-6dB at the resonance frequency of the Resonator.

Contribution in this field generally consist of the development of devices that focus on the reduction of pressure oscillations in one component or section of the system, for example, at the pump outlet, the controlled actuator or in the transmission lines. There is a need for the study of systems with multiple actuators that are controlled independently but interfere with each other's performance due to the transients generated in the system by their operation. The model developed in this thesis, considers the pressure fluctuations in the hydraulic circuit as a whole and focuses on the interaction of multiple actuators being controlled independently while being powered by the same pump. The reduction techniques investigated are evaluated based on the improvement in position control accuracy of the actuator.

1.1.2 Modelling hydraulic systems

There are three general approaches that can be taken when modelling a hydraulic system, namely white-box modelling, grey-box modelling and black box modelling [4]. White box models are the type of models which clearly define what the influencing variables are and how they influence the output response of the system. White box modelling of a system requires in-depth knowledge of the system and the physical equations governing it. A black box model would be the opposite extreme on this spectrum of modelling approach, with the model only drawing a functional relationship between the input and output but without any physical significance. A black-box model is identified using an experimental output or data set from the system using a dynamic test. The model is configured to have similar response characteristics as the experimental system. A grey box model is a combination of black box and white box modelling. The parts of the system that not being studied are modelled using a black box approach, and the components that need in-depth modelling are modelled using a white box approach. Grey-box modelling requires some prior knowledge of the system, such as the steady state performance. In this body of work, a grey box modeling approach is taken for the modelling of a hydraulic system. A black box approach is used for the modelling of components where the internal dynamics are not of significance to the measurement of crosstalk. A white box approach is used when

the modelling dynamics of the system are needed for capturing crosstalk and the loss of performance in the system.

1.1.2.1 Pump Modelling

In a hydraulic system, the pump acts as the source of flow and when combined with pressure compensation control or a relief valve, maintains the desired system pressure. It also fills the precharged accumulators with hydraulic fluid in the initial stages, which assist in providing instantaneous flow to individual loadframes during their operation. The pump characteristics greatly influence and pose limitations to the performance of each loadframe, making an accurate pump model an essential component in a hydraulic system model. Positive displacement pumps can be broadly classified into fixed displacement and variable displacement pumps[1]. As the name suggests, a fixed displacement pump provides a set amount of flow determined by the rotation speed of the motor. While this architecture is simpler, any excess flow provided is throttled through a bypass valve, which results in lower efficiency. On the other hand, a variable displacement pump can vary the flow provided to the system, so as to maintain a constant preset pressure and meet the load requirements of the system. This improves power and efficiency and reduces oil temperatures. The system under study, utilizes an Axial-Piston Variable Displacement Pump with pressure control or a 'Pressure Compensated Variable Displacement Pump' (PCVDP)[11], which senses the pressure at the outlet of the pump and adjusts the flow rate accordingly.

A significant amount of research work can be found on the modelling of variable displacement pumps [12–14]. Kaliafetis defined the governing equations of an axial-piston variable displacement pump and developed a mathematical model to model the flow response concluding that the main influencers of the outlet pressure dynamics are the control valve and the areas of the pistons that control the swashplate angle [8]. Similar work is done by Manring in the modelling of pump dynamics, but with the addition of insight into how the model output can be utilized to make design improvements with a positive impact on system rise time, settling time and pressure overshoot [12]. Manring concluded

that rise time of pressure is reduced by increasing the control piston volume but increases the settling time and the overshoot in pressure. Zeiger developed a method for modelling and improving the design of a swashplate controller, the dynamics of which define the performance of a variable displacement pump [14]. Kim and Cho conducted a sensitivity analysis on the parameters influencing the accuracy of a pump model, concluding that the flow gain of the pressure compensator, the displacement of the control cylinder and the specific displacement of the pump have the greatest influence on the system dynamics [9].

Barbosa and Aguirre develop a gray-box model of a hydraulic water pumping system (consisting of a fixed displacement pump) that is based on experimental data collected comparing the pump speed to the pressure at the outlet with good corroboration between the model and the system [10]. Casoli and Anthony developed a black box model of an excavator hydraulic system that uses a hydraulic pump [16]. The model corelates the motion of the excavator arm with the flow output of the pump.

Approaching a pump model with a white-box approach requires in-depth knowledge of the architecture of the pump and accurate dimensions and specifications of each component of the pump. This can prove to be quite difficult considering that the model would need to account for the variation in the machining tolerances that affect the performance of the pump. If the pump in the system under study were to be swapped with another pump of the same architecture, the white-box model would still have to be tuned to account for the variation in performance as the machining tolerances, part sizing such as piston volumes, control valve flow rating, spool dimensions, spring rates, clearances etc. which would vary from pump to pump. When switching to a pump of a different architecture, a new model would need to be developed from scratch, as the physical equations that govern it would change. In order to model crosstalk, the pressure and flow dynamics at the pump outlet for changes in the flow demand of the system are key outputs of the pump model. A black-box model approach is used in this study, using a ‘Hydraulic Flow Rate’ block in Simscape. A PID Controller is used to control the flow rate from this source. The gains of the controller

are tuned to match the response characteristics of a pressure compensated variable displacement pump.

1.1.2.2 Actuator modelling

The main objective in a testing laboratory is the precise control of the displacement of an actuator (mounted on a loadframe) to exert a desired force or strain on a specimen being studied. The motion of the actuator is controlled by flow from a servovalve mounted on it. The control loop consists of the position of the actuator as the input, a controller which compares the measured position with the command signal and commands the spool position in the servovalve with a proportional voltage input. PID controllers are the most common control strategies to this day, as they were easily understood by technicians and intuitive to use. The Ziegler-Nichols method is an experimental method of tuning PID controller gains to achieve the desired output from a system [17]. Rozali and Rehmat develop a black box model of an electrohydraulic actuator (EHA) using the System Identification Tool in MATLAB [18]. A PID Controller is then used to control the position of the EHA, and the Ziegler-Nichols method is employed to tune the controller to improve actuator performance.

Several modern approaches to servohydraulic control have been developed with improved response time and position tracking. An adaptive strategy for the control of an actuator is developed by Bobrow and Lum [19] using feedforward and a Linear Quadratic Regulator (LQR) to achieve better tracking performance than with a simple PID controller and better adapting to large changes in the system. Sharghi and Mohammadi develop a model for the control of servohydraulic actuators with feedforward utilizing a least-squares support vector machine(LS-SVM) that replaces the PID Controller [20]. The controller uses a hysteresis model to train the LS-SVM to reduce the error in positional control by 5% in the absence of fluid borne noise. Chae and Rabiee developed a method for real-time force control of servo-hydraulic actuators using adaptive series compensator and compliance springs for application in Real Time Hybrid Simulation (RTHS) [21].

In this thesis, a similar strategy as developed by Rozali and Rehmat is used to tune the actuator performance [18], but with the intention of replicating the performance of an actuator in a system experiencing crosstalk. The Zeigler-Nichols method is used to tune the actuator model to have good correlation with the experimental data collected to create a baseline test condition to evaluate crosstalk reduction techniques. In material testing application, often a perfectly tuned PID controller with the fastest response is not the ideal solution, and the required response time from the actuator varies depending on the application. For example, for the testing of small delicate ceramics using low magnitudes of force, it would be preferred to have a damped slow response, rather than a system with even a small amount of overshoot over the command signal.

1.1.2.3 Pipeline Modelling

In order to study the interaction of multiple loadframes in a hydraulic system, accurately capturing the pressure and flow dynamics in pipelines is crucial. Pressure fluctuations travel through the pipeline and are dependent on the bulk properties of the oil used in the system, and the sizing of the pipeline. Haas and Manhartsgruber use a lumped parameter approach to model fluid transients in hydraulic transmission lines [22]. In this approach, the pipeline is modeled as elements that are a combination of hydraulic resistance (R), inductance (L) and capacitance (C) and termed as the 'RLC' method. The dynamics of flow in a pipeline can be modeled using a distributed parameter model as in the model developed by Kenneth and Jan-Ove [23]. The properties of resistance of the pipeline, inertia of the fluid and capacitance are considered to be uniformly distributed throughout the length of the conduit. A popular and accurate method of modeling unsteady fluid transients is by the using the Method of Characteristics (MOC) approach to solve the partial differential equations used to define the flow in the pipeline [24]. Haas and Manhartsgruber show that the 'RLC' method or the lumped parameter approach has very good correlation with MOC. In this thesis, the pipeline dynamics are modelled using the 'segmented pipeline model' in Simscape Fluids which employs the 'RLC' method.

1.1.2.4 Modelling using Simscape

One of the goals of this thesis is to create a tool to measure crosstalk and evaluate reduction techniques that are easily reconfigurable depending on the laboratory setup analyzed. Such a tool should be able to allow the user to change the sizing of the loadframes and generate different combinations of command signals for the multiple loadframes. It should also allow a user without a programming background add, remove, and size components such as accumulators and pipelines. Simscape Fluids (MATLAB) provides a great platform for modelling of hydraulic systems . Simscape also provides detailed documentation on the modelling equations governing these components in the library. The modelling in Simscape uses 'blocks' for each component, that can be connected to create system layouts making it easy to quickly reconfigure an existing model to evaluate a new hydraulic system. While other software packages like AMESim have similar features, Simscape has a large user base amongst engineers in industry. Choosing Simscape over the other less popular options increases the potential for the tools developed in this thesis to have a larger reach amongst the hydraulics engineering community in the US.

The objective of this study is to create a system model of a hydraulic testing facility, with accurate sub-system models to study the impact of pressure fluctuations and transients on the position control accuracy of multiple loadframes termed as 'crosstalk' and use this model as a tool to evaluate methods to reduce it.

1.2 Thesis Overview

Chapter 1 : Introduction

- This chapter provides the motivation for the research, outlines prior research on hydraulic crosstalk, modelling of hydraulic components etc. and provides an outline of the thesis.

Chapter 2: Modelling of a Multiactuator Hydraulic System

- Developed a model of hydraulic testing laboratory consisting of loadframes, a hydraulic power unit (HPU) and hydraulic pipeline.
- Developed and experimentally validated component level models for each sub-system in the model.
- Defined and evaluated a baseline test case to study crosstalk using the system model.

Chapter 3: Measurement and Reduction of Hydraulic Crosstalk in a Multiactuator System

- Explored methods of reducing crosstalk including close coupled accumulation, RC filtering and 2^{nd} order RC filters.
- Evaluated the effectiveness of the methods of reducing crosstalk using the system model and comparing the results with the baseline test case.

Chapter 4: Conclusion

- This chapter provides concluding remarks on the model developed and methods of reducing crosstalk that are analyzed and evaluated.

Chapter 2

Modelling of a Multiactuator Hydraulic System

2.1 Introduction

In industrial testing setups, a common practice is to drive multiple testing stations or load frames with a single Hydraulic Power Unit (HPU). The HPU is often mounted at a large distance from the load frames - either in another room or at one corner of the facility - and is connected to them by rigid tubing that is fixed along the walls. In general, each load frame has an accumulator, and the fluid is metered to the actuators with servo valves to ensure precise control. The main objective of such a testing facility is to permit the usage of multiple load frames simultaneously without significant loss of control accuracy, while eliminating the cost of having one HPU per load frame. However, due to a single pressurized fluid supply and the difference in the nature of the tests performed in the loadframes, discrepancies in control tracking performance are found in the test results. This behavior is referred to as actuator crosstalk.

Figure 2.1 Loadframe for material testing [25]

Loadframes can be used to perform a variety of tests based on the design of the loadframe and the needs of the laboratory. Loadframes can be used for high cycle fatigue testing, where a large number of cycles (on the order of millions of cycles per specimen) of low force are applied to test the fatigue life of the specimen [26]. They can also be used for low cycle fatigue testing, where a smaller number of cycles of high force are applied. These tests may require the loadframe to apply cyclic compressive and tensile forces on the specimen [27]. Damper systems are tested by commanding large displacements to the damper and analyzing the shock absorption and the damping characteristics.

Loadframes can also be used to conduct wear simulation tests on materials, for example joint implants. These tests need the actuators of the loadframe to follow a path specified by ASME standards to ensure even loading or strain rates on specimen across millions of cycles. Tracking the command signal is key to accurate material characterization of the specimen.

Figure 2.2 MTS Bionix Knee wear simulation system[28]

Lab setups vary greatly depending on the size, function, and number of loadframes and HPUs as well as physical constraints of the lab space. In a typical material testing laboratory, 1-4 loadframes of varying sizes are spaced about 5-10m apart along the walls the laboratory (Figure 2.3). This gives the user access to the front of the loadframes, for ease of installing specimens and fixtures in the test space of the loadframe. The loadframes are connected to the HPU using hardline that runs along the walls of the lab, represented in Figure 2.3 by red and blue hardlines along the wall. The loadframes then connect to the hardline by flexible hoses. The HPU is usually, in the corner of the room or in the neighboring room to reduce noise in the lab. The hardline connects to the HPU using a short length (less than 1m) of flexible hose.

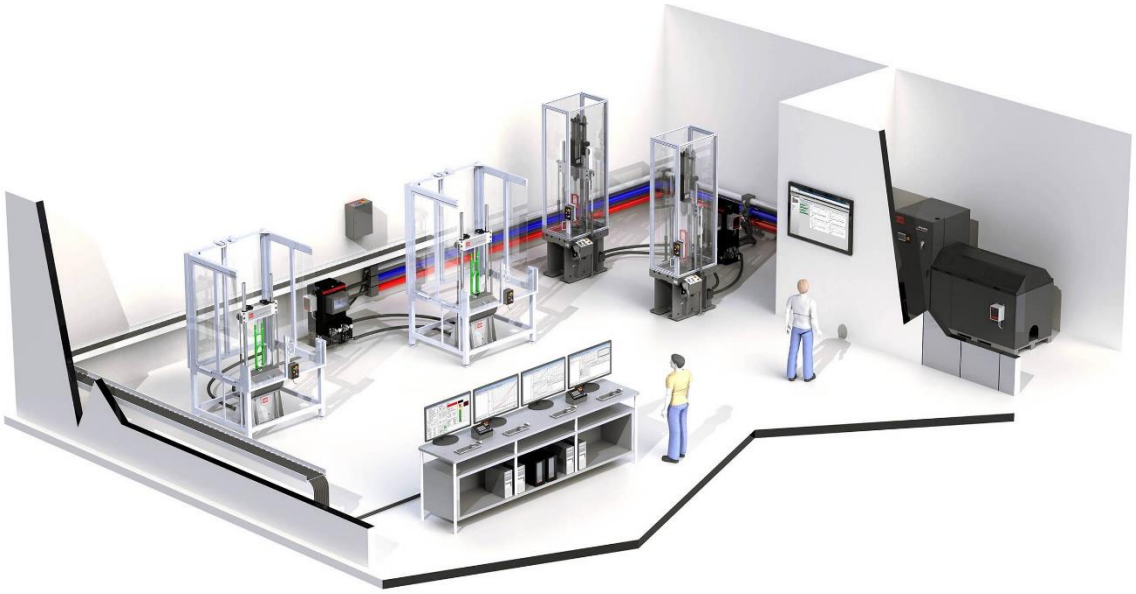

Figure 2.3 Typical Material Testing Lab [2]

Previous work in the field of fluid noise attenuation and hydraulic modelling focuses on component level models, developing methods of reducing fluid-borne noise and audible noise at the source [4–8, 29]. In this chapter, contributions are made to this field of research by considering a system level view with the objective of modelling crosstalk as the loss in performance of hydraulic actuators caused by the pressure fluctuations in the hydraulic circuit. In Section 2.2, a system level model is developed in Simscape Fluids of

a typical hydraulic testing laboratory setup to capture the pressure and flow dynamics at the HPU and at the loadframes. The aim of this model is to analyze crosstalk in multi-actuator systems driven by a single pump. The laboratory comprises of 2 loadframes that are powered by a single HPU and pipeline that connects them. The loadframes, pipeline and pump model are first developed at the component or subsystem level and validated with experimental data. These subsystems are then assembled together to create a hydraulics laboratory model. A baseline test setup is created to measure crosstalk, the crosstalk measuring parameters are defined and the results are discussed in Section 2.3. The results are interpreted and discussed in Section 2.4 and the contributions of this chapter and opportunities for future work are discussed in Section 2.5.

2.2 System Level Model

2.2.1 System Description

In this section, a model of a hydraulic testing lab is developed with the aim of capturing the pressure and flow dynamics at the pump and the loadframes as well as the control tracking performance of loadframes due to crosstalk. The system modelled in this chapter is based on a simple lab setup at MTS Systems comprising of an HPU, two loadframes and hydraulic pipeline system (Figure 2.4)

Figure 2.4 MTS Lab setup: A materials testing lab with three loadframes connected a hardline that run along the wall connecting them to the pump in the far corner of the room (Figure 2.5)

Figure 2.5 Hydraulic Power Unit : The pump unit in the corner of the test lab that powers the loadframes in Figure 2.4

This setup is schematically represented in Figure 2.6. The pipeline system includes hardlines running along the walls of the lab system with a pressure and return flow line to both loadframes. The HPU is positioned in the corner of the lab at a distance from the loadframes and is connected to the rigid pressure and return lines using short lengths of flexible hose. The loadframes are connected to this hardline using flexible hoses as well.

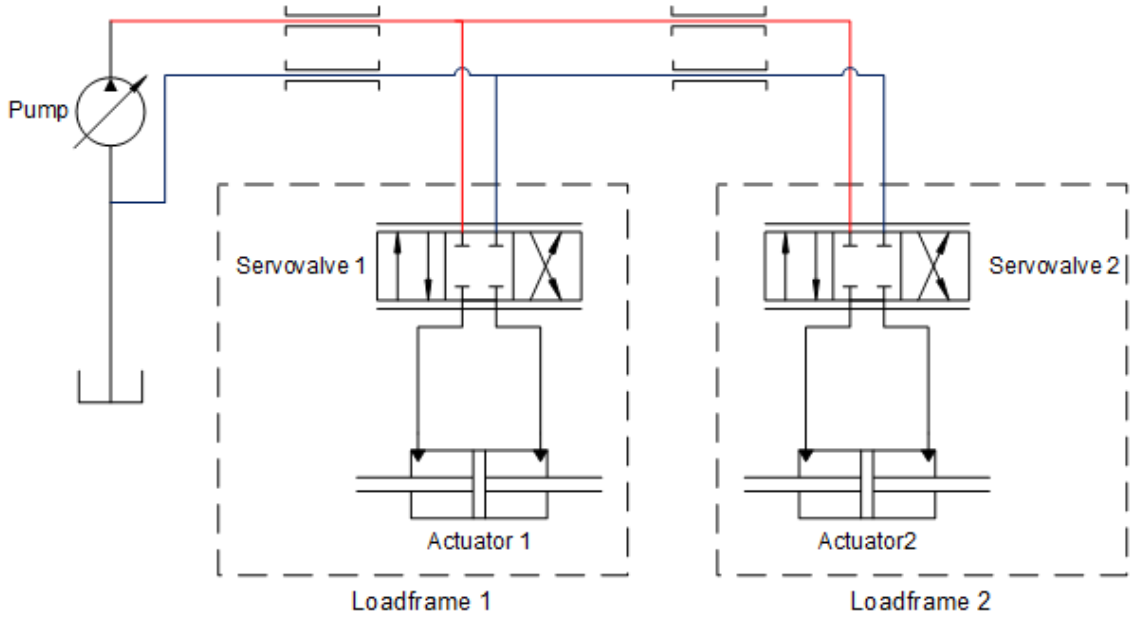

Figure 2.6 Schematic of Hydraulic Lab Setup

The specifications of the HPU, loadframes and hardlines are tabulated in Table 2.1. The loadframe specifications are based on MTS Landmark Loadframes [3], that are used generally for material testing applications. The pump specifications are based on MTS 515.30 HPUs [30], which is a 30gpm pump.

Table 2.1 Parameters of Hydraulic Lab Setup

Parameter	Value
HPU	
Model	515.30 [30]
Flow Rating	1.84 $x10^{-3} m^3/s$ (30gpm)
Operating Pressure	20.67MPa (3000psi)
Internal Diameter of Hose at pump outlet	31.8 mm (1.25in)
Length of Hose at pump outlet	1.5m
Loadframe	
Mass of Piston Rod	23.2 kg
Area of Piston Hub	5.148 $x10^{-4}$ m^2
Maximum stroke	167.6 mm (6.6in)
Servovalve Flow rating (MTS 252.25) [31]	9.46$x10^{-4}$ m^3/s (15gpm) @ 6.89 MPa (1000psi)
Maximum Area of opening of Servovalve	3.56 x 10^{-4} m^2
Length of Hydraulic hardline from Pump to Loadframe1 (Including hoses)	5m
Hardline	
Length of Hydraulic hardline from Loadframe1 to Loadframe 2	5m
Internal Diameter of Hydraulic hardline	25.4mm (1”)
Oil Properties (Exon Mobil DTE 25)	
Density	880 kg/m^3

The model for the system was developed in Simscape Fluids comprising of three major component models – pump model, loadframe model and pipeline model. In section 2.2.2, these component models are developed and validated individually and then combined to model the system layout described in Figure 2.6, with the pump model connected to each loadframe using the pipeline line model. The pump model captures the pressure and flow characteristics of the HPU at the pump outlet. The loadframe model captures the pressure dynamics at the loadframe as well as the position tracking performance of the actuator. The hardline model captures the fluid transients and the pressure ripple along the pipeline that connects the loadframes to the HPU. Finally, the solver configuration and parameters are explored and defined.

2.2.2 Component Models

2.2.2.1 Pump model – PID controlled Flow Source

In a hydraulic system, the pump acts as the source of flow and when combined with pressure compensation control or a relief valve, maintains the desired system pressure. It provides flow to each actuator in the system, in order for it to follow the commanded signal. It also fills the precharged accumulators with hydraulic fluid in the initial stages, which assist in providing instantaneous flow to individual loadframes during their operation. The system under study, utilizes a variable displacement pump with pressure control or a ‘Pressure Compensated Variable Displacement Pump’ (PCVDP), which senses the pressure at the outlet of the pump and adjusts the flow rate accordingly. The pressure at the outlet of a pump due to variation in pump flow rate as it meets the flow demand of the system is seen to respond like an underdamped second order system [15–17]. This allows one to characterize the pump response to a change in flow in terms of the rise time, settling time and peak value of the pressure fluctuations at the pump outlet.

For modelling the pressure dynamics of the system in the hardline and at the loadframes, the flow rate variation and the pressure response at the pump outlet are the required outputs of the pump model. The internal pressure dynamics in the pump, in the control pistons and the control valves can be neglected. This allows us to simplify the pump model

and treat it as a flow source controlled by a PID controller as seen in Figure 2.7. A PID Controller is a second order system, with the proportional, integral, and derivative gains being the values that can be tuned to match the rise time, settling time and peak overshoot in pressure seen in the pump response. The Simscape block 'Hydraulic Flow Rate Source' (MATLAB) [33] is used to command the flow at the outlet of the pump. Effectively, it sets the flow rate at a node, based on the pressure measured at the outlet, similar to the principle of operation of a PCVDP, which varies its swashplate angle and therefore flow rate based on the pressure sensed at the outlet.

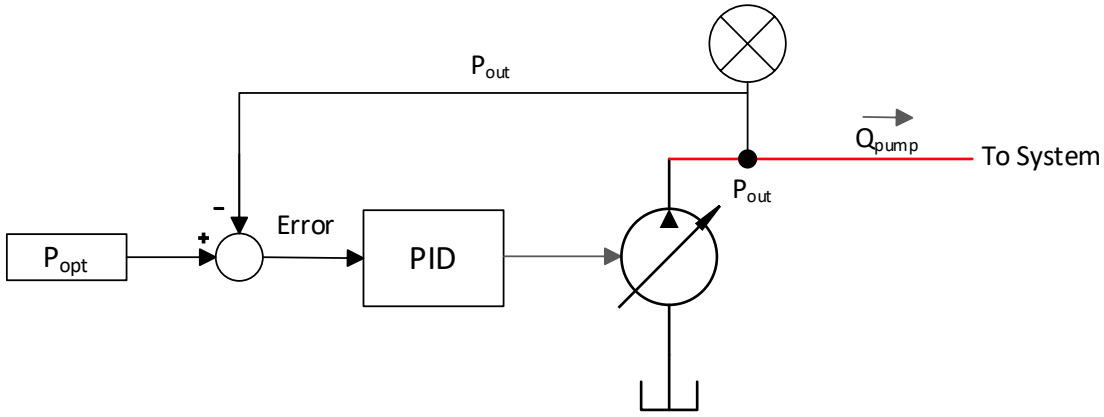

Figure 2.7 Pump Model (PID Controlled flow source)

In the model, pressure is measured at the outlet of the pump P_{out} and compared to the desired operating pressure of the system P_{opt}. The error, or the difference in pressure between the measured value and P_{opt}, is the input for the controller. The gains of the controller are tuned to match the response characteristics of the Pressure controller variable displacement pump using the Ziegler-Nichols Method [34]. In this method, the integral and differential gains of the controller are set to zero. The proportional gain is then increased until the system output is seen to have stable oscillations. The integral and differential gains are then set based on the desired behavior of the system.

2.2.2.1.1 Tuning of simplified pump model

The pressure dynamics at the pump outlet in response to variation in flow rate demanded by the system, is the key output of the pump model. In order to capture the pressure response characteristics of the pump under study, a simple hydraulic circuit with a switching valve, a PCVDP (Model: Rexroth AA 10VSO[11]), pressure transducer and hydraulic hoses was set up at MTS systems as per Figure 2.8 to collect experimental data. The pump is a PCVDP with a maximum flow rate of 30GPM [30]. The pressure transducer was installed at the outlet of pump with a flexible hose at a distance of 1m to record the pressure data. A switching valve (2-way,2 position) was connected to the pump using a flexible hose of 5m length. The flow through the switching valve was connected using a return line, back to the reservoir of the pump. The switching valve in this circuit, acts a variable orifice. The area of flow passage through the valve, can be set using the command voltage.

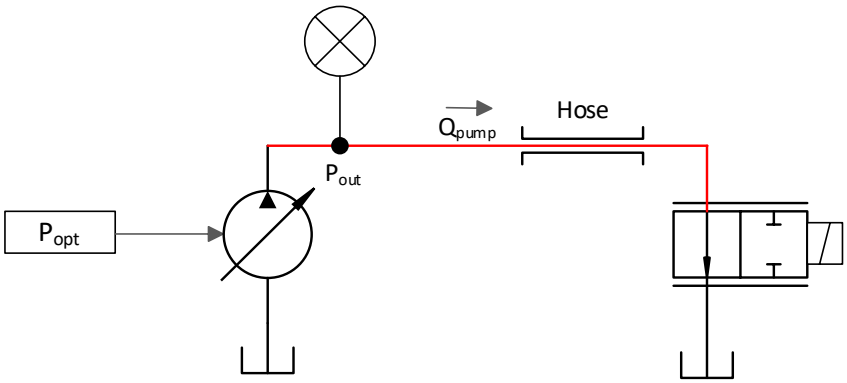

Figure 2.8 Lab setup for Pump Model validation

The system pressure was set at 20.67MPa (3000psi) (standard system pressure at MTS Systems). The maximum area of opening of the valve was 2.57cm^2. The valve was given step input commands in increments for 10% of maximum spool displacement within the valve. This results in a step change in the area of opening in the wave permitting more flow through it. The pressure in the system drops and the PCVDP responds by increasing

the flow rate to maintain system pressure. The pressure dynamics at the pump outlet were recorded using the pressure transducer at the pump outlet, as a response to the commanded step inputs to the servovalve.

A model was created in Simscape for the lab setup in Figure 2.8 using the PID controlled flow source as the pump. Flow through the valve at each time was calculated using the orifice equation:

$$Q = C_d A \sqrt{\frac{2\Delta P}{\rho}} \qquad \text{Eq. 2.2.1}$$

Where Q is the flow rate, $C_d$is the coefficient of flow through the orifice, which is assumed to be 0.6, ρ is the density of the hydraulic fluid and ΔP is the pressure differential across the orifice.

The pressure dynamics in the hose were modelled using the segmented pipeline model in section 2.2.2.2. The gains of the controller in the pump modelled were then tuned using the Ziegler-Nichols Method such that the pressure response matched the recorded experimental values at MTS closely. With the integral and differential gains of the controller set to zero, the proportional gain was increased until the settling time of the pressure at the pump outlet matched the settling time seen experimentally. Integral gain was then increased to reduce the steady state error to zero and to control the frequency of oscillation. Introduction of differential gain increased the frequency of pressure oscillation and reduced the magnitude significantly and best results were obtained with differential gain set to zero.

2.2.2.1.2 Pump model validation

The pump model was validated using the experimental setup described by the schematic diagram in Figure 2.8. Test cases were performed by commanding step changes of 10% increments of valve opening from 20% to 90%.

Figure 2.9 and Figure 2.10 compare the experimental data and model results for the pump response to the valve opening of 40% and 90% respectively. At 5 seconds, the command signal opens the valve to the commanded area of opening. For 40% valve opening, the pressure at the pump outlet is seen to oscillate with a peak value of 3060 psi and a minimum of 2945 psi (Figure 2.9). The pressure response has a setting time of 0.9 seconds with a frequency of approximately 5Hz. The pressure oscillations in the model are overlayed on the experimental findings and are seen to closely match within 10 psi. settling time is 0.9 seconds with a frequency of oscillation of 4.5Hz. Similar tracking is seen in the case of 90% valve area opening.

The pressure response recorded experimentally and in the model for 40% valve opening is shown in Figure 2.9 and for 90% valve opening is shown in Figure 2.10. The pressure dynamics at the pump outlet in the model (in red) is seen to closely match the experimental data (in black) in terms of settling time. The frequency of oscillation in the model is seen to be slightly slower than experimental results with a 10% difference, which is considered reasonably accurate for the purposes of this study.

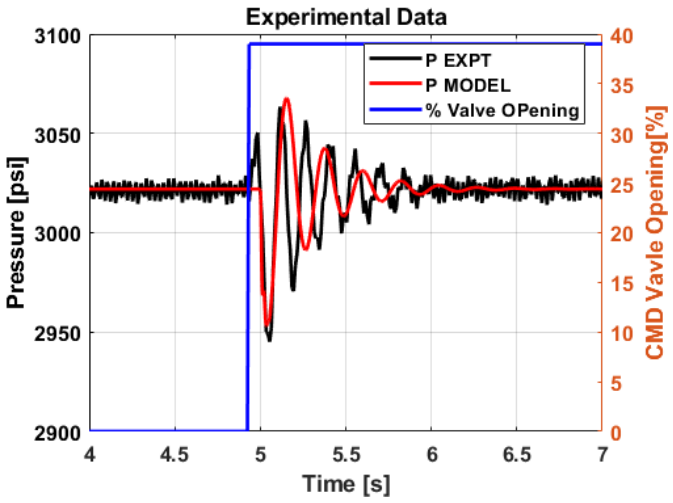

Figure 2.9 Pressure dynamics at pump outlet for 40% valve opening

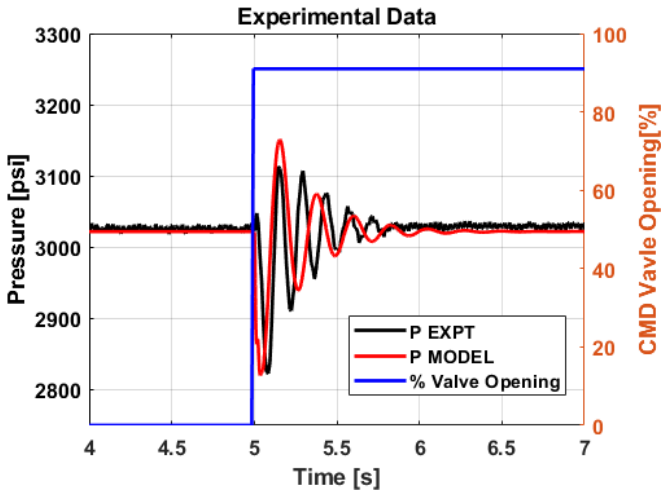

Figure 2.10 Pressure dynamics at pump outlet for 90% valve opening

The pump model controlled by the PID is considered reasonably accurate in capturing the response characteristics of a PCVDP. The PID controller gains for the pump model set using the Zeigler Nichols Method are tabulated in Table 2.2.

Table 2.2 PID Controller gains for Pump Model

Controller Gain	Value
Proportional (P)	4.8e-10
Integral (I)	1e-8
Differential (D)	0

2.2.2.2 Segmented Pipeline Model

The pressure and flow dynamics in the hardline is modelled as a lumped parameter model by dividing the pipeline into elements that each have hydraulic capacitance, resistance, and inertia[22]. This is achieved using the segmented pipeline model in Simscape Fluids. The length of the pipeline is divided into a calculated number of segments. Figure 2.11 shows a schematic diagram of a segmented pipeline where N_1, N_2, N_3 and N_n are nodes along the length of the pipeline that each have resistance, inertia, and a constant volume.

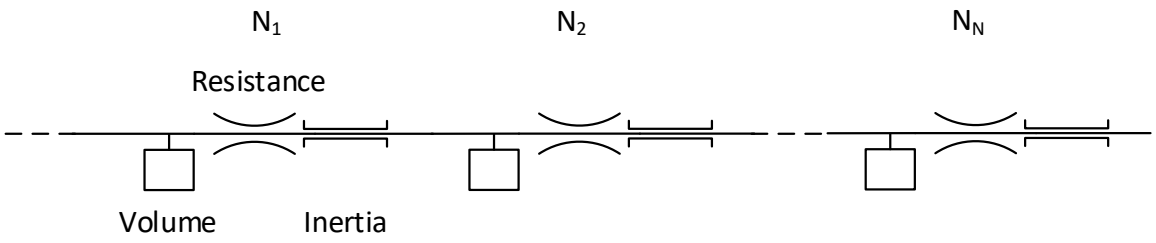

Figure 2.11 Segmented Pipeline Schematic Diagram

The number of segments for a given length of hardline is calculated based on the characteristic frequency of the system which would be the command signal. Streeter found that the maximum length permissible of each segment is 15% of the characteristic length [35]which is calculated as –

$$\lambda = \frac{c}{f} \qquad \text{Eq. 2.2.2}$$

Where λ is the characteristic length, c is the speed of sound in the fluid and f is the characteristic frequency.

The minimum number of segments is calculated as –

$$N = \frac{L}{0.15 * \lambda} \qquad \text{Eq. 2.2.3}$$

Where N is the number of segments and L is the total length of the pipeline.

The change in flow through each segment due to the pressure differential across it is calculated as

$$\frac{dQ}{dt} = \frac{\Delta P . A}{\rho L} \qquad \text{Eq. 2.2.4}$$

Where ΔP is the pressure differential between neighboring nodes, ρ is the density of the hydraulic fluid, L is the length of the pipe segment, A is the cross-sectional area of the segment and Q is the flow rate through the pipe.

Pressure loss due to friction is computed with the Darcy equation, in which losses are proportional to the flow regime-dependable friction factor and the square of the flow rate. The friction factor in turbulent regime is determined with the Haaland approximation [36]. The friction factor during transition from laminar to turbulent regimes is determined with the linear interpolation between extreme points of the regimes. As a result of these assumptions, the tube is simulated according to the following equations:

$$P = f_c \left(\frac{L}{D}\right)\left(\frac{\rho}{2A^2}\right) Q \qquad \text{Eq. 2.2.5}$$

Where, P is the pressure loss along the pipe due to friction, Q is the flow rate through the pipe, L is the length of the pipe segment, A is the cross-sectional area of the segment, D is the diameter of the pipeline, ρ is the density of the hydraulic fluid and $f$is the friction factor. f_c is calculated for different flow regimes as follows (White, F.M.) [1]

$$f = \begin{cases} 64/Re & for\ Re \leq\ Re_L \\ f_L + \dfrac{f_T - f_L}{Re_T - Re_L}(Re - Re_L) & for\ Re_L < Re < Re_T \\ \dfrac{1}{\left(-1.8log_{10}\left(\dfrac{6.9}{Re} + \left(\dfrac{r/D}{3.7}\right)^{1.11}\right)\right)^2} & for\ Re \geq Re_T \end{cases} \qquad \text{Eq. 2.2.6}$$

Where Re is the Reynolds, Re_T is the minimum Reynolds number for turbulent flow, Re_L is the maximum Reynolds Number for laminar flow, $f_L$is friction factor at the laminar border, f_T is friction factor at the turbulent border.

The pressure dynamics at each node in the segmented pipeline is calculated from the definition of the bulk modulus –

$$\frac{dP}{dt} = \frac{\beta}{V} Q \qquad \text{Eq. 2.2.7}$$

Where, β is the bulk modulus of the hydraulic fluid and V is the volume of the hydraulic pipeline.

The flow rates into the pipe in the first segment in the pipeline – connected to the HPU – is driven by the controller of the Pump model. The last segment in the pipeline is connected

to the servovalve of a loadframe. Since the valve is modelled as a variable orifice, the flow through the last segment is calculated using the orifice equation.

2.2.2.3 Accumulator Model

An accumulator is a hydraulic energy storage device that is used to reduce pulsation from a pump or a motor and supplying an excess flow demanded by system [1].The most common style of accumulator used are bladder style accumulators as seen in Figure 2.12 and Figure 2.13. They comprise of a precharged gas chamber, and a fluid chamber separated by a bladder. When the fluid pressure at the outlet of the accumulator exceeds the precharged pressure, fluid enters the accumulator and forms stored hydraulic energy (Figure 2.13 – C). The pressure in the gas and the oil in the accumulator are assumed to be in a state of quasi-equilibrium, with the gas pressure equal to the pressure of the oil at all times. When the pressure drops, the bladder expands discharging fluid into the system (Figure 2.13 – D).

Figure 2.12 Commercial Bladder Style Accumulators [37]

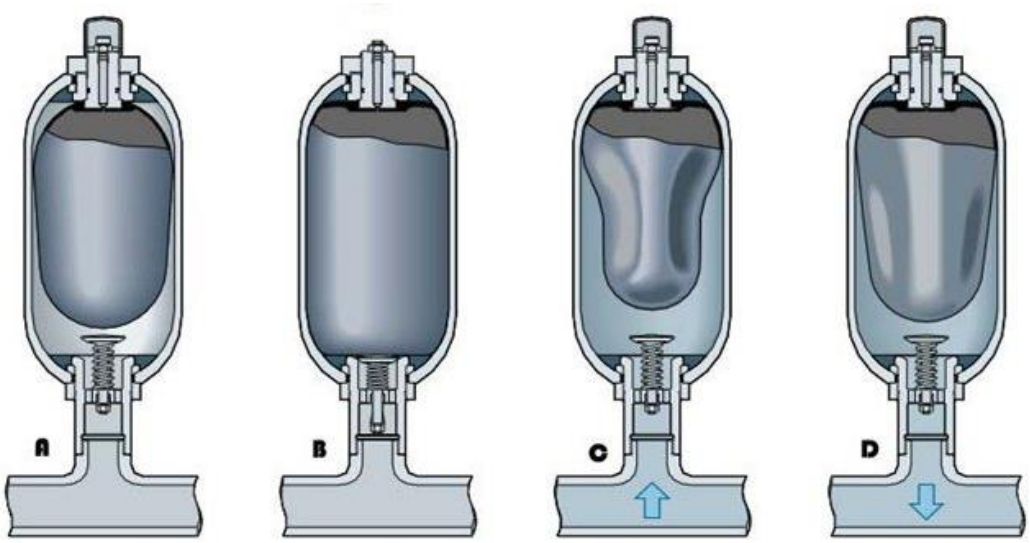

Figure 2.13 Bladder Style Accumulator [38]

The pressure-volume relation for the gas in the chamber is modelled by the polytropic equation $PV^k = constant$. Applying this relationship to the precharged state of the gas and the operating condition, where the pressure is balanced at the separator in the accumulator we get,

$$P_{gas,opt}(V_T - V_F)^k = P_{pr}{V_T}^k \qquad \text{Eq. 2.2.8}$$

Where $P_{gas,opt}$ is the pressure of the gas at current state which would be equal to the pressure at the outlet, $P_{pr}$is the precharge pressure, V_T is the total chamber volume and V_F is the oil volume that has entered the accumulator. A schematic representation of this is seen in Figure 2.14.

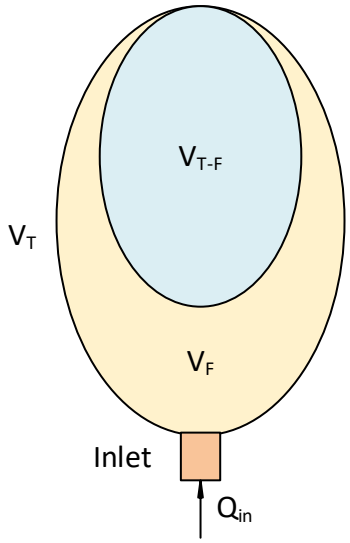

Figure 2.14 Schematic representation of the volumes in the accumulator

The flow rate into the accumulator is equal to change of the fluid volume V_F.

$$Q_{in} = \frac{dV_F}{dt} \qquad \text{Eq. 2.2.9}$$

The initial fluid volume is calculated using Eq. 2.2.8 with $P_{gas,opt}$ equal to the initial system pressure.

2.2.2.4 Loadframe Model

A loadframe comprises of an actuator, a servovalve, a controller and a rigid frame on which the components are mounted as seen in Figure 2.1. There are many variations of loadframes based on actuator sizing, load capacity, flow capacity of servovalve and load rating of the frame. In this study, the specifications for the 'Landmark 370.10' loadframes by MTS Systems have been used to validate the loadframe model. These loadframes are

rated for forces up to 100kN and are primarily used for material testing applications such as high cycle fatigue tests, low cycle fatigue tests, tensile tests, and impact tests. The loadframe model comprises of the actuator model and the servovalve model, which controls the flow to the actuator.

2.2.2.4.1 Servovalve Model

The servovalve is used to direct flow to the actuator. It is a proportional control valve that governs the flow paths through it by the precise control of an internal spool. The spool position is proportional to an input voltage. The position also determines the flow rate through the valve.

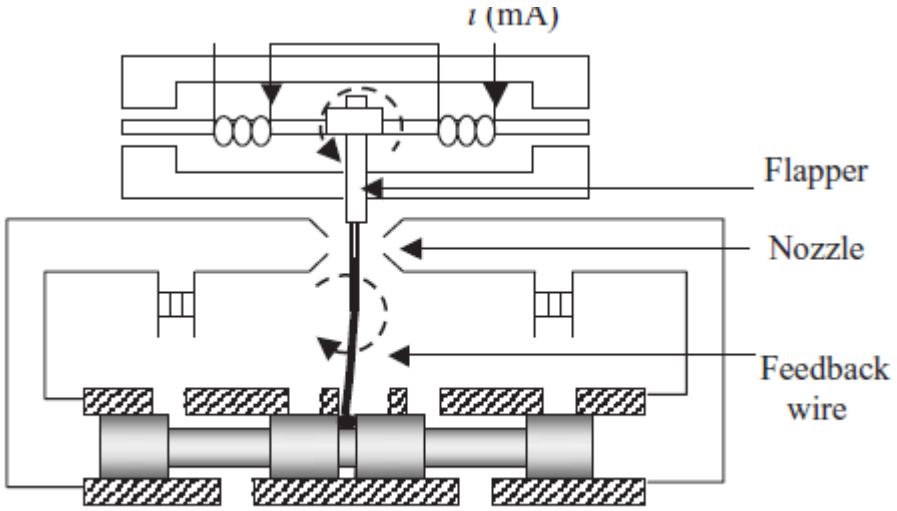

Figure 2.15 Schematic representation of a Servovalve [1]

Considerable research has been conducted to capture the internal dynamics of a directional flow control valve. Ledvon and Hruzik, developed a mathematical model of a proportional directional flow control valve by modelling the motion of the spool accounting for spring force, friction and inertia and the hard stop properties in the valve with good correlation between experimental and modelling results[27]. Xu and Ding expand on this work by applying a similar model to a three-stage valve additionally accounting for delay

in response of the servovalve[40]. Tordal and Klausen developed a black box model of a directional control valve using system identification capable of capturing the flow response of a servovalve (Model: Brevini HPV 41) to varying inputs of spool position [41]. The servovalves used in this study ate MTS 252.25 valves rated for 9.47e-4 m^3/s (15gpm) flow at 6.78MPa (1000psi). The roll off frequency for these valves is 170Hz which is significantly higher than the characteristic frequency of the pressure fluctuations modelled in this thesis. With this in mind, a valve is modelled using a gray box approach in this study.

In the model, the servovalve is modeled as a 4-way directional valve. The spool position is controlled by a command signal from a PID controller that takes the error of position of the actuator as the input. Through the servovalve there are four flow paths, namely P_A, P_B, T_A and T_B. As seen in Figure 2.16 Flow from servovalve to actuator [42] , in position 1, path P_A and T_B are maximally open. In position 2, path P_B and T_A are maximally open. The flow through the servovalve is modelled as flow through 4 variable orifices, one for each path of flow, as see in Figure 2.17. The servovalve is treated as critically lapped, with the direction of flow switching from position 1 to 2 as the spool passes the center of its stroke. The servovalve controller dictates the spool position which in turn determines the percentage of opening of each of these ports.

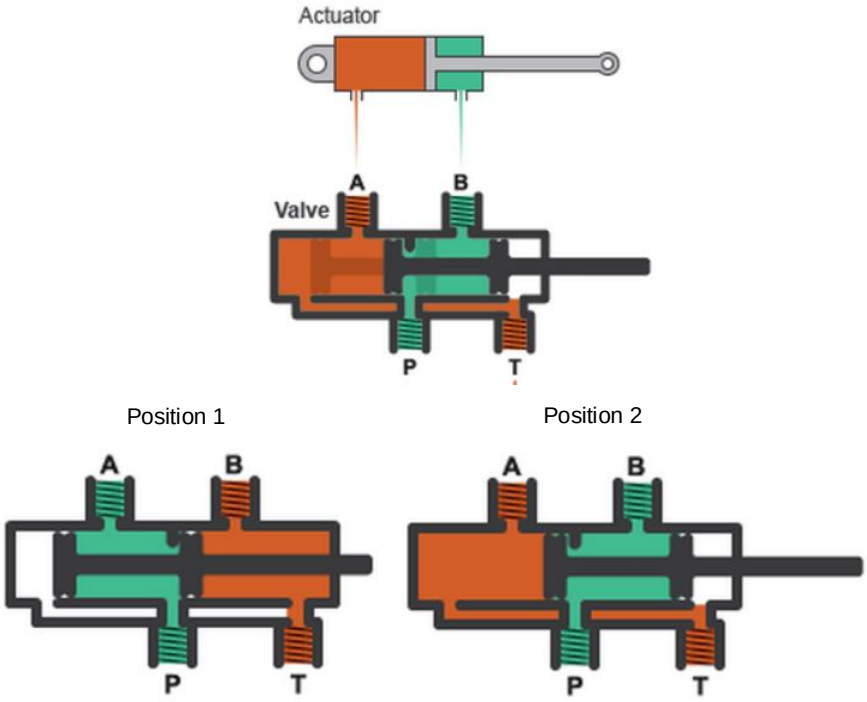

Figure 2.16 Flow from servovalve to actuator [43]

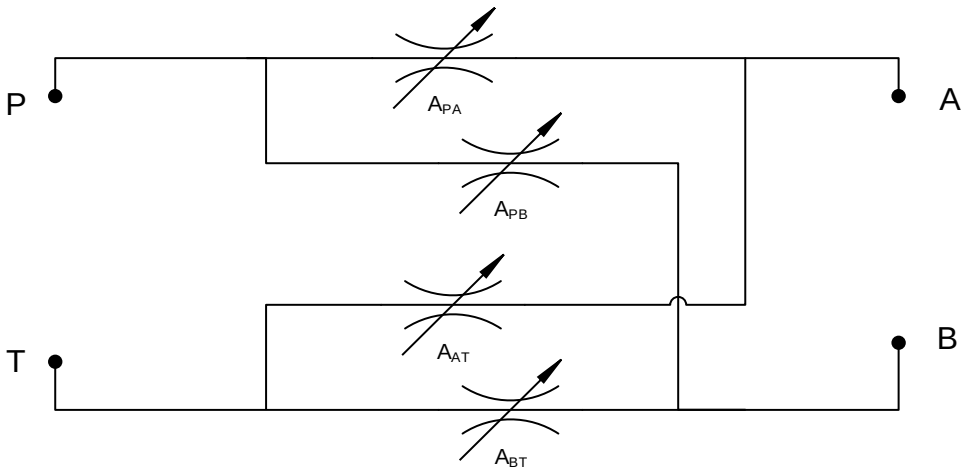

Figure 2.17 Servovalve flow paths

The area of the orifice for any spool position is calculated as –

$$A_{AT} = \frac{x_{AT}}{x_{AT,MAX}} A_{AT,MAX} \qquad \text{Eq. 2.2.10}$$

Where, $A_{AT}$is the area of the orifice, x_{AT} is the spool position in the valve, $x_{AT,MAX}$ is the spool position corresponding to maximum area of the orifice (in this case Position 2, Figure 2.16) and $A_{AT,MAX}$ is the maximum area of the orifice that can be calculated from the orifice equation–

$$A_{AT,MAX} = \frac{Q_{rated}}{C_d} \sqrt{\frac{\rho}{2\Delta P_{rated}}} \qquad \text{Eq. 2.2.11}$$

2.2.2.4.2 Actuator Model

The actuator is double-ended, which implies that the piston area is equal on both sides of the hub as seen in Figure 2.18. The displacement is considered to be 0 at the center of the stroke of the piston.

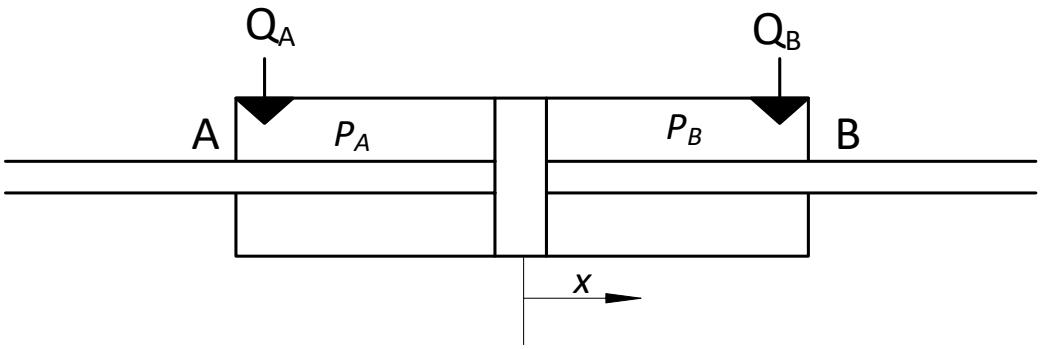

Figure 2.18 Actuator Model

The forces on the pistons hub, the flow rate into the ports of the actuator and the position of the actuator are modelled using the Simscape block – 'Double-Acting Hydraulic Cylinder' which is governed by the following equations

$$m\ddot{x} = A_A P_A - A_B P_B \quad \text{Eq. 2.2.12}$$

$$Q_A = A_A . v \quad \text{Eq. 2.2.13}$$

$$Q_B = A_B . v \quad \text{Eq. 2.2.14}$$

$$\frac{dx}{dt} = v \quad \text{Eq. 2.2.15}$$

The position of the piston in the actuator is controlled by a servovalve using a PID controller as seen in Figure 2.19. The position of the piston rod is measured using a LVDT that is affixed to the end of the piston rod. The error for the position of the piston of the actuator is calculated by comparing the position as measured by the LVDT and the command signal. This error forms the input for the PID controller. The controller output controls the spool position in the control valve. This varies the flow path (determined by spool position, Figure 2.16) and flow rate (area of the opening in the valve) through the valve. The piston moves along its stroke until the error in its position is driven to zero.

2.2.2.4.3 Loadframe Controller Tuning

The response of an actuator depends on the servovalve flow rating, the dimensions of the servovalve ports, the dimensions and specifications of the actuator, and the tuning of the controller gains. Using the lab setup described by Figure 2.19, experimental data was obtained for the position response of the actuator. A step command of 2cm was given to a Landmark Model loadframe, which was powered by an HPU connected to it by 5m of hard line. A 15gpm servovalve is used to control the flow to the actuator, as standard for this configuration of loadframe. The position data is tracked using an LVDT that is fastened to the piston rod of the actuator.

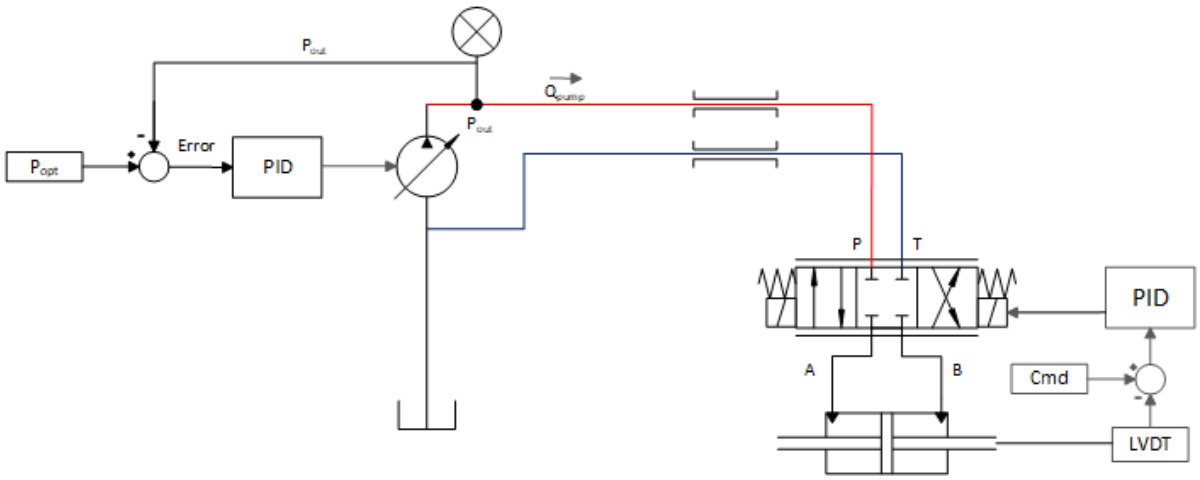

Figure 2.19 Tuning Loadframe Model

A model was setup in Simscape based on the schematic in Figure 2.19. The block diagram of the Simscape model can be found in Appendix A - Figure A. 1. The validated pump model from Section 2.2.2.1 was used as a flow source and the segmented pipeline model was used to model the hardline connecting the loadframe to the HPU.

The actuator was modelled using the Simscape block - 'Double-Acting Hydraulic Cylinder'. Physical properties of the loadframe such as mass and area of piston, servovalve flow

rating, stroke of actuator were based on the Landmark System and obtained from the MTS Landmark Technical Datasheet [3] and are tabulated in Table 2.3. The position of the piston is modelled using actuator model described in Section 2.2.2.4.2.

Table 2.3 Tuning of Loadframe Model Parameters

Property	**Value**
Mass of Piston	23.2 kg
Area of Piston Hub	5.148 $x10^{-4}$ m^2
Servovalve Flow rating	9.46$x10^{-4}$ m^3/s (15gpm) @ 6.89 MPa (1000psi)
Length of Hydraulic hardline from Pump to Loadframe	5m
Internal Diameter of Hydraulic hardline from Pump to Loadframe	25.4mm (1”)
System Pressure	20.67MPa (3000psi)

The PID gains of the servo valve controller in the model were tuned using the Zeigler-Nichols method [44] to closely match the step response as recorded experimentally. With the integral and differential gains of the controller set to zero, the proportional gain was increased until the settling time of actuator model matched the settling time seen experimentally. Integral gain was then increased to reduce the steady state error to zero. For this configuration of loadframe and servovalve, the PID controller gains are tabulated in Table 2.4.

Table 2.4 PID Controller gains for Loadframe Model

Controller Gain	Value
Proportional (P)	1e-2
Integral (I)	1e-5
Differential (D)	0

2.2.2.4.4 Loadframe Model Tuning

The loadframe model is validated using the experimental setup in Figure 2.19. The gains of the controller are tuned to closely match the displacement seen experimentally. The experimental data shows that the actuator has a rise time of 0.11s. Rise time is defined as the time taken for the response of the system to go from 10% to 90% of its final value [45]. The settling time defined as the time taken for the response to reach and stay within 2% of its final value [45] is measured as 0.13s. The response of the actuator model is seen to match these values within 0.5% or 0.1ms and with zero steady state error as seen in Figure 2.20.

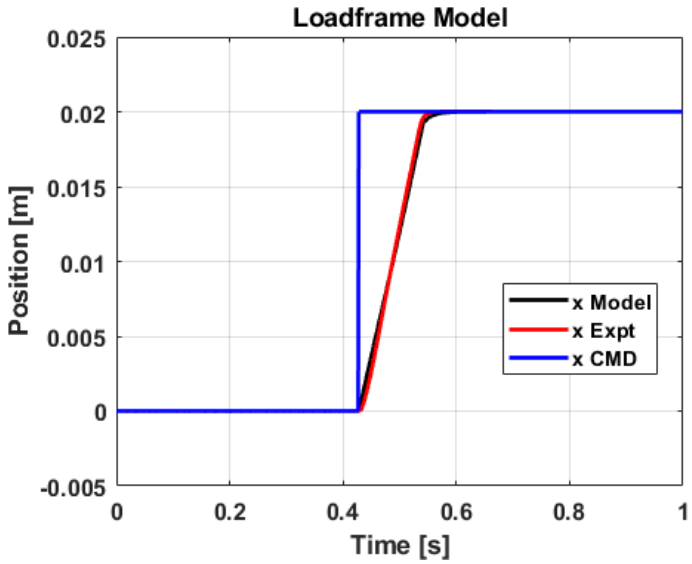

Figure 2.20 Position tracking of actuator (Model vs Experimental)

2.2.2.5 System model

The system described in Figure 2.6 is modelled by combining the individually validated models of the pump, loadframes and pipeline. The model is schematically represented in Figure 2.21. The Simscape model is documented in Appendix A for reference. The model contains a PCVDP pump (modelled as PID controlled flow source), two loadframes that are powered by the pump and a length of pipeline connected them which is modelled using the segmented pipeline model (Eq. 2.2.3 - Eq. 2.2.7).

This model is used to simulate a wide array of combinations of tests on the loadframes and specifically how the input to one loadframe influences the control performance of the other loadframe. The model records the pressure and flow dynamics at the pump and at the loadframes as well as the position response of the loadframe to the command signal.

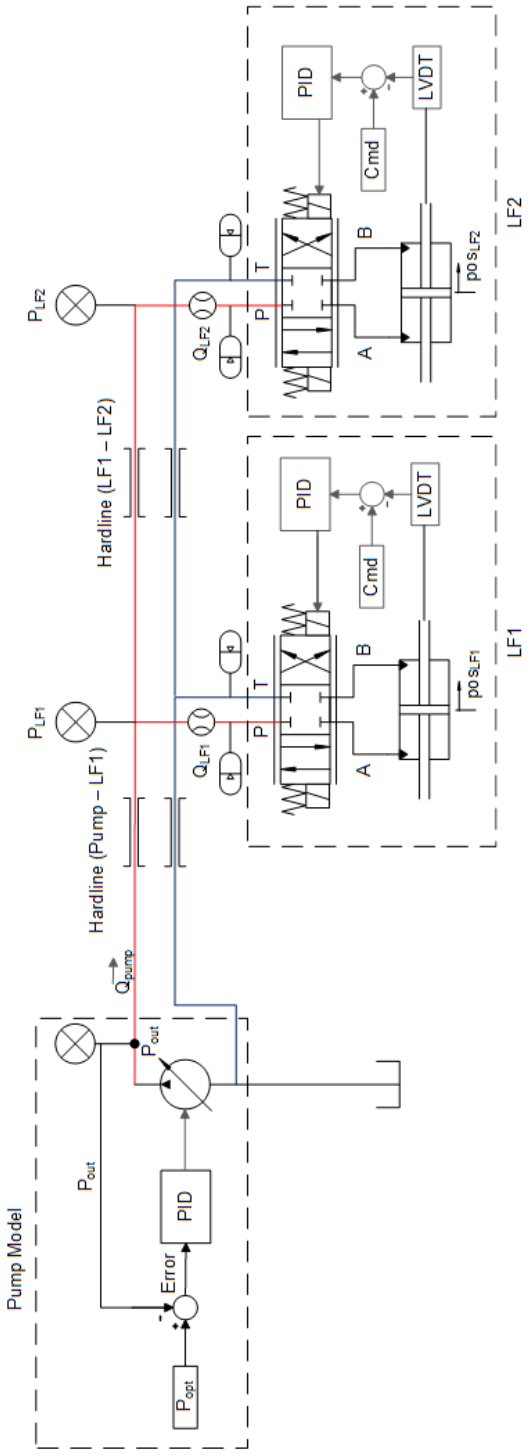

Figure 2.21 Schematic diagram of model for baseline test setup

2.2.2.6 Baseline System Parameters

The system model developed in Section 2.2.2.5 is used to create a baseline system to measure crosstalk in the current configuration of the system. The pump model is used to provide flow to two loadframes that are given different position command signals. The specifications and sizing of all system components are chosen based on standard 'Landmark' loadframes and MTS 515.30 HPUs [30] manufactured by MTS Systems and are tabulated in Table 2.1. Loadframe 1 and loadframe 2 are identical in specification and performance. Loadframe 1 (LF1) is used as a 'disturbance generator' and is given a step displacement command. The disturbance generated by loadframe 1, seen as pressure fluctuations in the hardline, impacts the tracking performance of loadframe 2. Loadframe 2 itself is following a sinusoidal position command and generates a pressure ripple in the hardline, at a frequency equal to the frequency of the commanded sinusoid. Loadframe 1 is connected to the HPU by 8m of hardline. The length of the hardline between loadframe 1 and 2 is 5m.

The following are the measures of crosstalk chosen in the simulation of the baseline system –

1. The magnitude of pressure ripple (amplitude of pressure wave) at LF2.
2. The magnitude of pressure ripple at HPU due to step command at LF1
3. The error in position tracking in loadframe2 due to flow demand of LF1

The results of simulation of the baseline system are then used as reference in the next chapter to measure the effectiveness of the techniques employed for the reduction of crosstalk.

The maximum flow capacity of the pump is 1.84 $x10^{-3}m^3/s$ (30gpm) with a leakage of 0.5gpm. Landmark loadframes have a maximum stroke of 167.6mm (6.6in) by design. Both pistons are positioned at the center of their stroke at the beginning of the simulation, and this is considered as the zero position. 1L Accumulators are installed at the

loadframes on the pressure (1L chamber volume, 1000psi precharge) and return lines (1L chamber volume, 50psi precharge pressure). The command signal for loadframe 1 (LF1) is a step displacement of 76.2 mm (3”), which would be the piston rod moving from mid-stroke to the end of its stroke. The command signal for loadframe 2 (LF2) is a sinusoidal wave of 10 Hz and 3 mm amplitude. The model records pressure at the pump and the two frames, flow rates to each loadframe and position tracking of both actuators and calculates the measures of crosstalk mentioned above.

2.2.2.7 Model Solver Configuration

The model is solved using the variable time step solver ‘ode23t’ [46]. Ode23t is a moderately stiff solver, based on the trapezoidal rule and commonly used for the solving of hydraulic models. The solver allows the user to define the allowable relative tolerance – the largest allowable solver error, relative to the size of each state during each time step. If the relative error exceeds the tolerance, the solver reduces the time step size to improve the accuracy of the solver. The absolute tolerance is the maximum acceptable error for each state as the value of the measured state approaches zero. At initialization, the solver sets the absolute tolerance by default as 0.001*(relative tolerance) [46]. As the simulation progresses, the absolute tolerance is resets to the product of maximum value of that state and the relative tolerance.

In the model, the key outputs are the pressure, flow rates and the position tracking. The minimum values of these states that can be recorded accurately experimentally are 6.89kPa (1psi), 6.3x 10^{-7} m^3/s (0.01gpm) and 0.1mm. In the simulations conducted, the maximum value for these states is seen to be 31MPa (4500psi), 0.005 m^3/s (80gpm) and 0.167m (6.6in). A convergence study was conducted on the system model to ensure that this value of relative tolerance gives accurate results. The relative tolerance for the solver is chosen to be 1e-5, which results in the maximum allowable error to be 0.31KPa (0.045psi), 5x10^{-8} m^3/s (8x10^{-4}gpm) and 1.6x10^{-3}mm. The results of this convergence study are documented in Appendix B. The maximum error in the model is smaller than the smallest significant values that can be experimentally recorded and sufficiently accurate

for the study of crosstalk. Increasing the relative error, does help with computational efficiency, speeding up the simulation time but comes at the cost of accuracy. The chosen value for relative tolerance, ensures high accuracy and reasonable simulation speed.

The values of the minimum time step size and maximum time step are set as ‘auto’ and are calculated by the solver based on the relative tolerance value.

2.3 Results

2.3.1 System Model – Baseline test case

The results of the simulation of the baseline system, specifically, the pressure and flow dynamics of the system and its impact on the tracking performance of the loadframes are discussed in this section.

Figure 2.22 shows the position tracking of LF1 (disturbance generator) to the commanded step input. The actuator is initially at mid-stroke (shown as 0m) and at 5 seconds is given a step command of 76.2mm - half of the maximum displacement of the actuator. The actuator travels to the commanded position with zero steady state error and 0.28 seconds settling time which corroborates well with the validated loadframe model in Section 2.2.2.4. Loadframe 2 is tracking a 10Hz, 3mm sinusoidal displacement command for the entire duration of the simulation.

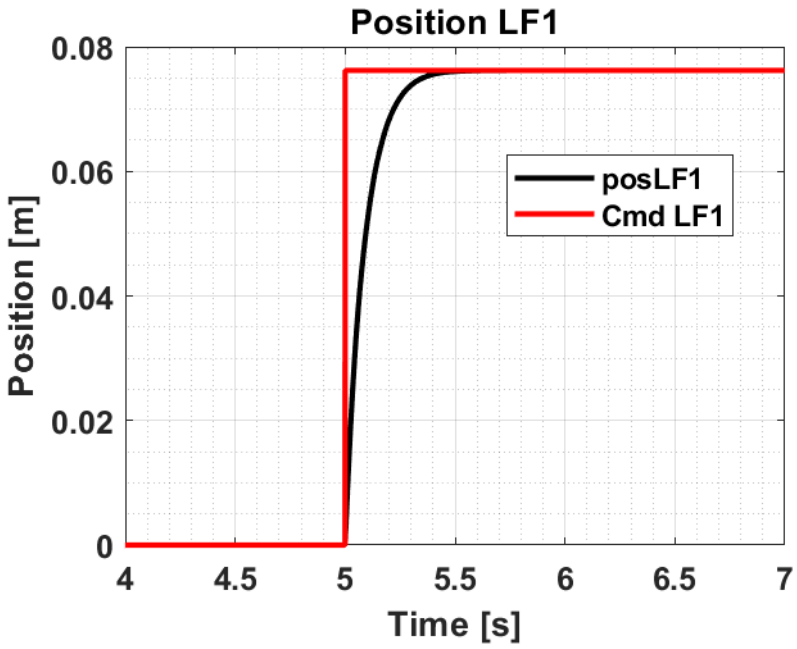

Figure 2.22 Position tracking of Loadframe 1

Figure 2.23 shows the pressure dynamics induced in the hardline at loadframe as a result of the displacement command at LF1 measured at P_{LF1} and P_{OUT} as in Figure 2.21. A constant pressure ripple of amplitude 0.31MPa (45psi) is measured at pump outlet and at loadframe 1 (prior to the step command at loadframe 1) due to the flow demand variation at loadframe 2, as the servovalve spool switches positions to change the direction of motion of the actuator. At 5.1s, the system pressure drops to 15.85MPa (2300psi) as the flow demand at loadframe suddenly increases to track the commanded step change in position. The pump increases the flow rate resulting in an overshoot in system pressure to 26.9MPa (3900psi) at 5.4s. The system reaches steady state in a settling time of 1.51s.

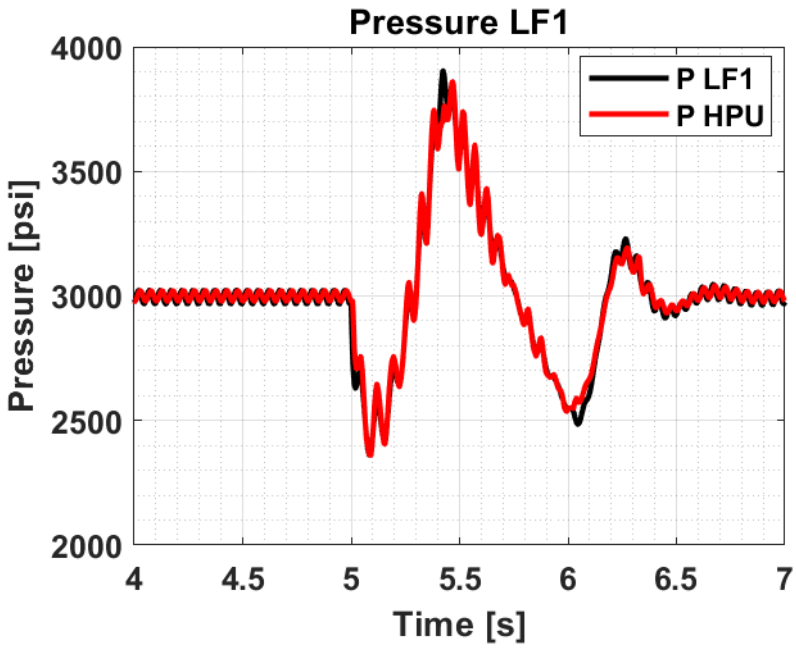

Figure 2.23 Pressure study at Loadframe 1 and HPU

Figure 2.23 shows the pressure dynamics at LF2 and the HPU measured at P_{LF2} and P_{OUT} as in Figure 2.21. Loadframe 2 induces a pressure ripple of magnitude 0.69MPa (100psi) in the hardline. The pressure fluctuations caused by loadframe 1, results in a similar drop to 16.2MPa (2350psi) and overshoot in pressure to 27.2MPa (3950psi) at loadframe 2.

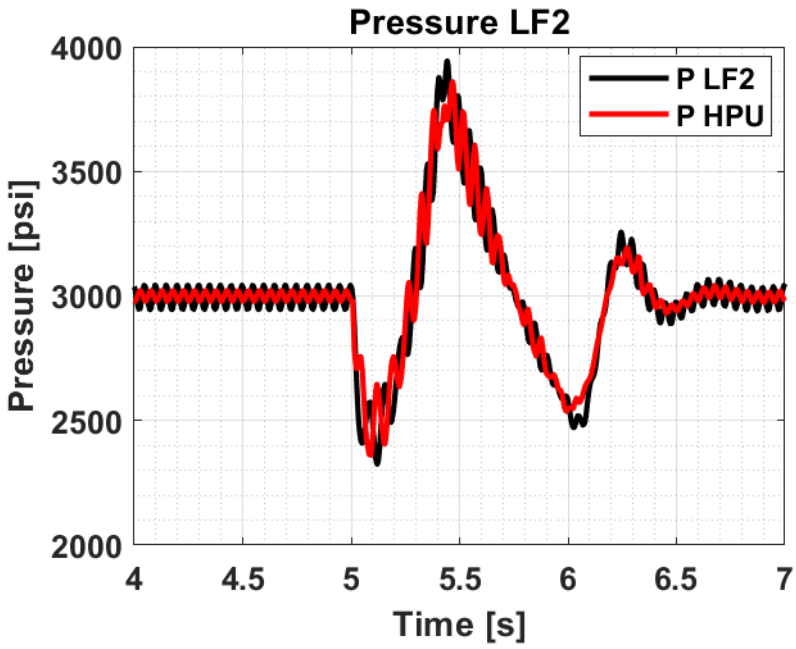

Figure 2.24 Pressure study at Loadframe 2 and HPU

Figure 2.25 shows the flow supplied by the pump and the flow rate through LF1 as measured at Q_{PUMP} and $Q_{LF1.}$ Initially the pump flow rate is seen to fluctuate between $4.29x10^{-4}$ m^3/s (6.8gpm) and 5.67 $x10^{-4}$ m^3/s (9gpm) to provide flow loadframe 2. At 5 seconds, the flow demand at loadframe 1 increases instantaneously to a peak value of 4.8 $x10^{-3}$ m^3/s (78gpm). The flow rate of the pump increases to $1.9x10^{-3}$ m^3/s (30gpm) which is the maximum flow rate of the pump. At 5.5 seconds when the system demand is met, the pressure in the system is at its peak value and sensing the rise in pressure, the pump reduces the flow rate to the minimum value. As the system pressure drops below the operating pressure, the pump increases the flow rate again to increase system pressure and reaches a steady state again, of oscillating between $4.29x10^{-4}$ m^3/s (6.8gpm) and 5.67 $x10^{-4}$ m^3/s (9gpm) as seen prior to the disturbance generated by loadframe 1.

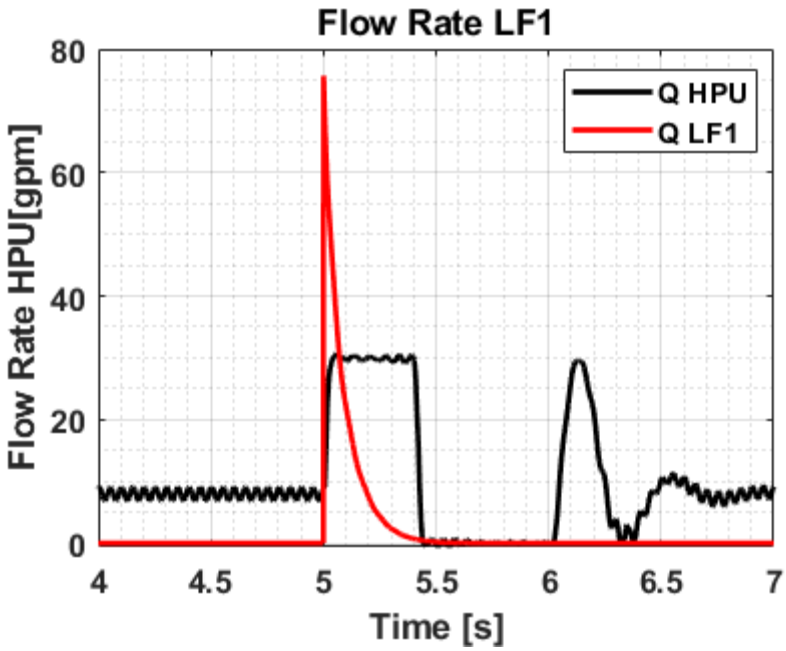

Figure 2.25 Flow rate at Loadframe 1 and HPU

Figure 2.26 shows the flow supplied by the pump and the flow rate through LF2 as measured at Q_{PUMP} and $Q_{LF2.}$ The flow demand of loadframe 2 (at steady state) is seen to vary from 0 to $7.57x10^{-4}$ m^3/s (12gpm) at a frequency of 20Hz, which corresponds to the 10Hz sinusoidal position command. The flow rate to the loadframe is seen to decrease to $7.27x10^{-4}$ m^3/s (11.5gpm) at 5.1s due to the large pressure drop in the hardline due to the step command at loadframe 1. As the system pressure increases and overshoots over the operating pressure (20.67MPa), the flow rate in to loadframe 2 increases to $7.88x10^{-4}$ m^3/s (12.5gpm) at 5.5s.

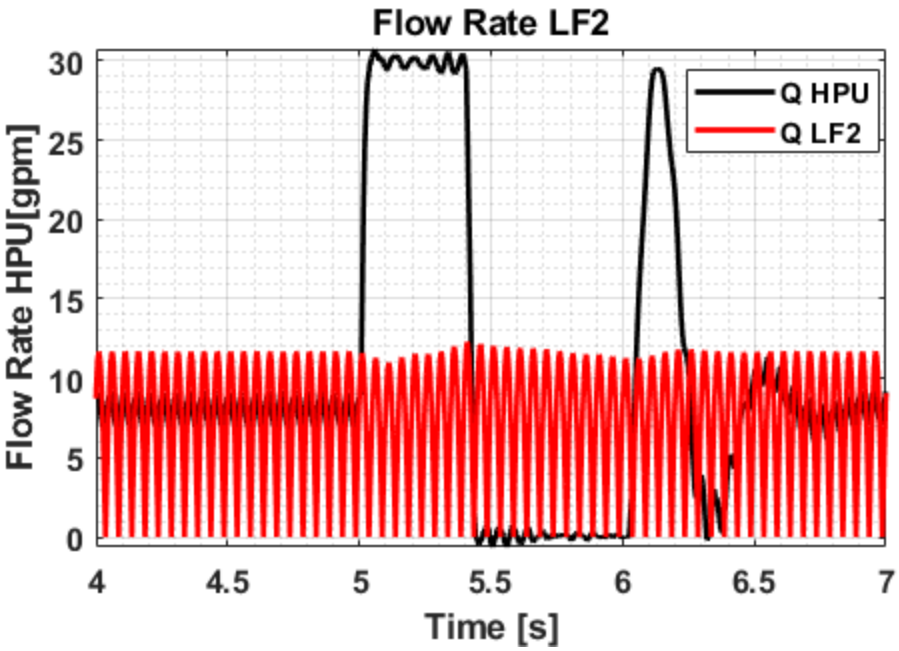

Figure 2.26 Flow rate at Loadframe 2 and HPU

Using a PID Controller without a feedforward or any compensation for sinusoidal positional control of loadframe 2 implies that the amplitude tracked by the actuator will be smaller than the command signal and with some phase lag. To eliminate this error more advanced control strategies have been discussed in 1.1.2.2 [19–21]. In this study, since simple PID control is used, the amplitude tracked by the actuator is seen to be 2.23mm (Figure 2.27). Deviation from this amplitude is used to calculate the error in position tracking.

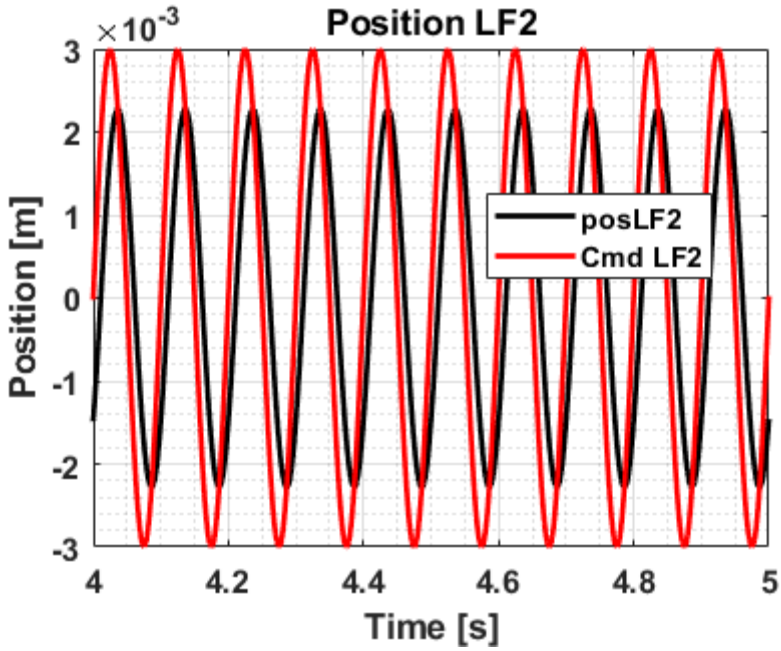

Figure 2.27 Position tracking of loadframe 2

Figure 2.28 shows the error in displacement tracking of loadframe 2 due to the disturbance generated at loadframe 1. The error is as a percentage of the amplitude of the command signal. At 5.2s, loadframe 2 is seen to have a -4.5% error, which shows that as a result of the pressure drop at loadframe 2, caused by the sudden flow demand at loadframe 1, the actuator amplitude reduced by 4.5%. At 5.5s, the error is +4.5%, due to the pressure spike at loadframe 2, caused by the overshoot in pressure due to response of the PCVDP to drop in system pressure. The error is seen to oscillate as the pressure rises and falls about the operating pressure and then returns to a steady state of 0% as the system pressure returns to operating pressure.

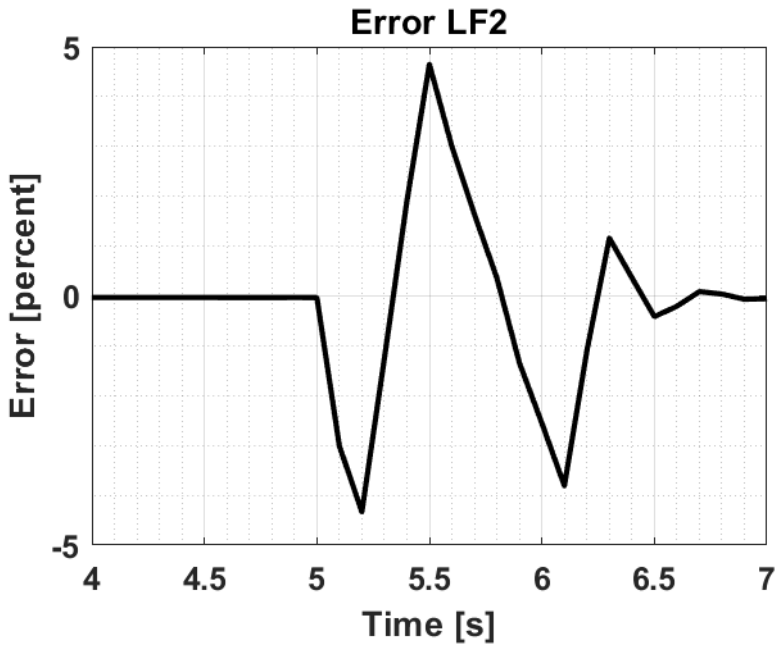

Figure 2.28 Error in position tracking for Loadframe 2

2.4 Discussion

2.4.1 Baseline System Model Test Setup

The results for the baseline test case are discussed in section 2.3. These results help quantify the crosstalk in three measures determined which are, the magnitude of pressure ripple due to sinusoidal oscillations at loadframe 2, the magnitude of pressure fluctuations due to a large step command to loadframe 1 and the error in position tracking at loadframe 2 as a result of the disturbance generated by loadframe 1.

Loadframe 2 generates a 0.69MPa (100psi) pressure ripple due to the switching of the servovalve. This pressure ripple travels along the hardline and reduces in magnitude as distance from loadframe 2 increases, due to the inertia of the fluid volume and the resistance provided by the friction in the pipeline. This pressure can have an impact on

the actuator motion and create unwanted noise in the system. This can also excite resonances in other loadframes connected to the system, losing tracking performance.

Loadframe 1 generates large pressure fluctuations due to the step command in displacement and flow response of the pump, with a drop in pressure to 15.85MPa (2300psi) which impacts the tracking performance of loadframe 2. An error of -4.5% in seen in the position tracking of loadframe 2 due to this drop in pressure. This means that the required rate and magnitude of strain are not achieved in the specimen installed. The pressure in the system rises to 26.9MPa (3900psi) due to the flow response of the PCVDP as it senses a pressure drop at its outlet. This overshoot in pressure results in a +4.5% error position tracking of loadframe 2. This means that the magnitude and the rate of strain experienced by the specimen exceeds the desired values, which results in poor material characterization. For example, if an elastomeric specimen was under study, the excess strain may result in the specimen undesirably entering the plastic region in the stress-strain curve.

To improve the performance of the hydraulic system, pressure ripple at loadframe 2 and the pressure fluctuations due to the disturbance at loadframe 1 must be reduced. The resultant error in position tracking of loadframe 2 must be reduced within an acceptable value. This would vary depending on the application and the desired accuracy of the laboratory. For the purposes of this study, 1% is arbitrarily chosen as an acceptable amount of error in position tracking. The baseline setup describes the current state before the implementation of crosstalk reduction techniques which are discussed and evaluated in the next chapter.

2.5 Inferences and Conclusion

In this chapter, sub-system models are developed for different components comprising a multiactuator hydraulic system in Simscape Fluids. Using Simscape Fluids blocks gives the model flexibility, allowing the user to easy add and remove components and relocate them within the hydraulic circuit as per the lab setup under study. The HPU is modelled

as variable flow source controlled by a PID controller. A methodology is defined for tuning the controller, such that response characteristics of the model match that of a pressure-compensated variable displacement pump. The pump model is validated using experimental data and is shown to be accurate in modelling the pressure dynamics shown by a PCVDP due to variation in flow demanded by the system.

A loadframe model is developed using a simplified servovalve model, an actuator model and accumulator model, that is capable of modelling the pressure dynamics in the hardline at the loadframe caused by the switching of the servovalve as well as the position tracking performance of the actuator. The loadframe model is validated using experimental data and is shown to be accurate in modelling the displacement response of the actuator to a given command signal.

A segmented pipeline model based on a lumped parameter model is analyzed in this chapter, to study the pressure dynamics in a pressurized hardline as a lumped parameter model, accounting for resistance, inertia, and compressibility in the pipeline. A methodology is developed for determining the number of segments required by the model to capture the desired dynamics of the system.

Using the component models, a system model of a typical material testing laboratory is developed to measure crosstalk consisting of an HPU, two loadframes and hardline connecting them. A baseline test case is defined and evaluated, to study the impact of one loadframe on the performance on the other. One loadframe is the disturbance generator in the system and the other loadframe is the one impacted. For the determined baseline case, the pressure ripple magnitude and error in position control tracking in the loadframe is quantified.

Future work on this model can focus on developing a white box model for the pump and the servovalve in the system. This would allow testing of improvement in actuator performance based on design changes in the pump and servovalve. A physical model of the servovalve would also help capture the higher frequency valve dynamics that are neglected in this model. The pump ripple generated in axial piston pumps is neglected in

this model. A white box approach in pump modelling can be used to evaluate the impact of pump ripple on the positional control accuracy of actuators.

In the next chapter, three measures to reduce crosstalk are identified, implemented in the system model developed in this chapter and evaluated using the baseline test case as a reference point, to measure their effectiveness.

Chapter 3
Measurement and Reduction of Hydraulic Crosstalk in a Multiactuator System

3.1 Introduction

A common motivation of using loadframes is the characterization of a specimen under study. A discrepancy in the displacement control leads to inaccurate results and a poor definition of the properties of the specimen. During sinusoidal position control, the flow rate to the actuator is varying at the same frequency as the actuator, generating a pressure ripple in the pipeline. In a system that comprises of more than one loadframe, the pressure ripple in the hardline can lead to poor position control in other loadframes as well as creating unwanted noise in the system [6]. For a loadframe testing dampers, there are sudden large demands in flow required by the actuator to follow a step displacement command. The HPU increases the flow rate to meet this demand, but there is a time lag in the pump response. This sometimes results in inadequate flow for another loadframe supplied by the same HPU, leading to poor position tracking and inaccurate results. In the event that the displacement amplitude is reduced from the command signal, the desired strain and strain rate is not experienced by the specimen. On the other hand, if the amplitude of displacement increases, the strain and strain rate experienced by the specimen are higher than value defined by the test, which may result in the specimen failing in a fewer number of cycles.

Significant research has been conducted in the field of fluid borne noise reduction, most of the work being associated with the development of a noise or pulsation reduction

device. Pan and Johnston (2016) developed a hybrid method of active and passive hydraulic noise cancellation with a focus on the reduction of audible noise generated by the system, specifically at the pump outlet [4]. A piezo electric actuator was used as the active component, varying the added compliance to the system at the pump outlet to reduce the pump pressure ripple. A flexible hose played the role of the passive component, reducing high frequency noise due to the added compliance. Yokota and Somada developed an active accumulator consisting of a piston controlled by piezoelectric sensor and a pressure transducer, and a passive accumulator installed at the pump outlet [7]. This device effectively reduced the high frequency pressure fluctuations produced by axial-piston pumps in the range of 500Hz-1KHz. Earnhart and Cunafare have designed a 'Compact Helmholtz Resonator' which comprised of a chamber with a compliant inner lining for the reduction of pressure fluctuations in hydraulic lines [9]. Haas and Lukachev explored the attenuation of pressure pulsations in short transmission lines generated by a switching valve using an RC filter [1]. This study is focused on the pressure pulsations generated in the short transmission lines between a switching valve and the actuator controller by it. The studies in this field focus on single component within the hydraulic circuit, for example the pump outlet, for the reduction of hydraulic noise. There is need for the study of the impact of the operation of multiple systems simultaneously and how they impact each other's performance.

In the previous chapter, a system level model was developed (in Simscape) that allows simulation of two loadframes that are powered by the same HPU. In this chapter, the system model will be used to perform computational experiments on different methods to reduce the influence of one loadframe on the tracking performance of another loadframe in the system, termed hydraulic crosstalk. To narrow the scope of study, a baseline test case was defined in Chapter 2 that will be used to compare to the crosstalk reduction approaches.

In this chapter, three methods of reduction of crosstalk are modelled and evaluated namely – close coupled accumulation, RC filters and second-order RC filters. The improvement in positional tracking and reduction of pressure ripple are measured and

reported using the Simscape model. The results for this study are presented in Section 3.3. The effectiveness of these methods is compared using the baseline test case as a reference. In the baseline test, error was measured to be +/- 4.5% of the desired displacement. The sizing study is conducted on the crosstalk reduction devices to reduce the error seen in position control to an acceptable value for each method. A cost comparison is conducted on the methods of crosstalk reduction, drawing a correlation between their expense and efficacy.

3.2 Modelling and Evaluation of Reduction Techniques for Crosstalk

In this section, three methods are explored, sized, modelled, and evaluated on the system baseline test case. The error in displacement control and pressure ripple was reduced to an acceptable value by sizing the accumulators and the restrictor orifice. To ensure consistency across cases, 1% error was chosen as an acceptable value for positional control. Additionally, cost comparison was conducted to evaluate the expense of each method corresponding to its effectiveness. While selecting component sizes, for instance, accumulator volume, off-the-shelf components available from vendors were preferred unless otherwise specified.

3.2.1 Closed Coupled Accumulation

Accumulators are hydraulic energy storage devices that are installed in a circuit to reduce the peak flow rate requirements of the pump, assist in fast flow supply to loadframes during transients, and reduce pressure fluctuations and shocks, which can protect the system. The capacitance of an accumulator is characterized by its volume and the precharged pressure of the gas volume.

To reduce large pressure fluctuations, we can add line-accumulation, which would be accumulators mounted on the hardline (Figure 3.1), or close-coupled accumulation, which would be accumulators mounted right at the loadframe (Figure 3.2). Close-coupled accumulators are typically smaller in volume. They are more effective in reducing high

pressure fluctuations at a loadframe than line accumulation, due to their proximity to the loadframe actuator.

Figure 3.1 Line Accumulation

Figure 3.2 Close Coupled Accumulation

The accumulator is modeled using the ‘Gas-Charged Accumulator’ Block in Simscape Fluids [43]. The physics of this block are governed by the equations discussed in Section

2.2.2.3. Close-coupled accumulators are added at both loadframes to reduce crosstalk in the system as seen in the schematic in Figure 3.3

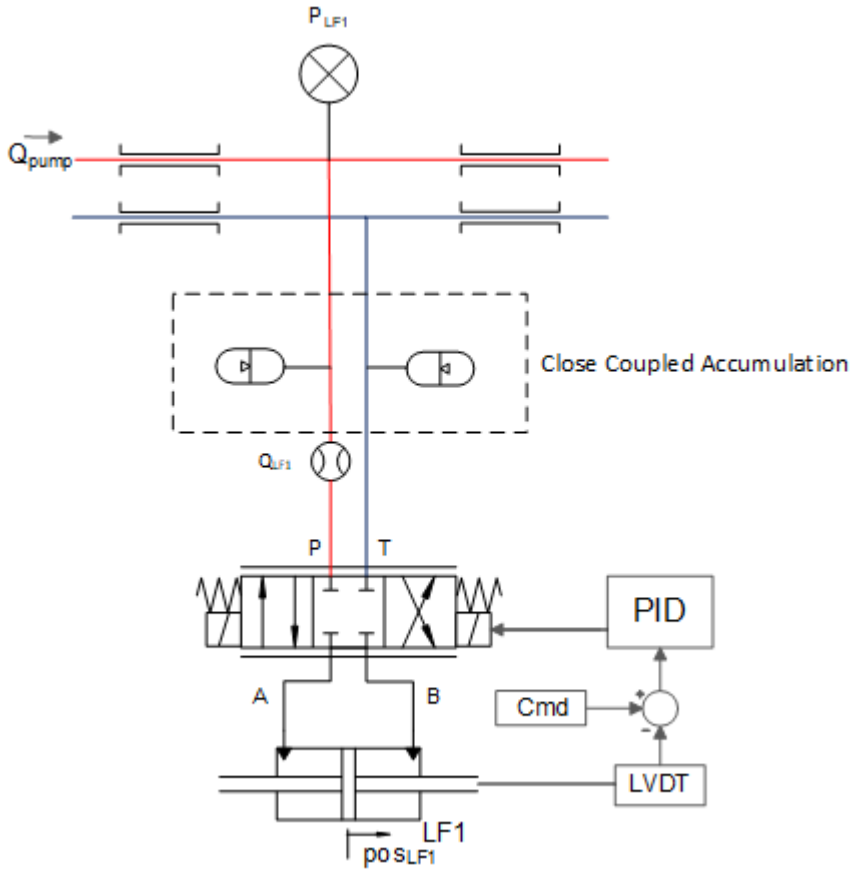

Figure 3.3 Close Coupled Accumulation: This schematic shows the installed close coupled accumulation close to the loadframes to reduce pressure pulsations

The parameters used to define the accumulator model are:

- Precharge pressure – The pressure of the gas with no oil in the accumulator prior to system initialization [3].
- Total Volume of Accumulator

- Minimum gas volume – In an accumulator, minimum dead volume is a part of the internal design to avoid damaging the bladder at higher pressures. In the model, this needs to be set as a non-zero value to ensure that pressure of the gas does not become infinite (mathematically) when the oil volume is equal to the volume of the accumulator. (Within the scope of our study, the highest internal pressure is 28MPa and the sizing of this parameter is not of significance).
- Initial Volume of Liquid – This is the initial volume of oil in the accumulator at the start of the simulation. Accurate calculation of this parameter reduces initial pressure transients in the system caused by the filling of the accumulator by the pump. This is calculated as:

$$V_{F,Initial} = V_T \left(\frac{{P_{gas,opt}}^{1/k} - {P_{pr}}^{1/k}}{{P_{gas,opt}}^{1/k}} \right) \qquad \textit{Eq. 3.2.1}$$

Where, $V_{F,Initial}$ is the initial volume of oil in the accumulator at the start of the simulation, $P_{gas,opt}$ is the operating pressure of the system (20.68MPa), P_{pr} is the precharge pressure of the gas, k is the specific heat ratio and V_T is the total volume of the accumulator.

In the interest of simplicity, these 4 parameters are sized identically for both loadframes. Henceforth, when it is stated that a 'X' gal accumulator is installed, it is implied that an accumulator of X gal volume is installed at both loadframes.

The baseline test case used a standard 0.25gal (0.94L) accumulator with a precharge pressure of 6.78MPa (1000psi), which is industry standard[25]. To study the reduction of crosstalk, increasing volumes of close coupled accumulators were evaluated for the test case. The volume of the accumulator was increased until the error was reduced below 1%, keeping the precharge pressure constant. Accumulators on the return line are precharged to 0.34MPa (50psi), which is the industry standard, are kept at an equal volume of 0.25gal (0.94L) for all studied cases. Results for the cases with accumulators of volumes 0.5gal (1.9L), 1.5gal (5.7L) and 2.0gal (7.6L) are documented in Section 3.3.1.

Accumulators can prove to be quite expensive hydraulic components with the cost increasing with the volume of the accumulator. Costs of each size of these accumulators including installation kits are obtained for a cost comparison study in Section 3.4.4.

3.2.2 RC Filter

In a hydraulic circuit, one can think of pressure and flow as analogous to voltage and current in an electrical circuit. This is referred to as the electrical analogy [1].The pressure drop between two points due to friction in a pipeline, or the pressure drop across an orifice are analogous to the voltage drop across a resistor in an electrical circuit. Similarly, accumulation in a hydraulic circuit is analogous to electrical capacitance. An RC filter (Figure 3.4) is an electrical circuit comprising of a resistor and capacitor connected in series [48]. It acts as a low pass filter – reducing the amplitude of frequencies greater than a certain value called the cut off frequency.

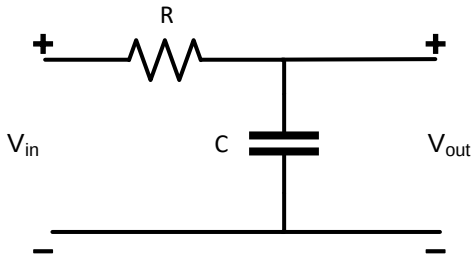

Figure 3.4 RC Filter

The cut off frequency in a RC filter is given by [45]

$$f_c = \frac{1}{2\pi RC} \qquad \textit{Eq. 3.2.2}$$

Where, f_c is the cutoff frequency, R is the resistance and C is the capacitance.

An analogous concept for an RC filter can be applied in a hydraulic circuit, by connecting an orifice (resistance) and accumulator (capacitance) near a loadframe as seen in Figure

3.5. The system acts like a low pass filter reducing the magnitude of pressure ripple in the hardline near the loadframe.

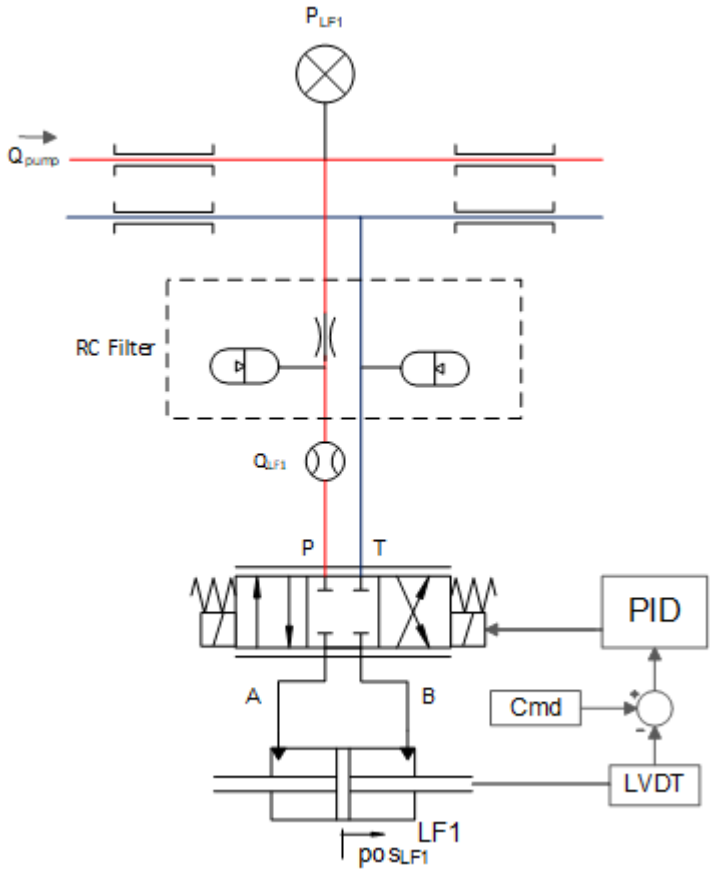

Figure 3.5 Hydraulic RC Filter

For hydraulic systems, the resistance can take the form of a restrictive pipeline or an orifice. Flow through an orifice, given by Equation 2.2.1, is nonlinear. The linearization of this equation gives us an equation that is analogous to Ohm's equation. Linearizing the orifice equation about flow rate Q_o results in:

$$\Delta P_{Q_o} = \frac{2Q_o}{K^2}Q - \frac{{Q_o}^2}{K^2} \quad \rightarrow v = iR \rightarrow \quad R = \frac{2Q_o}{K^2} \qquad \textit{Eq. 3.2.3}$$

Similarly, the compressibility equation can be used to get the value for hydraulic capacitance [1]:

$$\Delta Q = \frac{V}{\beta}\frac{dP}{dt} \quad \rightarrow \quad \Delta i = C\frac{dV}{dt} \quad \rightarrow \quad C = \frac{V}{\beta} \qquad \textit{Eq. 3.2.4}$$

The cut off frequency can be calculated from Eq. 3.2.2 - Eq. 3.2.4.

$$f_c = \frac{1}{2\pi\left(\frac{2Q_o}{K^2}\right)\left(\frac{V}{\beta}\right)} \qquad \textit{Eq. 3.2.5}$$

Performing dimensional analysis on Eq. 1.2.5 shows that the equation is dimensionally consistent.

A Hydraulic RC Filter is modelled in Simscape using the close coupled accumulator model discussed in Section 3.2.1 to model the capacitance in conjunction with a 'Fixed Orifice' block to model the resistance. The flow through the orifice is calculated using the orifice equation 2.2.1. The parameters required by the accumulator block are described in Section 3.2.1. The parameters for the orifice block are:

- Orifice Area
- Flow discharge coefficient – This is a semi-empirical parameter that depends on the orifice geometry. Typical range for this value is 0.6 to 0.8 depending on the orifice used and can be found in the manufacturers data sheet [5]. In this modelling effort, the value is assumed to be 0.7.

The orifice and accumulator Simscape blocks are connected in series as seen in Figure 3.5. The baseline test case contains a pressure ripple of 20Hz generated at loadframe 2 as it performs sinusoidal motion. To reduce this pressure ripple, the accumulator and the orifice should be sized such that the cut off frequency is less than 20Hz. Additionally, the

error must be reduced below 1% with the least amount of added accumulation as this would be the driving factor for the additional cost to the system.

A case with an RC filter, consisting of 0.5gal of close coupled accumulation and a 4mm diameter orifice is studied for the attenuation of crosstalk. For the baseline test case defined in Chapter 2, the average flow rate required by loadframe 2 is seen to be 5.04 x $10^{-4}m^3/s$ (8gpm) at steady state. Linearizing the orifice equation about this value of flow rate (Eq. 1.2.3), the resistance is calculated to be 7.81e+09 $kg/m^4.s$. The capacitance for the 0.5gal accumulator is calculated to be 1.568e-12 $m^4.s^2/kg$. The cut off frequency can be calculated using Eq. 1.2.5 to be 12.98Hz, which is lower than that frequency of pressure ripple (20Hz). The results for this case are reported in Section 3.3.2.

3.2.3 Second Order RC Filter

A second order RC filter, (Figure 3.6) consists of two RC filters connected in series. RC filters have a -20dB/decade roll off, which means that the gain of the system reduces by 20dB per decade. An Nth order RC filter (N RC filters connected in series) will have a roll-off gain of -20N dB/decade. Therefore, for a second order RC filter the roll-off gain is -40dB/decade. A second order RC filter is used when the first stage is unable to remove enough of the unwanted frequencies in an electrical circuit.

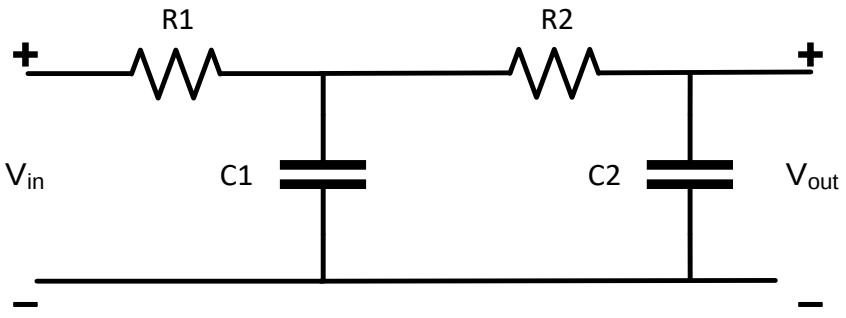

Figure 3.6 Second order RC Filter

The cutoff frequency of a 2nd order RC Filter is given by [48]:

$$f_{cutoff} = \frac{1}{2\pi\sqrt{R_1 R_2 C_1 C_2}} \qquad \textit{Eq. 3.2.6}$$

In a hydraulic circuit, the analogy of a second order RC circuit is two sets of orifice-accumulator pairs, connected in series as seen in Figure 3.7. This acts as a second order RC filter, reducing the pressure ripple with a higher roll-off than the first order RC filter.

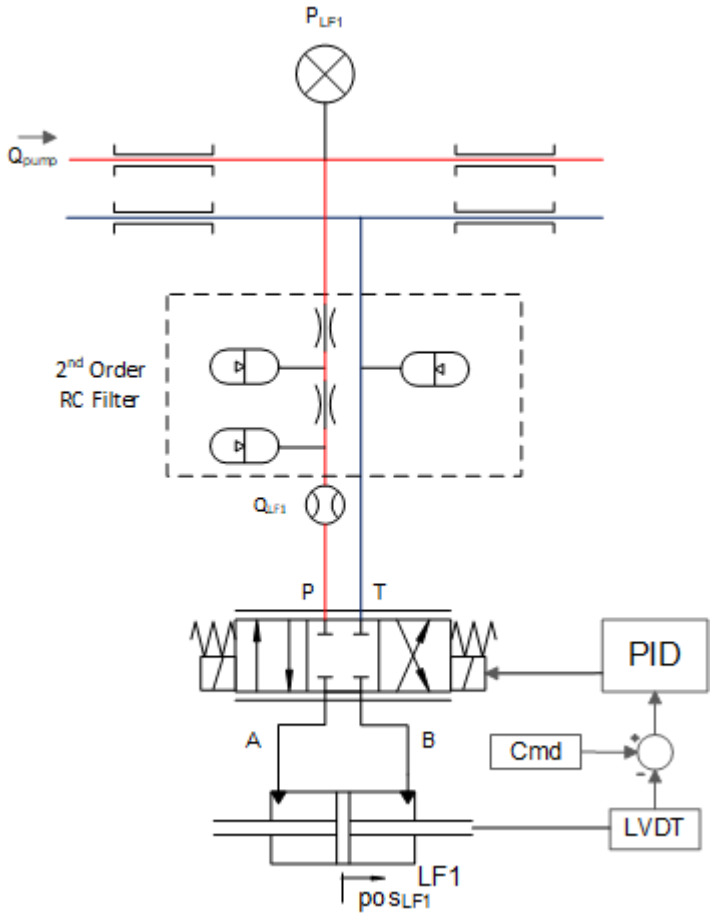

Figure 3.7 Hydraulic 2nd order RC Filter

A second order hydraulic RC filter is modelled using two RC filters modelled in Section 3.2.2 in series as in Figure 3.7 using the Simscape blocks 'Fixed Orifice' and 'Gas-Charged Accumulator'. The sizing of the components or the parameters in the blocks has the same goal as the previous two cases – reducing the error in positional control at loadframe 2 below 1%, while using the least amount of additional accumulation to keep the cost low. To offer a genuine comparison between 1st and 2nd order RC Filters, the cut off frequency must be approximately equal in both cases (12.98Hz), and so should the resistance and capacitance. Two cases of 2nd Order RC Filtering are studied in this chapter:

- Case 3A: Equal sized orifices to 1st order RC Filter: Two 0.25gal accumulators are added as capacitance and therefore the total volume is the same as in Section 3.2.2. The value of the capacitance is 1.568e-12 $m^4.s^2/kg$. Two orifices of diameter 4mm are used for as the resistances as in Figure 3.7. The resistance offered by the two orifices in series is 3.13e+10 $kg/m^4.s$. The cutoff frequency is calculated by Eq.1.2.6 to be 3.25Hz.
- Case 3B: Equal cut off frequency to 1st order RC Filter: Two 0.25gal accumulators are added as capacitance and therefore the total volume is the same as in Section 3.2.2. Since the capacitance is a function of volume, the value of the capacitance is the same as Section 3.2.2 and equal to be 1.568e-12 $m^4.s^2/kg$. To add a resistance of 7.81e+9 $kg/m^4.s$ (as in the case of the 1st order RC Filter) two orifices of diameter 5.656mm are used for as the resistances as in Figure 3.7.

The 2nd order RC filter for these two cases are tested using the system test case and the results are reported in Section 3.3.3.

3.2.4 Cost Comparison of Crosstalk Reduction

In Section 3.2.1 - 3.2.3, three crosstalk reduction methods are modelled. Costs of the components required for the implementation of these methods – including the cost of accumulators, orifices, fittings, and installation kits - are compared to draw a co-relation

between the effectiveness of these methods and the cost associated with them. The costing of the components is based on quotes from MTS Systems.

3.3 Results

The baseline model setup, commands and results are discussed in Chapter 2. All specifications of the loadframes (mass, dimensions, servovalve specifications, stroke, pump specifications) are tabulated in Table 2.1. The three identified methods of crosstalk reduction are tested, and the results of each case are shown below. The sizing of the added accumulation and resistance are tabulated in Table 3.3. Following are the cases discussed in this section:

- Case 1: Close Coupled accumulation
  - 0.5gal
  - 1.5gal
  - 2.0gal
- Case 2: RC Filter
  - 0.5gal Accumulator, 4mm Orifice
- Case 3: 2nd Order RC Filter
  - 0.25gal Accumulator (Qty:2), 5.656mm Orifices (Qty:2) – Equivalent Resistance and Cut off frequency to Case 2
  - 0.25gal Accumulator (Qty:2), 4mm Orifices (Qty:2) – Equivalent sizing to Case 2

3.3.1 Case 1 – Close Coupled Accumulation

In this section three cases of varying accumulation sizes are used to reduce crosstalk and a correlation between their sizing and effectiveness is drawn.

As described in Chapter 2, loadframe 1 plays the role of the disturbance generator in the test setup. The actuator is initially at mid-stroke (shown as 0m) and at 5 seconds is given a step command of 76.2mm (3”) - half of the maximum displacement of the actuator.

Figure 3.8 shows the position tracking of loadframe 2. The actuator travels to the commanded position with zero steady state error and 0.28seconds settling time. This validates that loadframe 2 tracks the commanded step input with the same response characteristics for all the studied sizes of accumulation when compared to the baseline tests case.

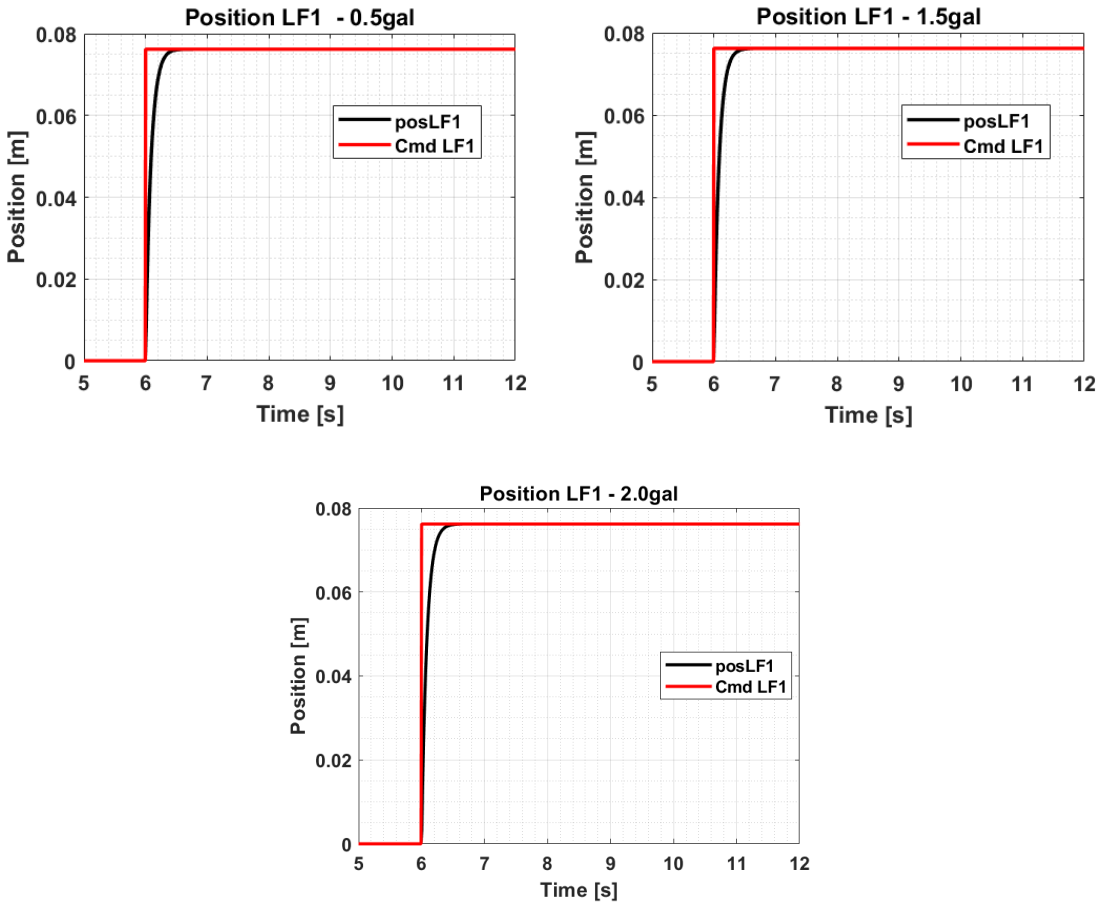

Figure 3.8 Position tracking of Loadframe 1

Figure 3.9 shows the pressure dynamics induced in the hardline due to the generated disturbance (Figure 3.8) by loadframe 1 at 6s and measured at the point of connection of loadframe 1 and the hardline (P_{LF1}) and the pump outlet (P_{OUT}) as in Figure 2.2.18 for the

three sizes of added accumulation. As the loadframe tracks the step displacement, the system pressure drops to below operating pressure as the flow demand at loadframe 1. The pump increases the flow rate resulting in an overshoot in system pressure. The system reaches steady state as the pressure returns to operating pressure. Increasing the volume of accumulation reduces the peak pressure and reduces initial pressure drop due to the disturbance by assisting the pump in meeting the flow demand of the system. The best case for minimum peak pressure and least drop in pressure is seen for the largest volume of accumulation tested at 2.0gal. However, with the increase of accumulator volume, the settling time is also seen to increase. This is due the longer time taken by the pump to replenish the fluid volume in the accumulator. The settling time is maximum for the case of 2.0gal of accumulation at 5.1 seconds.

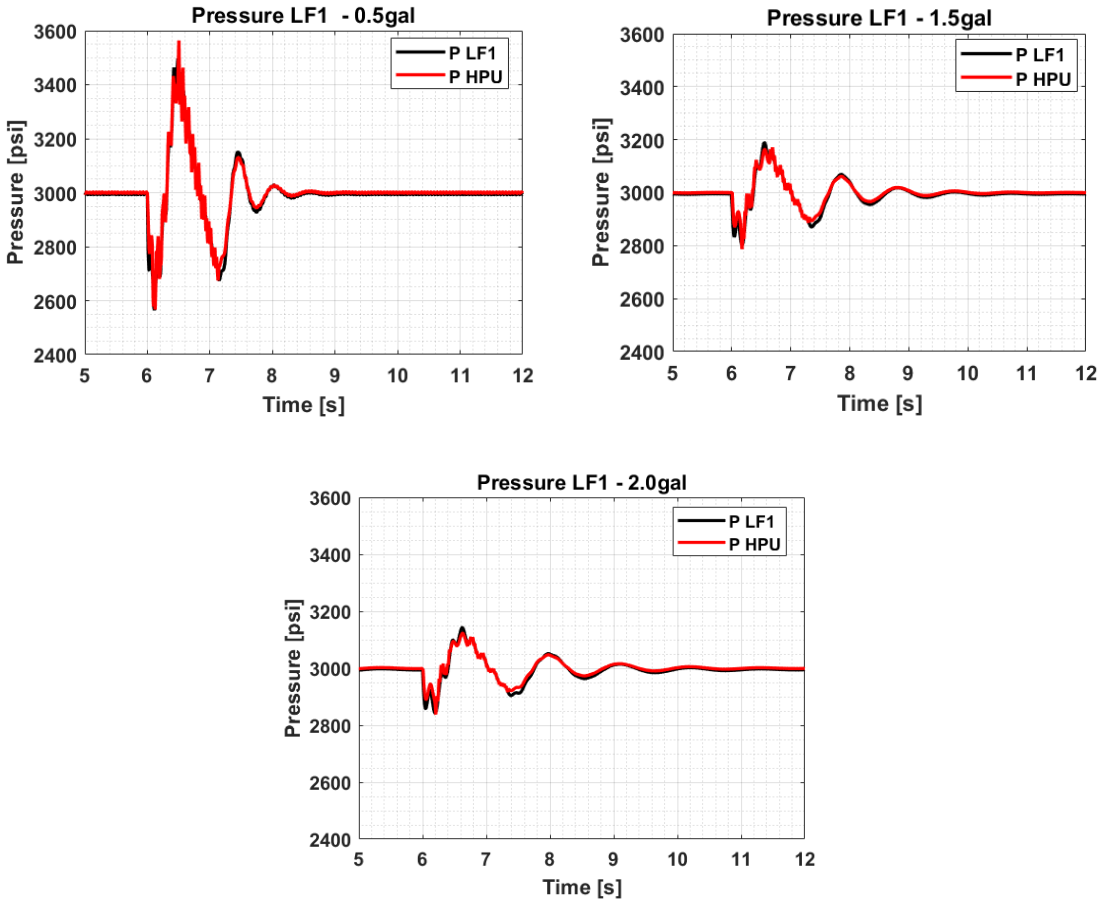

Figure 3.9 Pressure study at Loadframe 1 and HPU

Figure 3.10 shows the pressure dynamics at loadframe 2 and the HPU for the three cases of varying accumulation volume. In the absence of the disturbance generated by loadframe 1, a constant magnitude pressure at 20Hz is generated by loadframe 2 owing to the sinusoidal motion of its actuator. The magnitude of this ripple is tabulated in Table 3.1. The magnitude of this higher frequency ripple reduces as the accumulator volume increases. Loadframe 2 also experiences the pressure fluctuations generated by loadframe 1. The magnitude of this pressure ripple is reduced by approximately 10psi (0.07MPa) by the inertia and compliance of the hardline between the two loadframes.

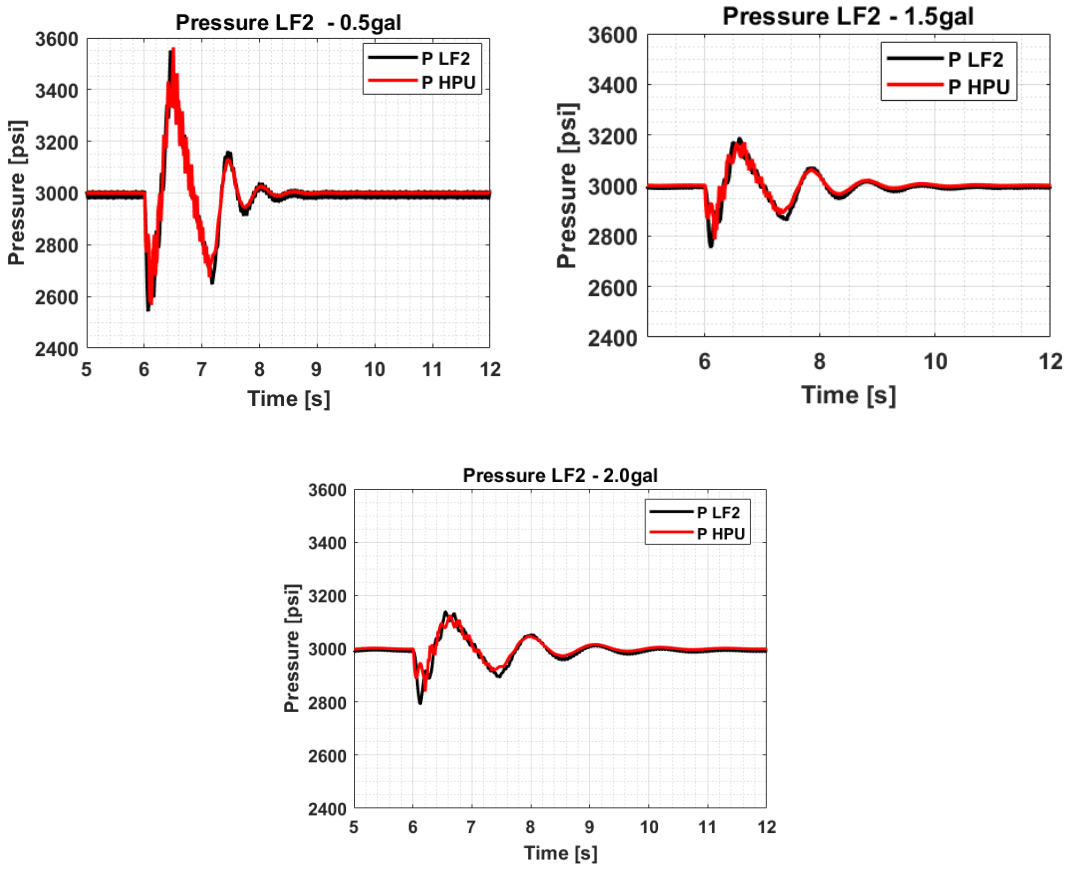

Figure 3.10 Pressure study at Loadframe 2 and HPU

Figure 3.11 shows the variation in flow rate demanded by loadframe 1 and the pumps flow response as measured at Q_{PUMP} and $Q_{LF1.}$ The peak instantaneous flow rate demanded is 76gpm(4.8e-3m^3/s), which is common across all cases being studied. The peak flow rate of the HPU is 30 gpm (1.9e-3m^3/s) which is the max flow rating of the pump. At 6s, the pump flow rate increases to 30gpm to meet the increased flow demand. As the pressure rises above operating pressure at 6.5s, the pump flow rate reduces to 0gpm. The pump flow rate is seen to rise again at 7.25 seconds as the system pressure drops below operating pressure. The pump flow rate oscillates, as the pressure in the system returns to steady state. The large volume of accumulation is seen to have the longest settling time.

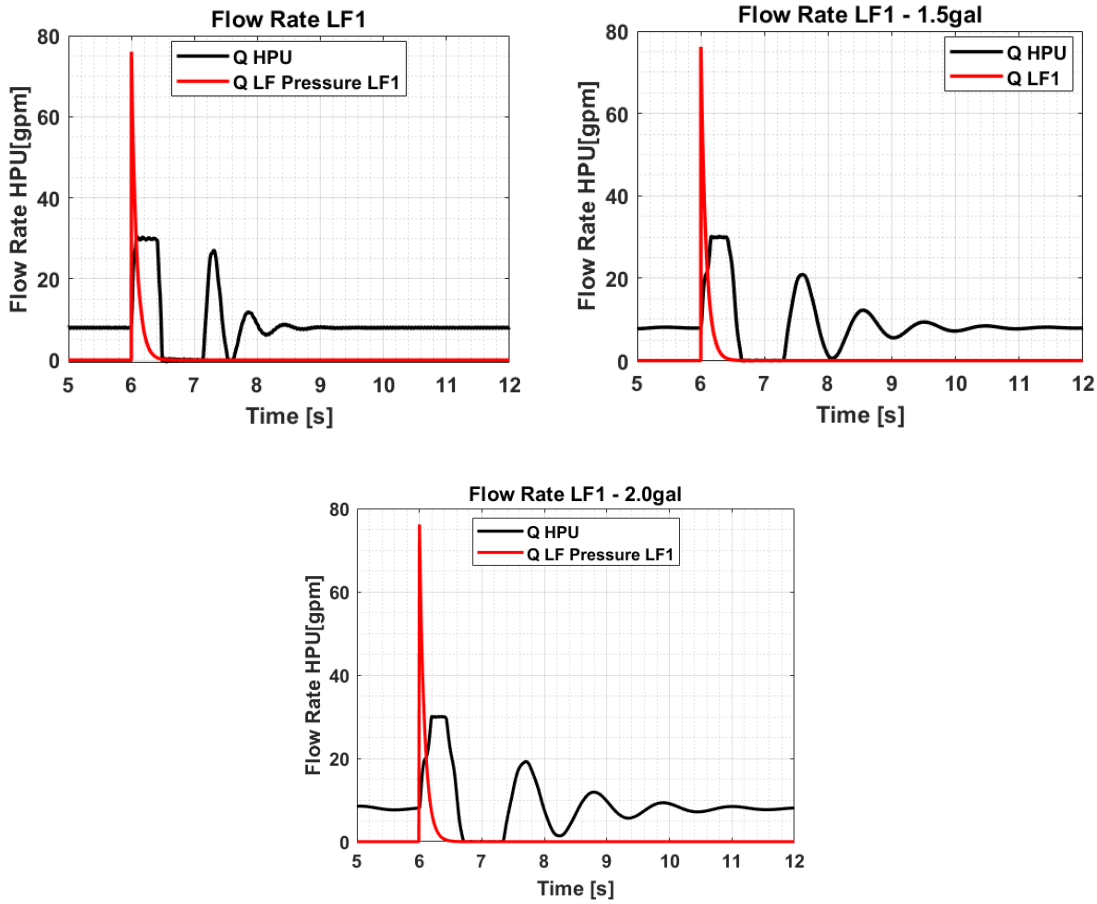

Figure 3.11 Flow rate at Loadframe 1 and HPU

Figure 3.12 shows the flow supplied by the pump and the flow rate through LF2 as measured at Q_{PUMP} and Q_{LF2} prior to the disturbance generated at loadframe 1. The flow demand of loadframe 2 (at steady state) is seen to vary from 0 to 7.57e-3 m^3/s (12gpm) at a frequency of 20Hz, which corresponds to the 10Hz sinusoidal position command. The pump flow rate is seen to vary at the same frequency as the pressure ripple generated at the loadframe by this flow variation travels down the hardline and is sensed at the pump outlet. As the volume of accumulation is increased, the magnitude of this pressure ripple reduces and therefore, the flow rate variation of the pump reduces too. For the case of 0.5gal of accumulation a 1.9e-5 m^3/s (0.3gpm) flow rate variation is seen at the pump outlet. For the case of 2gal of accumulation, this flow rate variation reduces to 6.3e-7 m^3/s

(0.01gpm). The low frequency variation, low amplitude variation in flow is generated due to the onset of the sinusoidal motion of loadframe 2. The settling time for this oscillation increases as the volume of accumulation increases. This flow variation does not have an adverse effect on the position control accuracy.

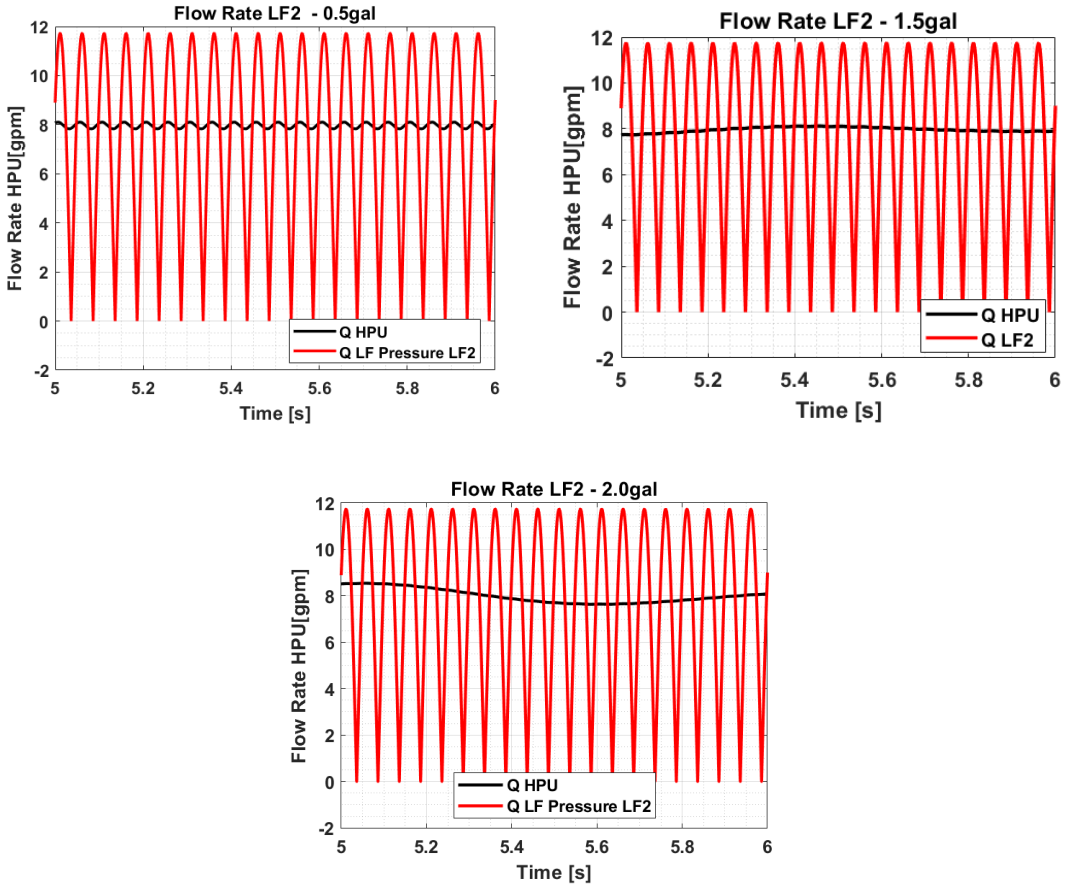

Figure 3.12 Flow rate at Loadframe 2 and HPU

Figure 3.13 shows the error in displacement tracking of loadframe 2 due to the disturbance generated at loadframe 1. The error calculated is as a percentage of the amplitude of the command signal that loadframe 2 is tracking. Before the generation of the disturbance at 6s, the steady state error is 0. The error is seen to reduce with the addition of close coupled

accumulation. With 0.5gal of accumulation, the error is seen to be -2.6/+2.6% - here, a negative error represents a reduction and positive represents an increase in the amplitude of the actuator motion in loadframe 2. Error reduces to -1.45/+1.2% with 1.5gal of accumulation. Error is seen to further reduce to -1.4/+0.8% for 2gal of accumulation which is deemed acceptable.

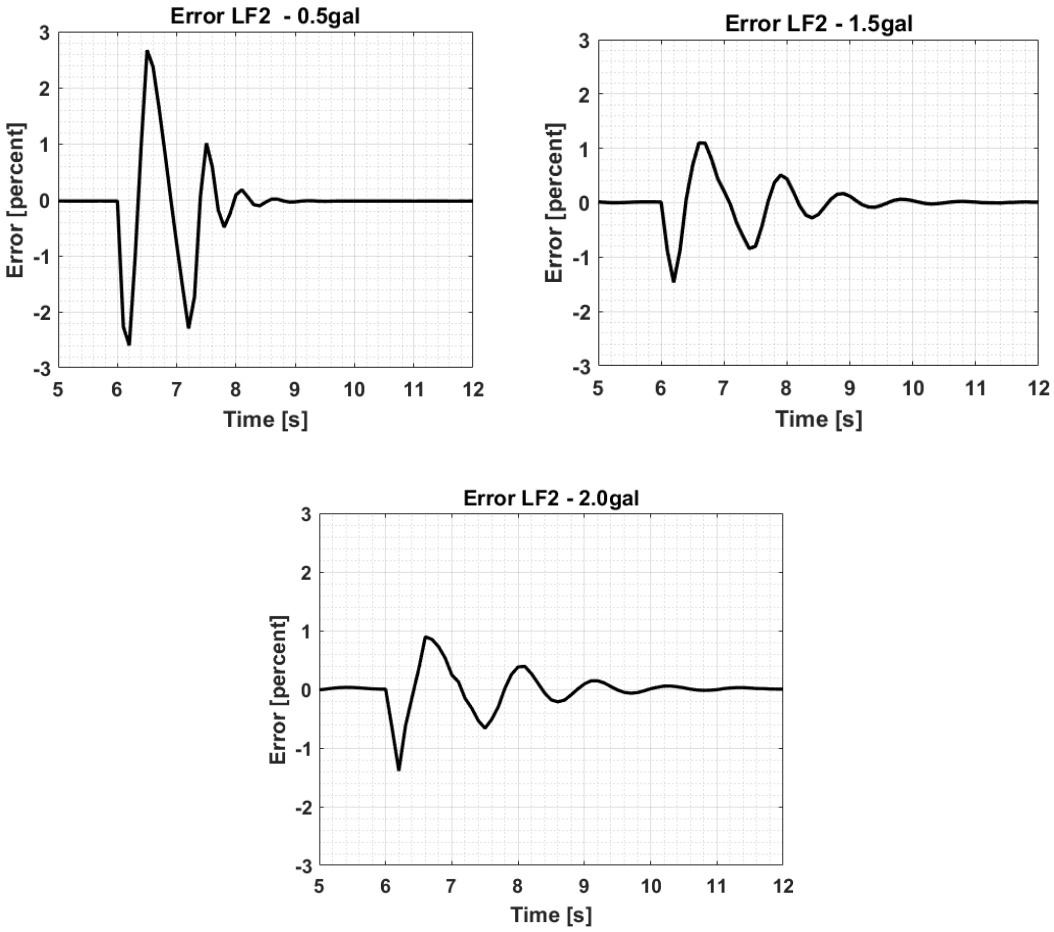

Figure 3.13 Error in position tracking for Loadframe 2

The peak pressure, settling time and pressure ripple magnitude, error in position tracking are tabulated in Table 3.1.

Table 3.1 Comparison of Accumulation Volume on Crosstalk Reduction

Volume of close coupled Accumulation	**0.5gal (1.9L)**	**1.5gal (5.7L)**	**2.0gal (7.6L)**
Peak Pressure at LF 1 (psi/MPa)	3550psi (24.44MPa)	3180psi (21.92MPa)	3140psi (21.65MPa)
Minimum Pressure in the system	2560psi (17.65MPa)	2785psi (19.20MPa)	2840psi (19.58MPa)
Pressure Ripple at LF 2 (psi/MPa)	29psi (0.2MPa)	8psi (0.05MPa)	5psi (0.03MPa)
Settling Time (seconds)	2.1	4.1	5.1
Error in position tracking at loadframe 2 (%)	-2.6/+2.6%	-1.45/+1.2%	-1.4/+0.8%
Peak flow demand from HPU	30gpm	30gpm	30gpm

3.3.2 Case 2 – RC Filter

A close coupled accumulator of 0.5 gallons in series with a 4mm orifice is used to install a hydraulic RC filter with a cut off frequency of 12.98Hz to reduce pressure pulsations and improve position tracking as described in Section 3.2.2.

Figure 3.14 shows the position tracking of LF1 (disturbance generator) to the commanded step input. The actuator is initially at mid-stroke (shown as 0m) and at 5 seconds is given a step command of 76.2mm (3”). The actuator travels to the commanded position with zero steady state error and 0.28seconds settling time i.e., with a similar performance as seen in Case 1 in section 3.3.1 Loadframe 2 is tracking a 10Hz, 3mm sinusoidal displacement command for the entire duration of the simulation.

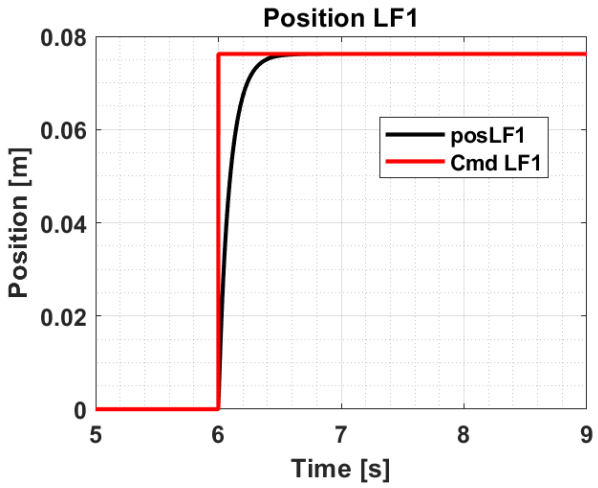

Figure 3.14 Position tracking of Loadframe 1

Figure 3.15 shows the pressure dynamics in the hardline as a result of the displacement command at loadframe 1 and measured at P_{LF1} and $P_{OUT.}$ The pressure is seen to drop to a minimum of 20.13MPa (2920psi) at the HPU at 6s and a minimum of 19.9MPa (2887psi) at loadframe 1 as the flow demand at loadframe increases. The pump flow rate increases to compensate for this pressure loss and the pressure rises to a peak value of 20.78MPa (3015psi) at LF1, with a settling time of 1.2 seconds to return to operating pressure.

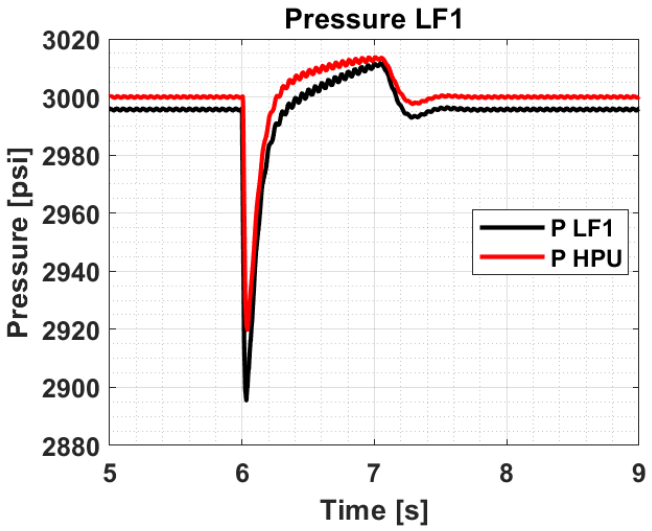

Figure 3.15 Pressure study at Loadframe 1 and HPU

Figure 3.16 shows the pressure at LF2 and the HPU. The pressure ripple generated at LF2 due to the sinusoidal command is measured to be under 1psi. The peak pressure at LF2 due to the step displacement of LF1 is measured to be 20.80 MPa (3017) psi with the pressure dropping to 19.91MPa (2888psi) at 6s.

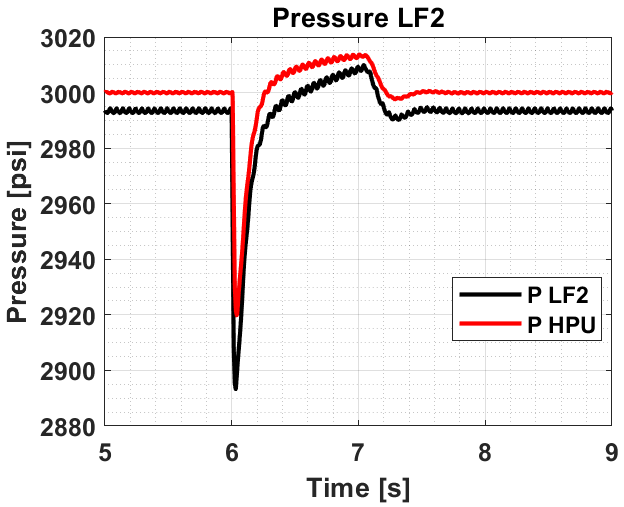

Figure 3.16 Pressure study at Loadframe 2 and HPU

Figure 3.17 shows the flow supplied by the pump and the flow rate through LF1 as measured at Q_{PUMP} and $Q_{LF1.}$ At 6 seconds, the flow demand at loadframe 1 increases instantaneously to a peak value of 4.8e-3 m^3/s (78gpm) as the loadframe tracks the input step command. The flow rate at the pump increases to a peak value of 1.2e-3 m^3/s (18.6gpm) to meet the flow demand of the system. As the pressure at the pump outlet falls by a smaller magnitude (Figure 3.15) as compared to Case 1, the pump does not increase the flow rate to maximum capacity (30gpm).

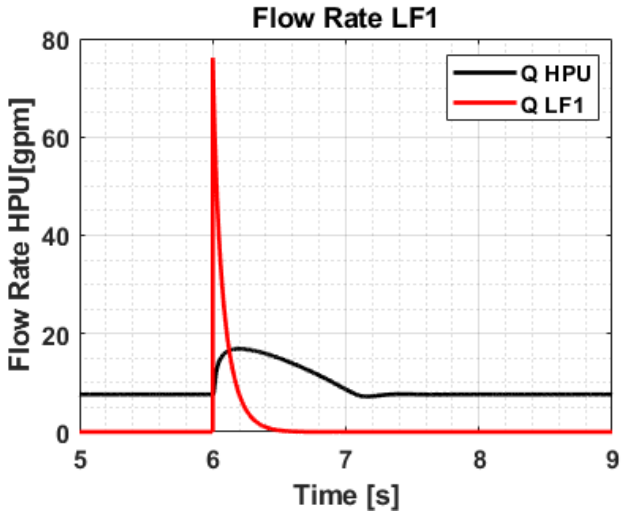

Figure 3.17 Flow rate at Loadframe 1 and HPU

Figure 3.18 shows the flow supplied by the pump and the flow rate through LF2 as measured at Q_{PUMP} and $Q_{LF2.}$ The plot shows a flow rate variation at 20Hz which corresponds to the 10Hz sinusoidal wave being commanded at loadframe 2. In in the absence of flow demand from LF1, at steady state, the HPU provides a steady flow rate of 8gpm with negligible flow rate variation from the pump.

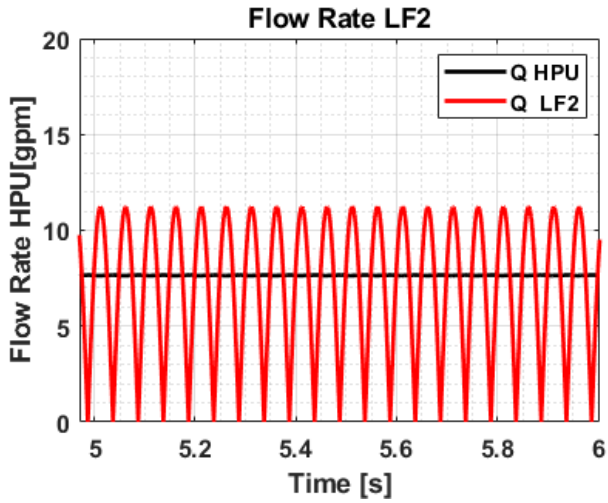

Figure 3.18 Flow rate at Loadframe 2 and HPU

Figure 3.15 and Figure 3.16 show that the pressure ripple due to disturbance generated by loadframe 1 has been reduced considerably compared to Case 1. This results in a reduction in error in the position tracking of loadframe 2. The error is seen to be -0.4/+0.04% for Case 2. This reduction of error is due to the significant reduction in overshoot in pressure in the system.

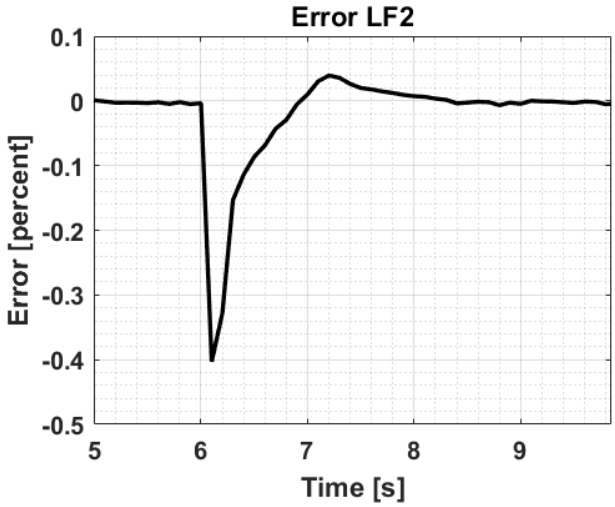

Figure 3.19 Error in position tracking for Loadframe 2

3.3.3 Case 3 – 2nd Order RC Filter

In this section, the results of the study of the effectiveness of a 2nd order RC Filter are reported. Two cases of 2nd order RC filters are studied as noted in Section 3.2.3 by testing on the baseline test case.

- CASE 3A - 0.25gal Accumulator (Qty:2), 4mm Orifices (Qty:2) – Equivalent orifice sizing to 1st Order RC Filter (Case 2)
- CASE 3B - 0.25gal Accumulator (Qty:2), 5.656mm Orifices (Qty:2) – Equivalent Resistance and Cut off frequency to 1st Order RC Filter (Case 2)

Figure 3.20 shows the displacement of loadframe 1 for the step input command for Case 3A and 3B. The actuator is initially at mid-stroke (shown as 0m) and at 6 seconds is given a step command of 76.2mm (3”). In both cases, actuator travels to the commanded position with zero steady state error and 0.28seconds settling time i.e., with a similar performance as seen in baseline test case. Loadframe 2 is tracking a 10Hz, 3mm sinusoidal displacement command for the entire duration of the simulation. This step command forms the disturbance generated in the system.

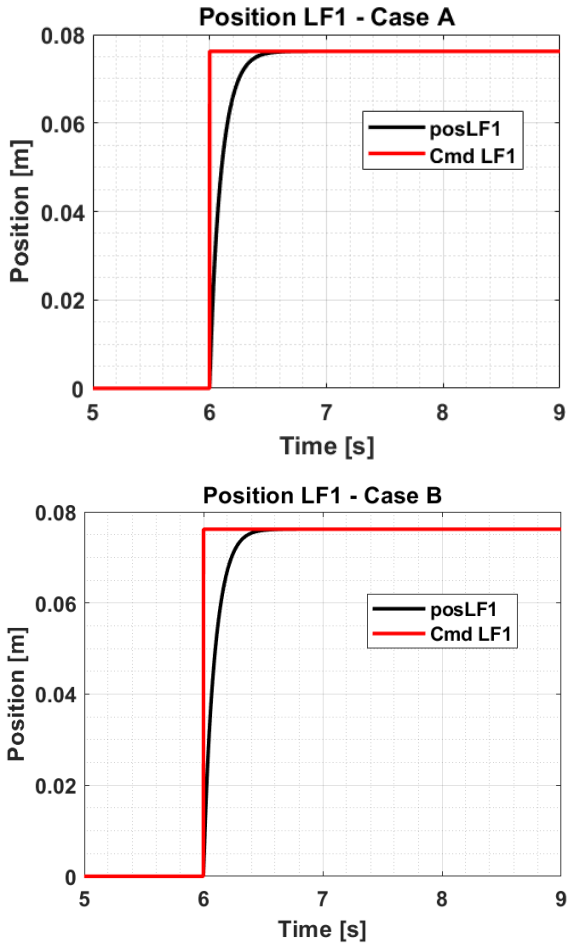

Figure 3.20 Position tracking of Loadframe 1

Figure 3.21 shows the pressure dynamics in the hardline as a result of the displacement command at loadframe 1 and measured at P_{LF1} and $P_{OUT.}$ A minimum pressure of 2914psi is seen at LF1 with a minimum of 2930 psi at the HPU. A peak pressure of 3035psi is seen at LF1, with a settling time of 1.2 seconds. As loadframe 1 tracks the step command, the system pressure falls as the flow is supplied to loadframe 1. The pressure is seen to drop to a minimum of 20.09MPa (2914psi) for Case 3A and 19.48MPa (2826psi) for Case 3B at 6s at loadframe 1 and a minimum of 20.20MPa (2930psi) at the HPU for Case 3A and 19.77MPa (2868psi) for Case 3B. The pump flow rate increases, as it senses the pressure drop, and the pressure rises to a peak value of 20.92MPa (3035psi) for Case 3A and

21.56MPa (3127psi) for Case 3B at LF1, with a settling time of 1.2 seconds to return to operating pressure. Case 3A shows better damping of pressure oscillations as compared to Case 3B, due to the higher resistance.

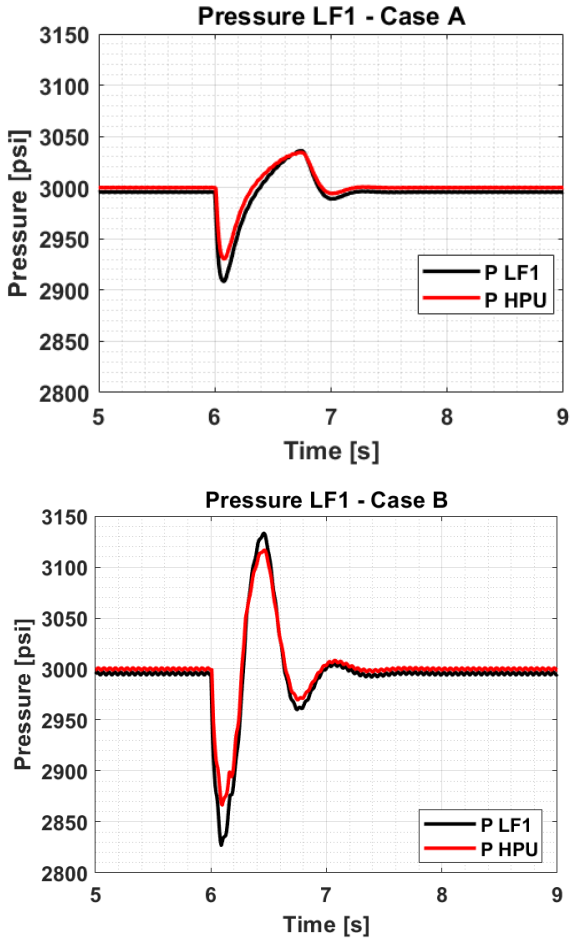

Figure 3.21 Pressure study at Loadframe 1 and HPU

Figure 3.22 shows the pressure as measured at LF2 and the HPU. The pressure ripple generated at LF2 due to the sinusoidal command is measured to be under 1psi for Case 3A and 8psi for Case 3B. The disturbance generated at loadframe 1 travels along the hardline and is measured at loadframe 2. The pressure is seen to drop to a minimum of 20.09MPa (2914psi) for Case 3A and 19.48MPa (2826psi) for Case 3B at 6s. The pump flow rate increases, as it senses the pressure drop, and the pressure rises to a peak value

of 20.92MPa (3035psi)) for Case 3A and 21.56MPa (3127psi) for Case 3B at LF2, with a settling time of 1.2 seconds to return to operating pressure.

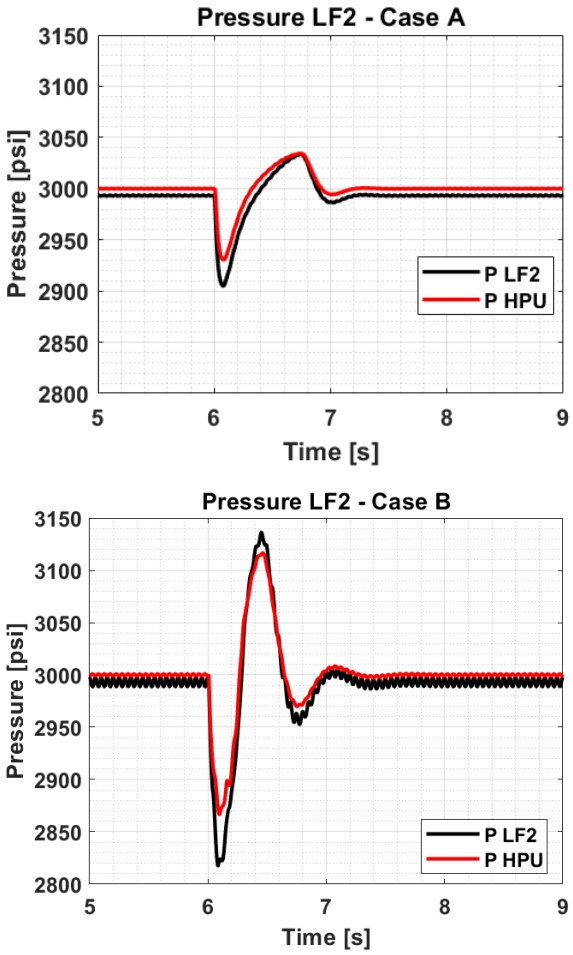

Figure 3.22 Pressure study at Loadframe 2 and HPU

Figure 3.23 shows the flow supplied by the pump and the flow rate through LF1 as measured at Q_{PUMP} and $Q_{LF1.}$ The peak instantaneous flow rate demanded is 76gpm, which is common across all cases being studied. The peak flow rate of the HPU is 21 gpm which is below the max flow rating of the pump.

Figure 3.23 shows the flow supplied by the pump and the flow rate to loadframe 1 during the disturbance generated at loadframe 1 as measured at the loadframe and at the pump.

At 6 seconds, the flow demand at loadframe 1 increases instantaneously to a peak value of 4.8e-3 m^3/s (78gpm) as the loadframe tracks the input step command. In Case 3A, the flow rate at the pump increases to a peak value of 1.3e-3 m^3/s (20.3gpm) to meet the flow demand of the system. In Case 3B, as the pressure drops by a larger magnitude (Figure 3.21) compared to Case 3A, the pump flow rate increases to 1.9e-3 m^3/s (30gpm) which is the maximum flow rating of the pump. The system pressure rises to operating pressure of 3000psi and the pump flow rate reduces to 8gpm.

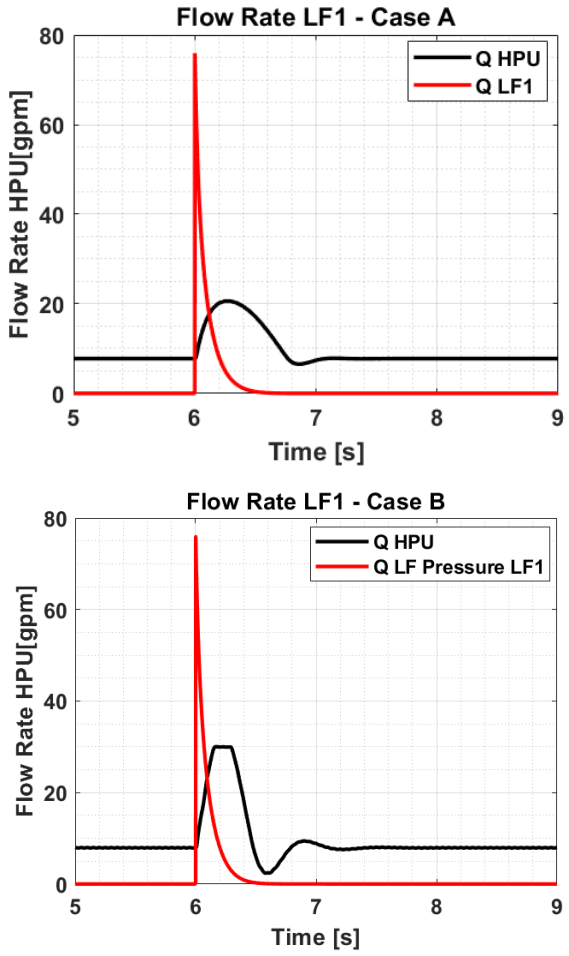

Figure 3.23 Flow rate at Loadframe 1 and HPU

Figure 3.24 shows the flow supplied by the pump and the flow rate through LF2 as measured at Q_{PUMP} and $Q_{LF2.}$ The plot shows a flow rate variation at 20Hz which

corresponds to the 10Hz sinusoidal wave being commanded. In in the absence of flow demand from LF1, at steady state, the HPU provides a steady flow rate of 5.04e-4 m^3/s (8gpm). In Case 3B, due to the larger pressure ripple originating at loadframe 2, the flow rate from the pump is seen to oscillate with an amplitude of 6.9e-9 m^3/s (0.11gpm) as the pump compensator varies the flow rate due to the pressure oscillation measured at the pump outlet.

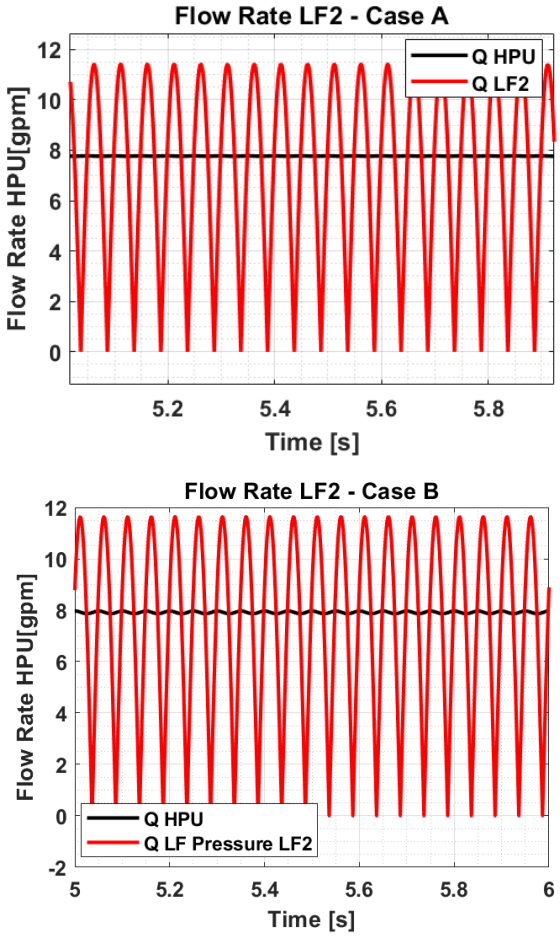

Figure 3.24 Flow rate at Loadframe 2 and HPU

Figure 3.25 shows the error in position tracking for Case 3A and B for the displacement of loadframe 2. In Case 3A, the error is reduced to -0.4/+0.17%. In Case 3B, the error in

position is seen to be -1.3/+0.8%. While the error in Case 3B is acceptable, it is still greater than a 1st order RC Filter with the same cut off frequency and resistance.

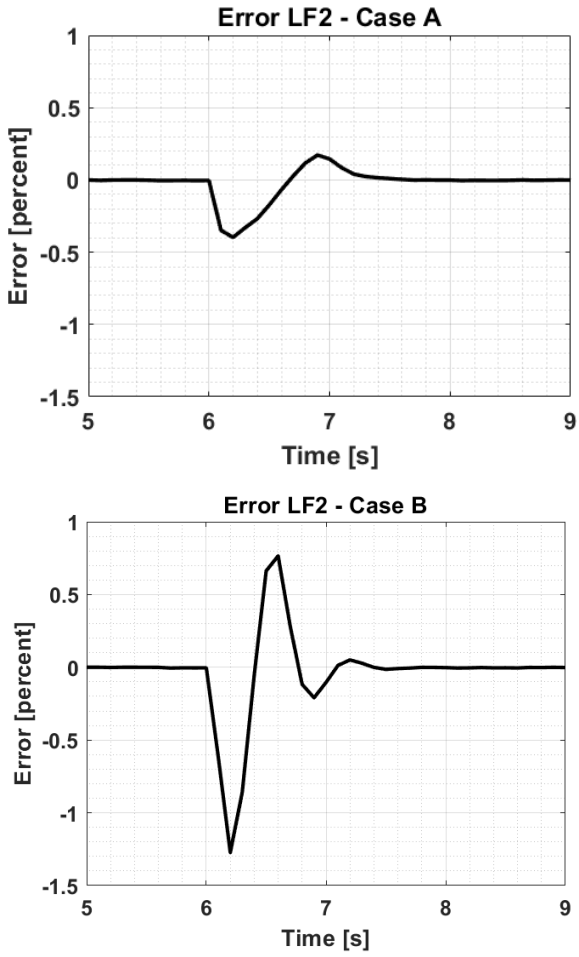

Figure 3.25 Error in position tracking for Loadframe 2

3.4 Discussion

The success of the crosstalk mitigation strategies is determined by the following objectives:

1. The magnitude of pressure ripple (amplitude of pressure wave) at LF2.
2. The magnitude of pressure ripple at HPU due to step command at LF1

3. The error in position tracking in LF2

The model described is studied for 3 test cases. The results of each test case, with the objectives above are discussed in this section and tabulated in Table 3.2.

3.4.1 Pressure ripple due to sinusoidal displacement at Loadframe 2

The pressure ripple originating at loadframe 2 is measured to be 0.68MPa (100psi) in the baseline test case as reported in Chapter 2. All reduction methods tested in Section 3.2 show good reduction of this pressure ripple. In Case 1, additional accumulation of 2.0gal is seen to reduce the magnitude of this ripple to 0.03MPa (5psi). Increasing the volume of the close coupled accumulators can help decrease this pressure ripple but the increase in settling time of larger pressure fluctuations as seen in Figure 3.9 is unfavorable.

The effective cut off frequency for the RC Filter can be calculated from Eq. 3.4.1 as 12.98 Hz for Case 2 (refer Table 3.3). The frequency of pressure ripple is 20Hz, and hence is above the cut-off frequency of the RC filter. The RC filter is seen to reduce the pressure ripple to 6.8KPa (1psi), using a smaller 0.5gal accumulator as compared to Case 1. In the case of high force application, it may be desired to have a larger orifice to reduce the pressure drop across the orifice, but this would require a larger accumulator to maintain the same cutoff frequency.

In Case 3A and 3B, two different orifice sizing for 2nd Order RC Filters are evaluated. In Case 3A, where the orifice sizing is the same as Case 2, the resultant resistance is greater (Table 3.3) as two orifices are placed in series. The pressure ripple reduces to 6.8KPa (1psi) which is similar to Case 2. In Case 3B, the orifices are sized such that the cut off frequency of the 2nd Order RC Filter is the same as in Case 2. The pressure ripple in this case is seen to be 55.2KPa (8psi). The pressure ripple is not reduced to the same magnitude as Case 2, despite having the same cutoff frequency and equivalent resistance. A possible reason for this is that the effectiveness of the 2nd accumulator in series may be hampered by the orifice installed between it and the servovalve. In the case of a 1st order RC filter, the accumulator is directly connected to the servovalve with minimal

resistance between the two components. For a 2nd order RC filter, resistance is offered by the orifice to the flow supplied by the second accumulator, reducing its ability to dampen the pressure ripple.

3.4.2 Pressure variation in system due to step displacement at LF1

In the baseline test setup, there is a large pressure drop in the system to 2300psi, and high peak pressure of 3900 psi, as the pump flow rate varies to meet the system flow demands. In all crosstalk mitigation cases, the pressure fluctuations at loadframe one due to the step displacement are seen to reduce significantly i.e., the pressure drop, and the peak pressure overshoot are both seen to reduce.

For Case 1, the increase in accumulation is seen to be proportional to reduction in pressure fluctuations with diminishing attenuation as the volume of the accumulator is increased over 2.0gal. In case 2, by using an RC Filter, the least pressure overshoot is seen with only 0.5gal of accumulation compared to Case 1. The lower amount of accumulation used in Case 2 also reduces the settling time for the pressure fluctuations. Case 3A shows the least drop in pressure in the system with similar effectiveness to the RC Filter in Case 2. Case 3B does not reduce the pressure fluctuations effectively compared to the RC filter despite having have the same cut off frequency, showing that for a 2nd order RC filter higher flow resistance is required to achieve the same crosstalk mitigation.

3.4.3 Error in displacement control of LF2

All crosstalk methods discussed are shown to reduce the error in position control of loadframe 2 due to the disturbance generated at loadframe 1. In Case 1, addition of accumulation is seen to reduce the error, however the increase in settling times in the hardline pressure fluctuations results in longer for the system to reach zero steady state error. Case 2 shows the best reduction for error with the 0.5gal of accumulation. This shows that additional resistance, helps in reducing the error in displacement control, without the need for larger accumulators.

3.4.4 Cost evaluation in crosstalk reduction techniques

There is an added cost associated with the installation of accumulators and orifices in the system. In Cases 1-3, the error and pressure ripple in the system are reduced to an acceptable value. The component costs are tabulated in Table 3.2 and are sourced from MTS Systems [25] and Parker Hannafin [37]. The most expensive components in the methods discussed in this chapter are accumulators with the cost increasing as the volume of the accumulator increases. For the cases studied, accumulator costs were seen to range from $1100 for 0.5gal, $2086 for 1.5gal and $3200 for 2.0gal. Orifices are relatively inexpensive, with the cost increasing as the orifice diameter reduces. This is due to the higher machining tolerances associated with smaller orifices. The 2^{nd} order RC Filter is seen to be the most cost effective. The RC filter is seen to be nearly as cost effective and may be the better solution in the case that a more compact solution is desired, with fewer components to install. Using only accumulation is the least cost effective, as a significantly larger accumulator is needed to achieve the required reduction in crosstalk.

Table 3.2 Comparison of crosstalk reduction

Case		Pressure ripple at LF2	Pressure ripple at LF1		Error in position	Cost
			Peak Pressure Rise	Min. Pressure Drop		
Units		[MPa/psi]	[MPa/psi]	[MPa/psi]	[%]	[$]
Baseline Testcase		0.68MPa (100psi)	26.9MPa (3900psi)	15.85MPa (2300psi)	+4.5/-4.5	-
Close coupled accumulators	0.5gal	0.2MPa (29psi)	24.44MPa (3550psi)	17.65MPa (2560psi)	+2.6/-2.6	$2200
	1.5gal	0.05MPa (8psi)	21.92MPa (3180psi)	19.20MPa (2785psi)	+1.2/-1.45	$2786
	2.0gal	0.03MPa (5psi)	21.65MPa (3140psi)	19.58MPa (2840psi)	+0.8/-1.4	$3119
RC Filter		6.8KPa (1psi)	20.78MPa (3015psi)	19.9MPa (2887psi)	+0.04/-0.4	$2400
2nd Order RC Filter	Case 3A	6.8KPa (1psi)	20.92MPa (3035psi)	20.09MPa (2914psi)	+0.17/-0.4	$1600
	Case 3B	55.2KPa (8psi)	21.56MPa (3127psi)	19.48MPa (2826psi)	+0.8/-1.3	$1600

Table 3.3 Comparison of Resistance and Capacitance of system

Case		Accumulator Volume	Orifice Diameter	Hydraulic Resistance	Hydraulic Capacitance	Cutoff Frequency
Units		[Gal]	[mm]	[kg/m^4.s]	[m^4.s^2/kg]	[Hz]
Close coupled accumulators		0.5	-	-	1.57e-12	-
		1.5	-	-	4.71e-12	-
		2.0	-	-	6.27e-12	-
RC Filter		0.5	4	7.81e+9	1.57e-12	12.98
2nd Order RC Filter	Case 3A	0.25 + 0.25	4	3.13e+10	1.57e-12	3.25
	Case 3B	0.25 + 0.25	5.656	7.81e+9	1.57e-12	12.98

3.5 Conclusion

In Chapter 2, a system level model was developed consisting of a pump, hydraulic pipeline, and two loadframes. A baseline test condition was defined where one loadframe functioned as the disturbance generator and a second loadframe was the 'impacted' as it lost position tracking accuracy due to the pressure fluctuations generated in the system. Three methods of crosstalk reduction were modelled and evaluated in this chapter. The performance of these methods was evaluated based on the reduction in pressure ripple in the system, improvement in position control and cost-effectiveness of the solution.

Close coupled accumulation is shown to be an effective method of reducing hydraulic noise provided adequate volume of accumulation is added to the system for the lab setup and the tests being carried out. RC filters are shown to be the most effective method for crosstalk reduction. Significant improvement in position tracking and reduction in pressure ripple is achieved with lower volumes of accumulation by the addition of resistance. 2nd

order RC Filters are shown to be less effective than RC filter with equivalent cut off frequencies. However, with additional resistance, 2nd Order Filters are shown to be effective measures of crosstalk reduction at a lower expense of installation. In this study, the two orifices in a 2nd order RC filter are sized equally which may hamper the effect of the second accumulator installed in series. In future work, an optimization study can be conducted to evaluate the ideal sizing of both orifices to improve the effectiveness of this method of crosstalk mitigation.

The use of accumulation independently is shown to be the most expensive method of crosstalk reduction. The work done in this chapter in crosstalk modelling represents the first stage of modeling the interaction between hydraulic systems and their impact on the performance required. Future work includes broadening the study by expanding to different test cases with different command signals, sizing of loadframes as well as modelling of other crosstalk reduction methods to evaluate their effectiveness.

Chapter 4
Conclusion

4.1 Thesis Review

Materials Testing is a precise science with a large range of tests to accurately characterize the mechanical properties of a specimen. These properties can be tensile, compressive, failure, fatigue to name a few. Oil-hydraulic loadframes are the most popular choice in this industry owing to their large force to weight ratio. Testing setups comprising of multiple loadframes are susceptible to hydraulic crosstalk which reduces the positional control accuracy. In this thesis a tool to measure crosstalk in a testing facility is developed and methods to mitigate it are evaluated.

Research in the field of servohydraulic control is typically focused on the improvement of the performance of components in a hydraulic circuit – pumps, valves, accumulator, actuators etc. There is a lack of research that study the system as whole and focuses on the interactions between these components. A need was identified to study the impact on the performance of loadframes due to noise generated in the system by other components. In this thesis, an initial step was taken towards studying pressure dynamics and position control performance at a system level.

A gray box approach was taken towards taken for the modelling of a hydraulic system in Simscape Fluids. A black box approach is used for the modelling of components where the internal dynamics are not of significance to the measurement of crosstalk, such as the modelling of the pump. A white box approach is used when the modelling dynamics of the system are needed for capturing crosstalk and the loss of performance in the system, such as the modelling of the pipeline, accumulators, and the actuator. A pump model is developed using a variable flow source in Simscape controlled by a PID controller. The

dynamic pressure response of a Pressure-Compensated Variable Displacement Pump (MTS 515.30 HPU) [30] was recorded for step changes in flow demand. The PID controller in the model is tuned using the Ziegler-Nichols method such that the response of the model closely matched the experimental data.

A loadframe model is developed consisting of a double-ended actuator, a servovalve, accumulators and a controller. The servovalve was modelled with a grey box approach as a simplified directional valve. This assumption allowed the model to neglect the internal dynamics of the valve as the roll frequency of valve operation was significantly higher at 170Hz, compared to the frequencies studied within the scope of this thesis. Experimental data was collected for the response of the loadframe for step commands of displacement. The PID Controller was tuned such that the model response closely matched the experimental data. The pressure and flow dynamics of in the pipeline were modelled using a lumped parameter model in Simscape. The pipeline was divided into segments with each segment having the properties of resistance, inertance and capacitance. The number of segments was determined by the characteristic frequency of the system. Using these component models a system level model was developed comprising of one pump, pipeline and two loadframes – one acting as a disturbance generator and the other one to measure the impact of the disturbance on positional control accuracy.

A convergence study was conducted to determine the solver parameters to be used for the model. A relative tolerance of 1e-5 was found to give consistently accurate results. A baseline test case was evaluated with one loadframe performing a step command as the disturbance and the other tracking a sinusoidal position command. A +/- 4.5 % error in position tracking due to the disturbance generated in the system. The pressure and flow dynamics of the system at the loadframes and the pump due to the disturbance generated are recorded.

Methods of reducing this error were identified namely close coupled accumulation, RC filtering and second order RC filtering. These methods were then modeled in Simscape and implemented in the system model, sized such that the error is reduced to be under

1%. All the methods investigated are shown to be effective in reducing crosstalk but vary greatly in the cost and sizing of components required to achieve desired crosstalk mitigation and control accuracy. Increasing sizes of close couped accumulation are evaluated to reduce crosstalk in the system. Volume of the accumulator is shown to be proportional to the effectiveness in reduction of pressure fluctuations in the system. An increase in volume is also shown to be directly associated with the increase in settling time of the system which is undesirable.

Hydraulic RC filters consist of accumulation and resistance in form of orifices connected in series. RC filters were shown to be the effective method of crosstalk attenuation with the capacity to reduce error in positional tracking under 0.5% with only 25% of accumulator volume and 30% less expense, when compared to using only close coupled accumulation. RC Filters are also shown to be 29.9% more effective in reducing high frequency pressure ripple generated at the servovalve due to the sinusoidal tracking of loadframes as compared to using only accumulation.

Second order RC filters are shown to be effective crosstalk attenuator but with lower effectiveness when compared to a RC filter of equivalent cut-off frequency and resistance. A second order RC filter shows 12% less reduction of pressure ripple when compared to a first order RC filter with equivalent resistance and cut off frequency. This is hypothesized to be due to resistance offered by the second orifice to one of the accumulators, reducing the effective dampening of the pressure pulsations at the loadframe. Second order RC filters are shown to be the most cost-effective methods of crosstalk mitigation discussed within this thesis costing 33% less than an equivalent RC filter and 50% less than an equally effective close couple accumulator.

4.2 Recommendations for Future Work

The aim of the research conducted in this thesis is to create a toolbox of crosstalk reduction techniques and a platform to evaluate them for different lab setups. Future work

could involve modelling and evaluating more crosstalk reduction techniques to add to this toolbox. The model can be expanded to include loadframes with rotary actuators that are used for torsion tests. Chapter 1 discusses more crosstalk reduction devices including active accumulators, active piezo-electric actuators to vary compliance of a system which can be modelled and tested on the system model developed in this thesis.

Within the model, component level models can be improved to capture additional dynamics of the system. The pump is currently modelled with a black box approach. While this provides reliable results and quick modelling of new pump architectures, one cannot use this approach to improve the pump design to mitigate crosstalk. Future work can include developing a physical model for a pump and integrating it with the system model. Different architectures of pumps can be evaluated for the reduction of pressure ripple. The impact of changes in the pump design on crosstalk mitigation can then be evaluated. Similarly, the valve model in this study is simplified and does not capture the internal dynamics of a valve. To augment to this model, a physical model of a valve can be integrated to it with the aim to model tests at higher frequencies where the valve performance is not optimal. The effectiveness of the second order filter can be improved by conducting an optimization study on the diameters of the two orifices keeping the resistance and cut off frequency of the system constant.

An optimization tool can be developed using the system model to evaluate the sizing of accumulators, resistances, pumps and loadframes for a desired level of accuracy in the initial settling up a laboratory.

Bibliography

[1] J. Watton, *Fundamentals of Fluid Power*. Cambridge University Press, 2009.

[2] MTS Systems, “MTS Systems Articles - Fox Laboratory.”

[3] MTS Systems, “MTS Landmark System Technical Datasheet 370.10,” Eden Prairie, MN, 2016.

[4] M. Pan, N. Johnston, and A. Plummer, “Hybrid Fluid-borne Noise Control in Fluid-filled Pipelines,” in *Journal of Physics: Conference Series*, Oct. 2016, vol. 744, no. 1. doi: 10.1088/1742-6596/744/1/012016.

[5] M. Pan, C. Yuan, B. Ding, and A. Plummer, “Novel Integrated Active and Passive Control of Fluid-Borne Noise in Hydraulic Systems,” *Journal of Dynamic Systems, Measurement, and Control*, vol. 143, no. 9, Sep. 2021, doi: 10.1115/1.4049734.

[6] R. Haas, E. Lukachev, and R. Scheidl, “An RC filter for Hydraulic switching control with a transmission line between valves and actuator,” *International Journal of Fluid Power*, vol. 15, no. 3, pp. 139–151, Jan. 2014, doi: 10.1080/14399776.2014.970974.

[7] S. YOKOTA, H. SOMADA, and H. YAMAGUCHI, “Study on an Active Accumulator. (Active Control of High-Frequency Pulsation of Flow Rate in Hydraulic Systems).,” *JSME International Journal Series B*, vol. 39, no. 1, pp. 119–124, 1996, doi: 10.1299/jsmeb.39.119.

[8] A. Waitschat, F. Thielecke, P. Kloft, C. Nisters, R. M. Behr, and U. Heise, “Compact Fluid-Borne Noise Silencers for Aviation Hydraulic Systems,” Oct. 2015. doi: 10.1115/FPMC2015-9517.

[9] N. E. Earnhart and K. A. Cunefare, “Compact helmholtz resonators for hydraulic systems,” *International Journal of Fluid Power*, vol. 13, no. 1, pp. 41–50, 2012, doi: 10.1080/14399776.2012.10781045.

[10] B. H. G. Barbosa, L. A. Aguirre, C. B. Martinez, and A. P. Braga, “Black and gray-box identification of a hydraulic pumping system,” *IEEE Transactions on Control Systems Technology*, vol. 19, no. 2, pp. 398–406, Mar. 2011, doi: 10.1109/TCST.2010.2042600.

[11] Rexroth Bosch Group, “Axial piston variable pump A10VSO Technical Document,” 2012.

[12] N. D. Manring and R. E. Johnson, “Modeling and Designing a Variable-Displacement Open-Loop Pump,” 1996. [Online]. Available: http://www.asme.org/about-asme/terms-of-use

[13] P. Kaliafetis and T. H. Costopoulos, “MODELLING AND SIMULATION OF AN AXIAL PISTON VARIABLE DISPLACEMENT PUMP WITH PRESSURE CONTROL,” 1995.

[14] G. Zeiger and A. Akers, “Dynamic Analysis of an Axial Piston Pump Swashplate Control,” *Proceedings of the Institution of Mechanical Engineers, Part C: Journal of Mechanical Engineering Science*, vol. 200, no. 1, pp. 49–58, Jan. 1986, doi: 10.1243/PIME_PROC_1986_200_093_02.

[15] S. D. Kim, H. S. Cho, and C. O. Lee, “A Parameter Sensitivity Analysis for the Dynamic Model of a Variable Displacement Axial Piston Pump,” *Proceedings of the Institution of Mechanical Engineers, Part C: Journal of Mechanical Engineering Science*, vol. 201, no. 4, pp. 235–243, Jul. 1987, doi: 10.1243/PIME_PROC_1987_201_115_02.

[16] P. Casoli, A. Anthony, and M. Rigosi, “Modeling of an Excavator System - Semi Empirical Hydraulic Pump Model,” *SAE International journal of commercial vehicles*, vol. 4, no. 1, pp. 242–255, 2011, doi: 10.4271/2011-01-2278.

[17] A. O’Dwyer, *Handbook of PI and PID controller tuning rules*, 2nd ed.. London: Imperial College Press, 2006.

[18] S. M. Rozali, M. F. Rahmat, N. Abdul Wahab, R. Ghazali, and Zulfatman, “PID controller design for an industrial hydraulic actuator with servo system,” in *Proceeding, 2010 IEEE Student Conference on Research and Development - Engineering: Innovation and Beyond, SCOReD 2010*, 2010, pp. 218–223. doi: 10.1109/SCORED.2010.5704005.

[19] J. E. Bobrow and K. Lum, “Adaptive, High Bandwidth Control of a Hydraulic Actuator,” *Journal of Dynamic Systems, Measurement, and Control*, vol. 118, no. 4, pp. 714–720, Dec. 1996, doi: 10.1115/1.2802347.

[20] A. H. Sharghi, R. K. Mohammadi, M. Farrokh, and S. Zolfagharysaravi, “Feed-forward controlling of servo-hydraulic actuators utilizing a least-squares support-vector machine,” *Actuators*, vol. 9, no. 1, p. 11, 2020, doi: 10.3390/act9010011.

[21] Y. Chae, R. Rabiee, A. Dursun, and C. Kim, “Real-time force control for servo-hydraulic actuator systems using adaptive time series compensator and compliance springs,” *Earthquake engineering & structural dynamics*, vol. 47, no. 4, pp. 854–871, 2018, doi: 10.1002/eqe.2994.

[22] R. Haas and B. Manhartsgruber, “Simulation of fluid transients, for nonlinear fluids, with a lumped parameter model,” *PAMM*, vol. 9, no. 1, pp. 505–506, Dec. 2009, doi: 10.1002/pamm.200910225.

[23] P. Krus, K. Weddfelt, and J.-O. Palmberg, “Fast Pipeline Models for Simulation of Hydraulic Systems,” *Journal of dynamic systems, measurement, and control*, vol. 116, no. 1, pp. 132–136, 1994, doi: 10.1115/1.2900667.

[24] W.-G. Sim and J.-H. Park, “Transient Analysis for Compressible Fluid Flow in Transmission Line by the Method of Characteristics,” *KSME international journal*, vol. 11, no. 2, pp. 173–185, 1997, doi: 10.1007/BF02944891.

[25] MTS Systems, “MTS Landmark Testing Solutions (System Brochure) 2020,” Eden Prairie, MN, 2020.

[26] Christ, *Fatigue of Materials at Very High Numbers of Loading Cycles Experimental Techniques, Mechanisms, Modeling and Fatigue Life Assessment*. Wiesbaden: Springer Spektrum, 2018.

[27] K. Pöhlandt, *Materials Testing for the Metal Forming Industry*. Berlin, Heidelberg: Springer Berlin Heidelberg, 1989.

[28] MTS Systems, “MTS System Bionix Multistation Wear Simulators Brochure,” Eden Prairie, MN.

[29] N. Earnhart, K. Marek, and K. Cunefare, “Novel, compact devices for reducing fluid-borne noise,” 2011. doi: 10.4271/2011-01-1533.

[30] MTS Systems, “MTS SilentFlo™ 515 Hydraulic Power Units,” Eden Prairie, MN, 2020.

[31] MTS Systems, “MTS Model 252 Servovalves.”

[32] W. Kemmetmüller, F. Fuchshumer, and A. Kugi, “Nonlinear pressure control of self-supplied variable displacement axial piston pumps,” *Control Engineering Practice*, vol. 18, pp. 84–93, 2010, doi: 10.1016/j.conengprac.2009.09.

[33] MATLAB, “MATLAB - Hydraulic Flow Rate Source.”

[34] K. J. Åström and T. Hägglund, “Revisiting the Ziegler–Nichols step response method for PID control,” *Journal of Process Control*, vol. 14, no. 6, pp. 635–650, Sep. 2004, doi: 10.1016/j.jprocont.2004.01.002.

[35] V. L. W. E. B. Streeter, *Hydraulic transients*. McGraw-Hill, 1967.

[36] F. M. White, *Viscous Fluid Flow*. McGraw-Hill, 1991.

[37] Parker Hannafin, “Bladder Accumulator - BA Series,” 2021.

[38] ReasonTek, “Bladder style Accumulators,” *https://www.reasontek.com/bladder-accumulators*.

[39] M. Ledvoň, L. Hružík, A. Bureček, and M. Vašina, “Static and dynamic characteristics of proportional directional valve,” *EPJ Web of Conferences*, vol. 213, p. 02052, 2019, doi: 10.1051/epjconf/201921302052.

[40] B. Xu, R. Ding, J. Zhang, and Q. Su, “Modeling and dynamic characteristics analysis on a three-stage fast-response and large-flow directional valve,” *Energy Conversion and Management*, vol. 79, pp. 187–199, Mar. 2014, doi: 10.1016/j.enconman.2013.12.013.

[41] S. S. Tørdal, A. Klausen, and M. K. Bak, “Experimental System Identification and Black Box Modeling of Hydraulic Directional Control Valve,” *Modeling, Identification and Control*, vol. 36, no. 4, pp. 225–235, 2015, doi: 10.4173/mic.2015.4.3.

[42] MATLAB, “MATLAB - 4-Way Directional Valve.”

[43] MATLAB, “Matlab - Documentation of Simscape Fluids.”

[44] T. Hägglund and K. J. Åström, “Revisiting The Ziegler-Nichols Tuning Rules For Pi Control,” *Asian Journal of Control*, vol. 4, no. 4, pp. 364–380, Oct. 2008, doi: 10.1111/j.1934-6093.2002.tb00076.x.

[45] N. S. Nise, *Control systems engineering* . John Wiley & Sons, 2009.

[46] MATLAB, “MATLAB - Ode23t.”

[47] N. Manring, *Hydraulic control systems*. Hoboken, N.J.: John Wiley, 2005.

[48] M. Herpy, *Active RC filter design*. Amsterdam ; New York : Budapest: Elsevier ; Akadémiai Kiadó, 1986.

Appendix A: Simscape Models

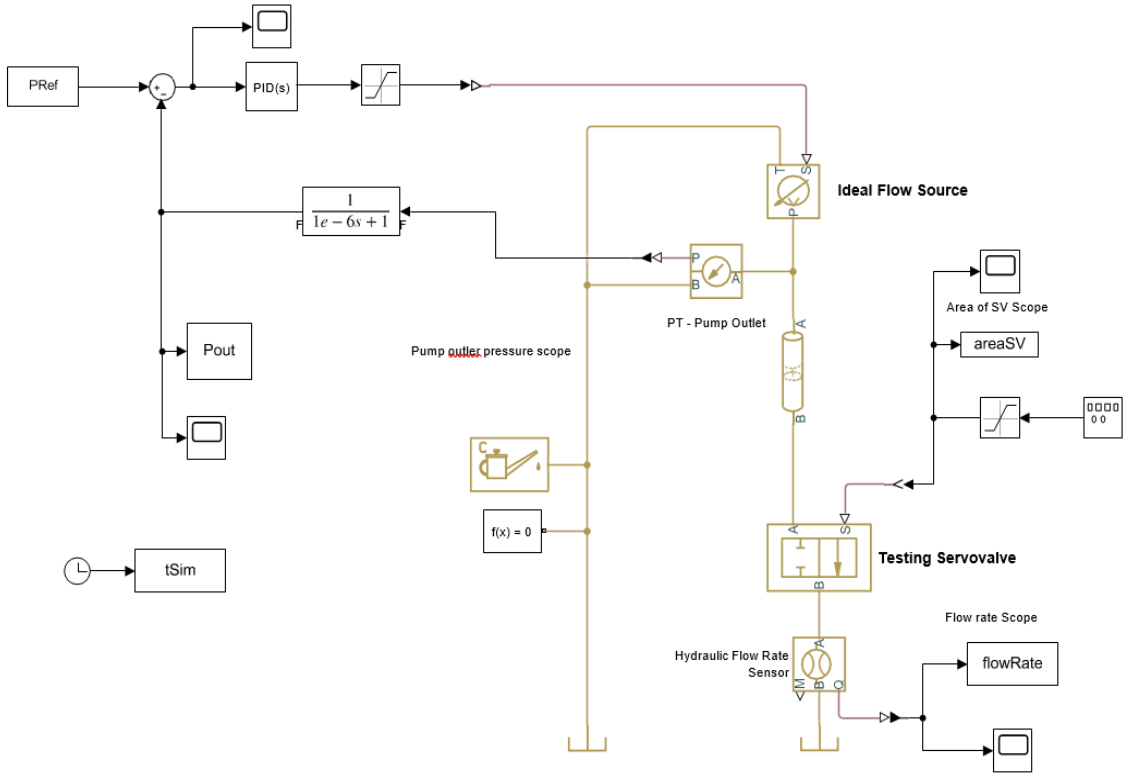

Figure A. 1Simscape Fluids Model for validation of Pump Model

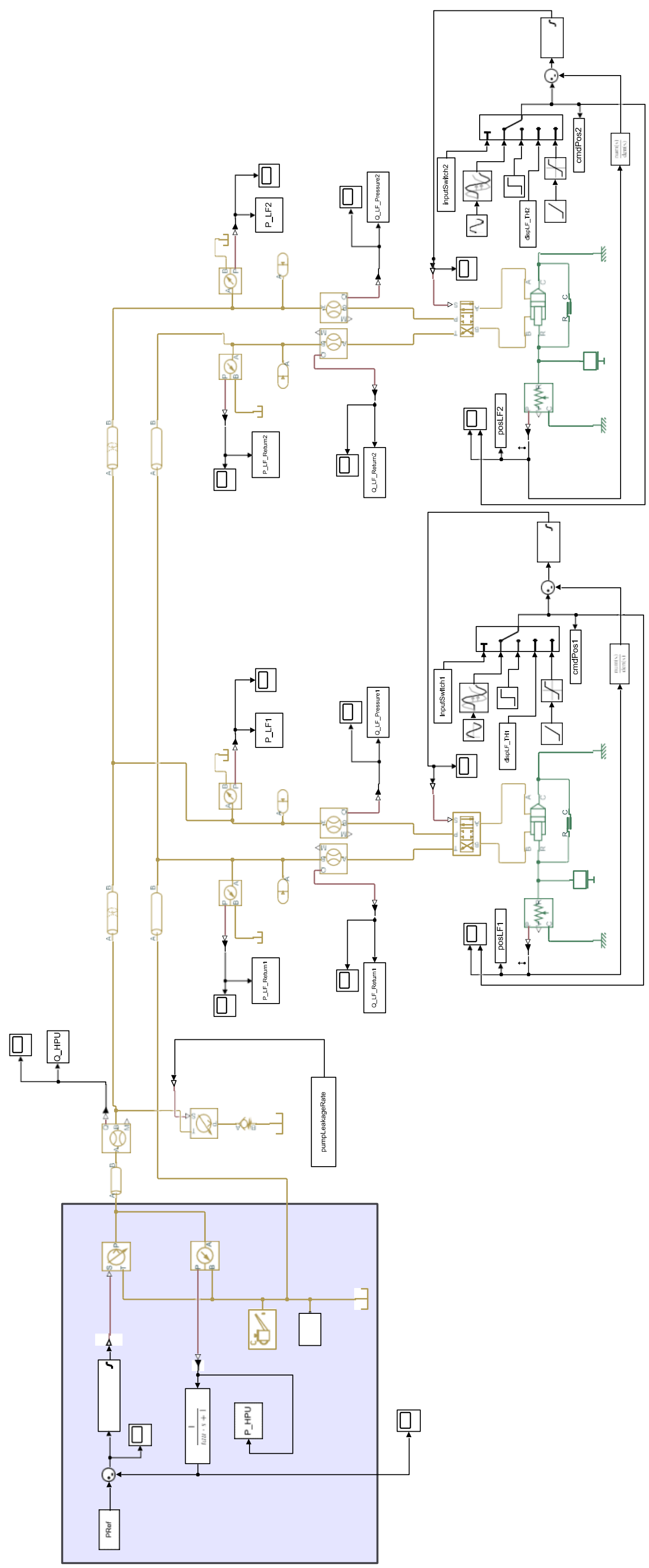
P_LF2
Q_LF_Pressure2
InputSwitch2
dispLF_TH2
cmdPos2
posLF2
P_LF_Return2
Q_LF_Return2
P_LF1
Q_LF_Pressure1
InputSwitch1
dispLF_TH1
cmdPos1
posLF1
P_LF_Return1
Q_LF_Return1
Q_HPU
pumpLeakageRate
P_HPU
PRef

Figure A. 2 Simscape System Model for Evaluation of Crosstalk

Appendix B: Convergence study of model

The system model developed in Chapter 2 is evaluated for decreasing values of relative tolerance (1e-3, 1e-4, and 1e-5) for the baseline test case setup. The results of the simulation are documented in this appendix. The model is seen to be equally accurate at all three values of relative tolerance. A simulation of 5second takes 20.58s with 1e-3 relative tolerance, 29.45s with 1e-4 relative tolerance and 45.26s with 1e-5 relative tolerance.

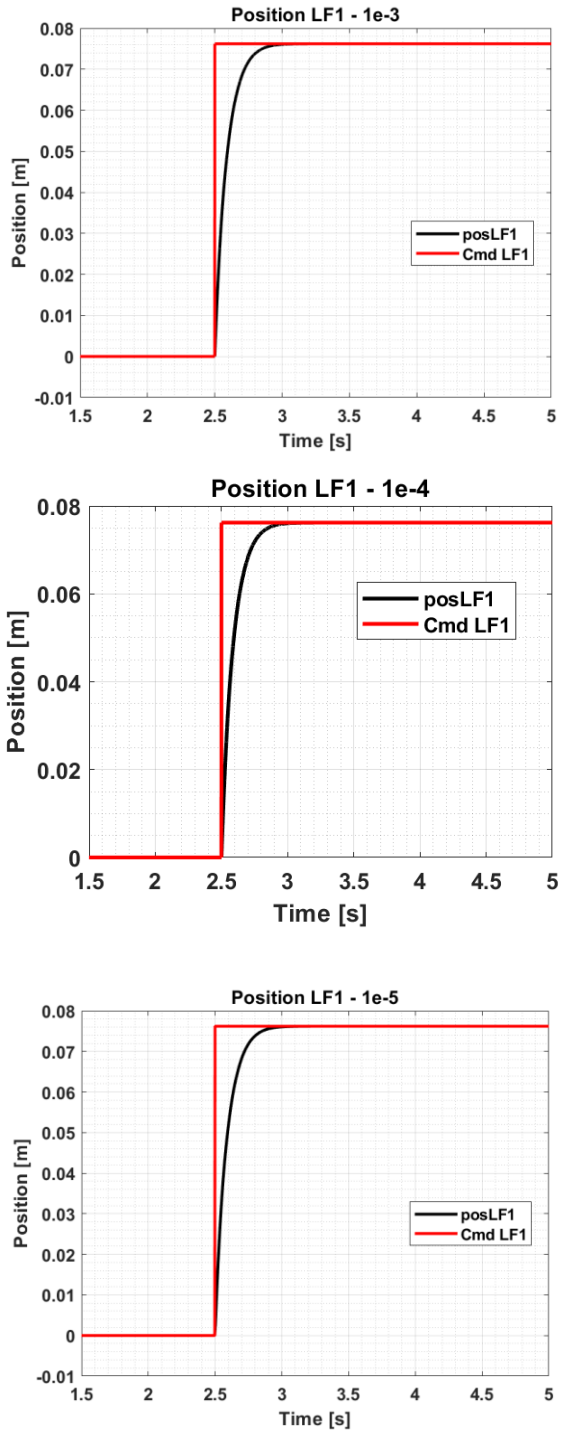

Figure B. 1 : Comparison of Loadframe 1 position with Relative tolerance

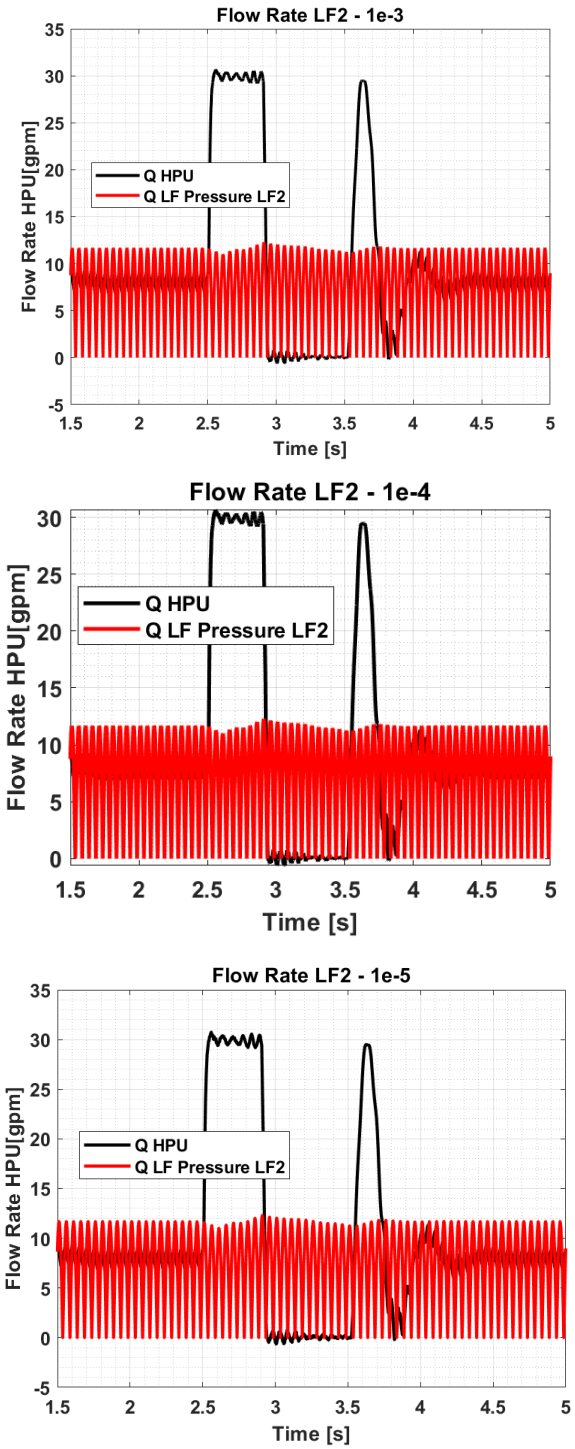

Figure B. 2 Comparison of flow rate of Loadframe 2 with Relative tolerance

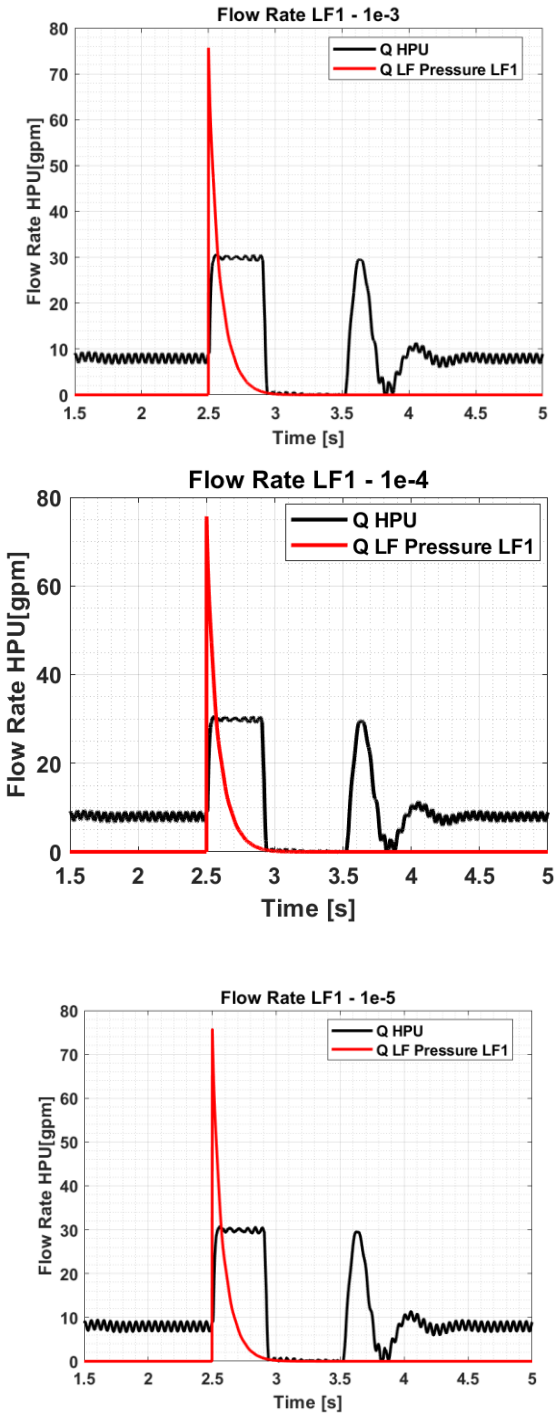

Figure B. 3 Comparison of flow rate of Loadframe 2 with Relative tolerance

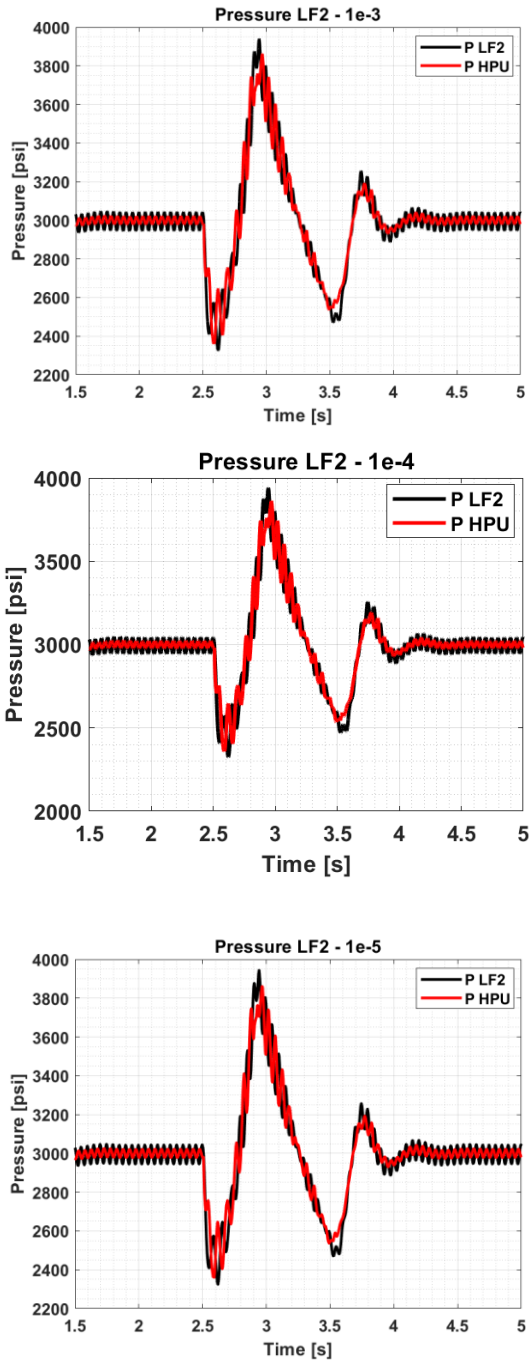

Figure B. 4 Comparison of Pressure at Loadframe 2 with Relative tolerance

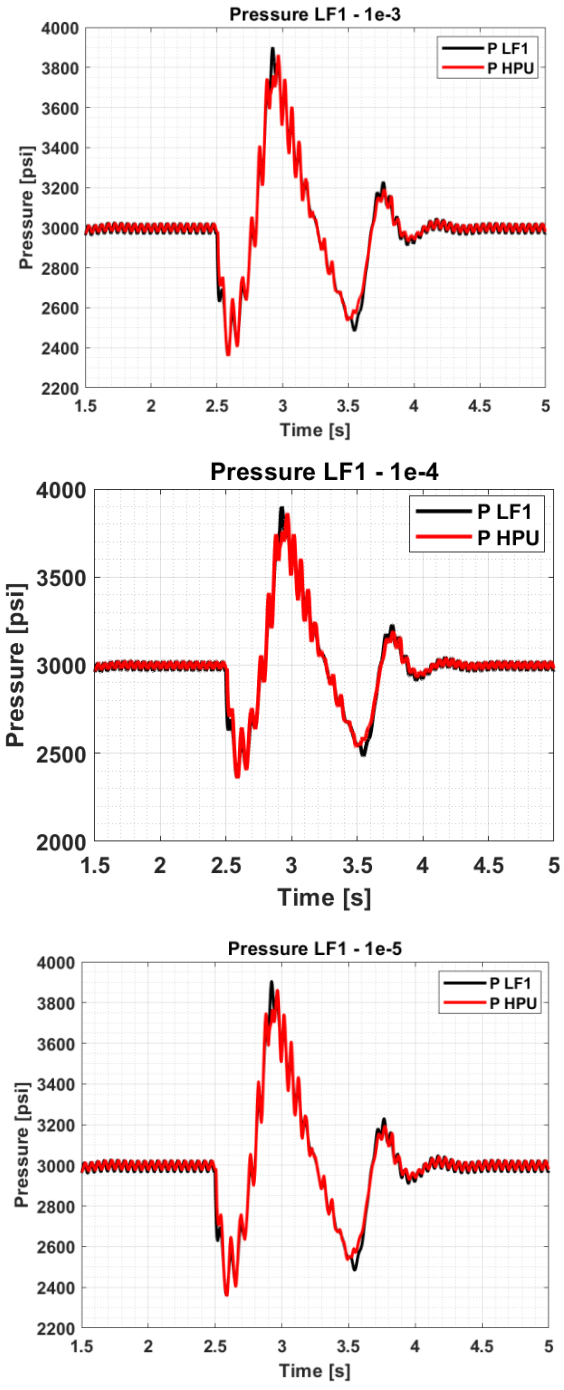

Figure B. 5 Comparison of Pressure at Loadframe 1 with Relative tolerance

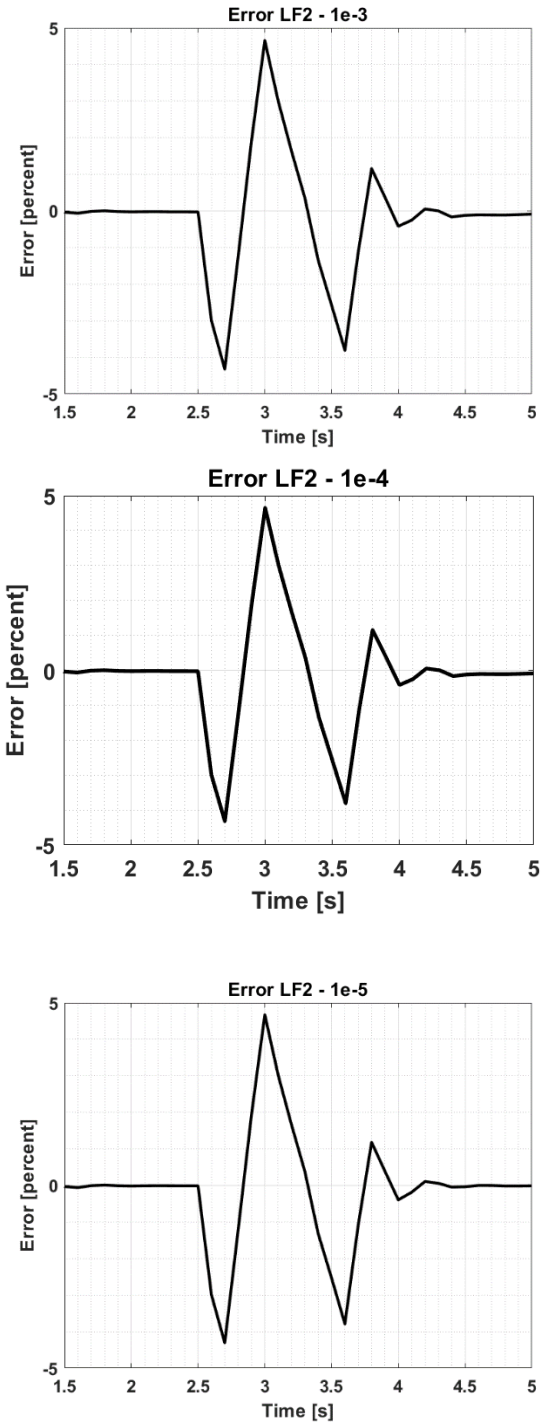

Figure B. 6 Comparison of error in position control of Loadframe 2 with Relative tolerance